

CalVal Envisat
CLS.DOS/NT/06.300
Version : 0rev1, April 19, 2007
Nomenclature : SALP-RP-MA-EA-21376-CLS

Ramonville, April 19, 2007

**Envisat RA2/MWR ocean data validation and
cross-calibration activities. Yearly report 2006.**

Contract N° 03/CNES/1340/00-DSO310

	AUTHORS	COMPANY	DATE	INITIALS
WRITTEN BY	Y. Faugere N. Granier A. Ollivier	CLS CLS CLS		
APPROVED BY	J.Dorandeu	CLS		
QUALITY VISA	AQM	CLS		
APPLICATION AUTHORISED BY	N.Picot P.Leloup	CNES CNES		

CLS CalVal Envisat	Envisat validation and cross-calibration activities	Page : i.2 Date : April 19, 2007
Ref: CLS.DOS/NT/06.300	Nom.: SALP-RP-MA-EA-21376-CLS	Issue: 0rev1

DISTRIBUTION LIST		
COMPANY	NAMES	COPIES
CLS/DOS	J.DORANDEU	1 electronic copy
	V.ROSMORDUC	1 electronic copy
	P.ESCUDIER	1 electronic copy
DOC/CLS	DOCUMENTATION	1 electronic copy
CNES	P.LELOUP	2 copy + 1 electronic copy
CNES	N.PICOT	1 electronic copy
CNES	P.BOUBE	1 electronic copy
CNES	J.LAMBIN	1 electronic copy

CLS CalVal Envisat	Envisat validation and cross-calibration activities	Page : i.3 Date : April 19, 2007
Ref: CLS.DOS/NT/06.300	Nom.: SALP-RP-MA-EA-21376-CLS	Issue: 0rev1

CHRONOLOGY ISSUE

Control Initials	ISSUE	DATE	REASON FOR CHANGE
	0/0	2006/12/29	Creation
	0/1	2007/01/02	1 appendix added

CLS CalVal Envisat	Envisat validation and cross-calibration activities	Page : i.4 Date : April 19, 2007
Ref: CLS.DOS/NT/06.300	Nom.: SALP-RP-MA-EA-21376-CLS	Issue: 0rev1

LIST OF ACRONYMS

TBC	To Be Confirmed

CLS CalVal Envisat	Envisat validation and cross-calibration activities	Page : i.5 Date : April 19, 2007
Ref: CLS.DOS/NT/06.300	Nom.: SALP-RP-MA-EA-21376-CLS	Issue: 0rev1

List of Tables

1	<i>Processing version</i>	3
2	<i>IPF versions</i>	4
3	<i>CMA versions</i>	5
4	<i>Editing criteria</i>	13
5	<i>SSH definition</i>	44

CLS	Envisat validation and cross-calibration activities	Page : i.6
CalVal Envisat		Date : April 19, 2007
Ref: CLS.DOS/NT/06.300	Nom.: SALP-RP-MA-EA-21376-CLS	Issue: 0rev1

List of Figures

1	<i>Chronology of USO Correction computation.</i>	7
2	<i>Monitoring of the percentage of missing measurements relative to what is theoretically expected over ocean</i>	9
3	<i>Envisat missing measurements for cycle 50</i>	10
4	<i>Pass segments unavailable more than 5 times between cycles 41 and 51. The numbers on the map indicate the pass number. The colour indicates the occurrence of unavailability</i>	10
5	<i>Cycle per cycle percentages of missing MWR measurements</i>	11
6	<i>Cycle per cycle percentages of data impacted by the S-Band anomaly</i>	12
7	<i>% of edited points by sea ice flag over ocean</i>	12
8	<i>Cycle per cycle percentages of edited measurements by the main Envisat altimeter and radiometer parameters: top-left) Standard deviation of 20 Hz range measurements > 25 cm, Number of 20-Hz range measurements < 10 top-right) Square of off-nadir angle (from waveforms) out of the [-0.2 deg², 0.16 deg²] range, dual frequency ionosphere correction out of [-40 , 4 cm] bot-left) Ku-band Significant wave height outside > 11 m, Ku band backscatter coefficient out of the [7 dB, 30 dB] range bot-right) MWR wet troposphere correction out of the [-50 cm, -0.1 cm] range.</i>	14
9	<i>SSH-MSS out of the [-2, 2m] and edited using thresholds on the mean and standard deviation of SSH-MSS on each pass</i>	16
10	<i>left) Cycle mean of the number of 20 Hz elementary range measurements used to compute 1 Hz range. right) Cycle mean of the standard deviation of 20 Hz measurements.</i>	17
11	<i>Histogram of RMS of Ku and S range (cm)</i>	18
12	<i>Cycle mean of the square of the off-nadir angle deduced from waveforms (deg²).</i>	19
13	<i>Histogram of off-nadir angle from waveforms (deg²)</i>	20
14	<i>Global statistics (m) of Envisat Ku and S SWH top-right) Mean and top-left) Standard deviation. bot-right) Mean Envisat-Jason-1 Ku SWH differences at 3h EN/J1 crossovers computed with 120 days running means. bot-left) Mean. ERS-2-Envisat Ku SWH collinear differences over the Atlantic Ocean.</i>	21
15	<i>Histogram of Ku and S SWH (m)</i>	22
16	<i>Global statistics (dB) of top) Envisat Ku and S Sigma0 Mean and Standard deviation. middle) Mean Envisat-Jason-1 Ku Sigma0 differences at 3h EN/J1 crossovers computed with 120 days running means. bottom) Mean and Standard of ERS-2-Envisat Ku Sigma0 collinear differences over the Atlantic Ocean.</i>	24
17	<i>Histogram of Ku and S Sigma0 (dB)</i>	25
18	<i>Comparison of global statistics of Envisat dual-frequency and JPL-GIM ionosphere corrections (cm). top) Cycle mean and standard deviation of Dual Frequency and GIM correction. bot) Mean and standard deviation of the differences</i>	26
19	<i>Scatter plot of MWR correction according to ECMWF model (m)</i>	27
20	<i>Comparison of global statistics of Envisat MWR and ECMWF wet troposphere corrections (cm). top) Cycle mean and standard deviation of MWR and ECMWF corrections bot) Mean and standard deviation of the differences.</i>	28
21	<i>Monitoring of the (ERS-2 - Envisat) brightness temperatures</i>	29
22	<i>Monitoring of the (ERS-2 - Envisat) wet troposphere correction</i>	29
23	<i>Maps of the time invariant 35-day crossover mean differences (cm) for Envisat averaged in (3° x 3°) geographical bins over cycles 10 to 40 (left) and over cycles 41 to 51 using the new POE orbit using a new gravity model (right).</i>	31

CLS	Envisat validation and cross-calibration activities	Page : i.7
CalVal Envisat		Date : April 19, 2007
Ref: CLS.DOS/NT/06.300	Nom.: SALP-RP-MA-EA-21376-CLS	Issue: 0rev1

24	<i>Time varying 35-day crossover mean differences (cm). Cycle per cycle Envisat crossover mean differences. An annual cycle is clearly visible. Diamonds: shallow waters (1000 m) are excluded. Triangles: shallow waters excluded, latitude within [-50S, +50N], high ocean variability areas excluded</i>	32
25	<i>Standard deviation (cm) of Envisat 35-day SSH crossover differences depending on data selection. Dots: without any selection. Diamonds: shallow waters (1000 m) are excluded. Triangles: shallow waters excluded, latitude within [-50S, +50N], high ocean variability areas excluded.</i>	33
26	<i>Comparison of the Standard deviation (cm) of Envisat (dot) and Jason-1 (diamond) 10-day SSH crossover differences</i>	33
27	<i>Mean of Envisat Sea Level depending on data selection. Dots: without any selection. Diamonds: shallow waters (1000 m) are excluded. Triangles: shallow waters excluded, latitude within [-50S, +50N], high ocean variability areas excluded.</i>	34
28	<i>Mean of Envisat -Jason-1 differences at 10-day dual crossovers. Dots: Global. Diamonds: Northern Hemisphere. Triangle: Southern Hemisphere.</i>	35
29	<i>Envisat and Jason-1 MSL trend over the period 2003-2006 (left), Envisat - Jason-1 MSL trend (right)</i>	36
30	<i>Envisat and Jason-1 MSL trend over the period 2003-2004 (top left), 2004-2005 (top right), 2005-2006 (bot)</i>	36
31	<i>Mean per day of the correction since the beginning of the USO anomaly.</i>	37
32	<i>Raw period (left). Spline filtered period (top right). Associated correction (bottom right)</i>	38
33	<i>SLA without (left) and with (right) the USO Correction on cycle 46 affected by the anomaly.</i>	39
34	<i>(Predictive model USO Correction - Operational USO Correction) mean differences (left). Average USO Correction differences per pass for Cycle 46 and 47(right).</i>	40
35	<i>Predictive model USO Correction (Red) and Operational USO Correction (Black) for tracks 200 to 210 of cycle 46 (slow change of the mean USO value) (left) and for track 1 of cycle 46 (quick change of the mean USO value) (right).</i>	41
36	<i>Mean per day of Correction Step=100s and Correction Step=86400s.</i>	43
37	<i>SSH Crossover mean difference, using SSH1 over cycles 31 to 40 (top left), using SSH2 over cycles 31 to 40 (top right),and using SSH3 over 41 to 50 (bottom)</i>	45
38	<i>Scatter plot of SSH crossover mean difference (cm) according to Significant wave height (cm) using SSH3 (left) and using SSH4 (right) over cycles 41 to 50</i>	46
39	<i>Crossover mean difference using SSH3 (left) and using SSH4 (right) over cycles 41 to 50</i>	46
40	<i>Crossover mean difference using SS4 + GIM ionosphere correction over cycles 41 to 50</i>	47
41	<i>Amplitude (cm) of the annual signal on the mean at crossovers estimated in 10x10 deg boxes (using GOT00 tide model)</i>	48
42	<i>Amplitude (cm) and phase (deg) of the annual signal on the mean at crossovers estimated in 10x10 deg boxes</i>	49
43	<i>Amplitude (cm) and phase (deg) of the annual signal on the mean at crossovers estimated in 10x10 deg boxes using FES04</i>	49
44	<i>Amplitude (cm) and phase (deg) of the annual signal on the mean at crossovers estimated in 10x10 deg boxes using FES02</i>	49
45	<i>Amplitude (cm) and phase (deg) of the annual signal on the mean at crossovers estimated in 10x10 deg boxes using FES99</i>	50
46	<i>Difference of the amplitude (cm) of the annual signal estimated using GOT00 and FES04 tide</i>	50
47	<i>Amplitude (cm) of the annual signal on the mean at crossovers estimated in 10x10 deg boxes using no tide correction</i>	50
48	<i>Q1 oceanic tide component of Fes04 and difference between Q1 component of FES04 and GOT00</i>	51

CLS	Envisat validation and cross-calibration activities	Page : i.8
CalVal Envisat		Date : April 19, 2007
Ref: CLS.DOS/NT/06.300	Nom.: SALP-RP-MA-EA-21376-CLS	Issue: 0rev1

49	<i>O1 oceanic tide component of Fes04 and difference between O1 component of FES04 and GOT00</i>	51
50	<i>P1 oceanic tide component of Fes04 and difference between P1 component of FES04 and GOT00</i>	51
51	<i>K1 oceanic tide component of Fes04 and difference between K1 component of FES04 and GOT00</i>	51
52	<i>N2 oceanic tide component of Fes04 and difference between N2 component of FES04 and GOT00</i>	52
53	<i>M2 oceanic tide component of Fes04 and difference between M2 component of FES04 and GOT00</i>	52
54	<i>S2 oceanic tide component of Fes04 and difference between S2 component of FES04 and GOT00</i>	52
55	<i>K2 oceanic tide component of Fes04 and difference between K2 component of FES04 and GOT00</i>	52
56	<i>Amplitude (cm) and phase (deg) of the annual signal on the mean at crossovers estimated in 10x10 deg boxes using Delft orbit</i>	53
57	<i>Amplitude (cm) and phase (deg) of the annual signal on the mean at crossovers estimated in 10x10 deg boxes using Delft orbit and FES04 tide</i>	53
58	<i>Delft - CNES (GRIM5) mean differences (left), Delft - CNES (EIGEN-CG03C) mean differences (right).</i>	54
59	<i>Crossover mean differences over cycles 41 to 47. SSH using the Delft orbit (right) and CNES orbit (left).</i>	55
60	<i>Difference of variance [Var(SSH(POE Delft))-Var(SSH(POE CNES))]</i> (cm ²)	55
61	<i>Mean per day of the difference between the radiometric corrections and the ECMWF model: Jason-1, T/P, GFO, et ENVISAT.</i>	66
62	<i>Map of the difference between ENVISAT radiometric corrections and the ECMWF model. Left hand map shows the average on one year (02/12/2003 to 02/12/2004). Right hand map shows the associated standard deviation.</i>	67
63	<i>Difference between ENVISAT radiometric and the ECMWF model corrections as a function of latitude. Black plain curves (-) represent the mean difference, black dotted lines (- -) represent the standard deviation and the red curves (-) represent the number of valid measurements repartition.</i>	68
64	<i>Difference between ENVISAT radiometric and the ECMWF model corrections as a function of distance to coast. Black plain curves (-) represent the mean difference, black dotted lines (- -) represent the standard deviation and the red curves (-) represent the number of valid measurements repartition.</i>	69
65	<i>Difference between ENVISAT radiometric and the ECMWF model corrections as a function of distance to coast. Better accounting of Side Lobe effect for the new V7 version compared to V6 version.</i>	70
66	<i>Spectra of Envisat and Jason-1 SLA using 20Hz measurements(left) and 1Hz measurements (right).</i>	72
67	<i>Filtering technique</i>	73
68	<i>Map of standard deviation of difference between $\sigma(S_{HF}(EN))$ and $\sigma(S_{HF}(J1))$ with GDR a (top left), GDR b (top right) and Envisat mean water vapour (bottom)</i>	73
69	<i>MSL over global ocean since the beginning of T/P mission on the left and since the beginning of Jason-1 mission on the right.</i>	80
70	<i>MSL over global ocean since the beginning of T/P mission on the left and since the beginning of Jason-1 mission on the right after removing annual, semi-annual and 60-day signals.</i>	81

CLS CalVal Envisat	Envisat validation and cross-calibration activities	Page : i.9 Date : April 19, 2007
Ref: CLS.DOS/NT/06.300	Nom.: SALP-RP-MA-EA-21376-CLS	Issue: 0rev1

71	<i>MSL and SST over global ocean for the T/P period on the left, and after removing annual, semi-annual and 60-day signals on the left.</i>	81
72	<i>MSL slopes over Jason-1/TOPEX overlapping period for T/P (left) and Jason-1 (right), MSL slope differences between Jason-1 and T/P (bottom)</i>	82
73	<i>MSL slopes over Envisat/Jason-1 overlapping period for Envisat (left) and Jason-1 (right), MSL slope differences between Jason-1 and Envisat (bottom)</i>	83
74	<i>T/P MSL and SST slopes over 13 years</i>	84
75	<i>Adjustment errors of T/P MSL and SST slopes over 13 years</i>	84
76	<i>Adjustment errors of T/P MSL and SST slopes over 13 years before and after "El Niño"</i>	85

CLS CalVal Envisat	Envisat validation and cross-calibration activities	Page : i.10 Date : April 19, 2007
Ref: CLS.DOS/NT/06.300	Nom.: SALP-RP-MA-EA-21376-CLS	Issue: 0rev1

Contents

1	Introduction	1
2	Quality overview	2
3	Data used and processing	3
3.1	Data used	3
3.2	Processing	5
4	Missing and edited measurements	9
4.1	Missing measurements	9
4.2	Missing MWR data	10
4.3	Edited measurements	11
4.3.1	Measurements impacted by S-Band anomaly	11
4.3.2	Measurements impacted by Sea Ice	11
4.3.3	Editing by thresholds	12
4.3.4	Editing on SLA	15
5	Long term monitoring of altimeter and radiometer parameters	17
5.1	Number and standard deviation of 20Hz elementary Ku-band measurements	17
5.2	Off-nadir angle from waveforms	19
5.3	Significant Wave Height	21
5.4	Backscatter coefficient	23
5.5	Dual frequency ionosphere correction	26
5.6	MWR wet troposphere correction	27
6	Sea Surface Height performance assessment	30
6.1	SSH definition	30
6.2	Single crossover mean	30
6.3	Variance at crossovers	31
7	Envisat SSH bias and Mean Sea Level trends	34
7.1	SSH definition	34
7.2	Envisat Bias	34
7.3	MSL trends	35
8	Particular investigation	37
8.1	The Ra-2 USO anomaly and its associated correction	37
8.1.1	Introduction	37
8.1.2	USO correction method	37
8.1.3	Correction availability	39
8.1.4	Validation over ocean	39
8.1.4.1	Quality assessment of the corrected GDR	39
8.1.4.2	Comparison to the correction proposed by R Scharroo	40
8.1.4.3	Analysis of the validity of the long term drift component of the new correction	42
8.1.5	Conclusion	42
8.2	Analysis of the geographical feature of EN/J1 SSH Differences	44
8.2.1	Introduction	44
8.2.2	Main data product changes on Envisat and Jason-1	44

CLS	Envisat validation and cross-calibration activities	Page : i.11
CalVal Envisat		Date : April 19, 2007
Ref: CLS.DOS/NT/06.300	Nom.: SALP-RP-MA-EA-21376-CLS	Issue: 0rev1

8.2.3	Comparison of SSH performance	45
8.2.4	Comparison of SSH performance with new SSB for Jason-1	45
8.2.5	Impact of GIM	46
8.2.6	Conclusion	46
8.3	Analysis of the annual signal at EN SSH crossover	48
8.3.1	Introduction	48
8.3.2	Estimation using the reference SSH	48
8.3.3	Impact of tide on the annual signal	48
8.3.3.1	Change of tide correction	48
8.3.3.2	Comparison between GOT00 and FES04 tidal waves	50
8.3.4	Impact of orbit on the annual signal	53
8.4	Comparison Orbit POE and Delft	54
8.4.1	Orbit differences	54
8.4.2	Performance at crossovers	54
8.5	The B Side configuration performances	56
8.6	Wet tropospheric correction	66
8.6.1	Monitoring per day of the wet troposphere correction differences (radiometer - model) and long term monitoring	66
8.6.2	Geographical correlations of the wet troposphere correction differences (radiometer - model)	67
8.6.3	Stability of the corrections when approaching coasts	69
8.6.4	Conclusion	71
8.7	High frequency analysis	72
8.7.1	Spectral analysis	72
8.7.2	Filtering technique	72
9	Conclusion	74
10	Appendix 1: Mean Sea Level (MSL) and Sea Surface Temperature (SST) comparisons	79
10.1	SSH definition for each mission	79
10.2	MSL and SST time series	80
10.2.1	MSL over global ocean	80
10.2.2	SST over global ocean	81
10.3	Spatial MSL and SST slopes	82
10.3.1	Methodology	82
10.3.2	Spatial MSL slopes over Jason-1 period	82
10.3.3	Spatial MSL slopes over Envisat period	83
10.3.4	Spatial SST and MSL slopes since the beginning of T/P mission	84
10.3.5	"El Niño" impact on SST and MSL slope estimations	85
11	Appendix 2: Instrument and platform status	86
11.1	ACRONYMS	86
11.2	Cycle 010	86
11.3	Cycle 011	86
11.4	Cycle 012	87
11.5	Cycle 013	87
11.6	Cycle 014	87
11.7	Cycle 015	87
11.8	Cycle 016	88

CLS CalVal Envisat	Envisat validation and cross-calibration activities	Page : i.12 Date : April 19, 2007
Ref: CLS.DOS/NT/06.300	Nom.: SALP-RP-MA-EA-21376-CLS	Issue: 0rev1

11.9 Cycle 017	88
11.10 Cycle 018	88
11.11 Cycle 019	89
11.12 Cycle 020	89
11.13 Cycle 021	89
11.14 Cycle 022	89
11.15 Cycle 023	90
11.16 Cycle 024	90
11.17 Cycle 025	90
11.18 Cycle 026	90
11.19 Cycle 027	90
11.20 Cycle 028	91
11.21 Cycle 029	91
11.22 Cycle 030	91
11.23 Cycle 031	91
11.24 Cycle 032	91
11.25 Cycle 033	92
11.26 Cycle 034	92
11.27 Cycle 035	92
11.28 Cycle 036	92
11.29 Cycle 037	92
11.30 Cycle 038	92
11.31 Cycle 039	93
11.32 Cycle 040	93
11.33 Cycle 041	93
11.34 Cycle 042	93
11.35 Cycle 043	93
11.36 Cycle 044	94
11.37 Cycle 045	94
11.38 Cycle 046	94
11.39 Cycle 047	94
11.40 Cycle 048	95
11.41 Cycle 049	95
11.42 Cycle 050	95
11.43 Cycle 051	95

CLS CalVal Envisat	Envisat validation and cross-calibration activities	Page : i.13 Date : April 19, 2007
Ref: CLS.DOS/NT/06.300	Nom.: SALP-RP-MA-EA-21376-CLS	Issue: 0rev1

APPLICABLE DOCUMENTS / REFERENCE DOCUMENTS

CLS CalVal Envisat	Envisat validation and cross-calibration activities	Page : 1 Date : April 19, 2007
Ref: CLS.DOS/NT/06.300	Nom.: SALP-RP-MA-EA-21376-CLS	Issue: 0rev1

1 Introduction

This report is an overview of Envisat validation and cross calibration studies carried out at CLS during the year 2006. It is basically concerned with long-term monitoring of the Envisat altimeter system over ocean. Data from GDR cycles 10 through 51 spanning four years have been used for this analysis. All relevant altimeter parameters deduced from Ocean 1 retracking, radiometer parameters and geophysical corrections are evaluated and tested. This work is routinely performed at CLS, as part of the SSALTO and funded by ESA through F-PAC activities (SALP contract N° 03/CNES/1340/00-DSO310 Lot 2C). In this frame, besides continuous analyses in terms of altimeter data quality, Envisat GDR Quality Assessment Reports (e.g. Faugere et al. 2004) are routinely produced in conjunction with data dissemination. Some of the results described here were presented in the "15 years of altimetry" symposium (Venice, March 2006), the OSTST meeting (Venice, March 2006) and at the Quality Working Group (QWG) meeting (Toulouse, May 2006 and October 2006).

The work performed in terms of data quality assessment also includes cross-calibration with Jason-1 and ERS-2. This kind of comparisons between coincident altimeter missions provides a large number of estimations and consequently efficient long-term monitoring of instrument measurements. This enables the detection of instrument drifts and inter-mission biases essential to obtain a consistent multi-satellite data set.

After a preliminary section describing the data used, the report is split into 5 main sections: first, data coverage and measurement validity issues are presented. Second, monitoring of the main altimeter and radiometer parameters is performed, describing the major impact in terms of data accuracy. Then, performances are assessed and discussed with respect to the major sources of errors. Then, Envisat Sea Surface height (SSH) bias and MSL issues are analysed. Finally, an additional part presents the particular investigations that have been performed during this year.

CLS CalVal Envisat	Envisat validation and cross-calibration activities	Page : 2 Date : April 19, 2007
Ref: CLS.DOS/NT/06.300	Nom.: SALP-RP-MA-EA-21376-CLS	Issue: 0rev1

2 Quality overview

Nearly four years of Envisat altimetric observations over ocean are available in Geophysical Data Record (GDR) products. A major instrumental anomaly impacted Ra2 data this year, the USO anomaly on February 2006, the 13th. In May 2006, the instrument sub-system Radio Frequency Module (RFM) was switched to its B-side. Unfortunately, an anomaly occurred on the S-Band transmission power. On June the RFM was then switched to its nominal configuration side (A-side). A ground segment correction was developed and implemented in August and allowed Envisat altimetric data to recover its nominal quality.

Apart from that event, Envisat data show good general quality over ocean. The new IPF/CMA configuration set in operation in September 2005 improved the products quality. The unavailability of data is lower than 5% on most of the cycles from cycle 23 onwards. The MWR availability has also strongly improved. Moreover, some modifications were performed by ESA in 2005 to decrease the duration of the S-Band anomaly events. Statistics and performances of altimeter and radiometer parameters are consistent with expected values using the USO auxiliary correction.

CLS CalVal Envisat	Envisat validation and cross-calibration activities	Page : 3 Date : April 19, 2007
Ref: CLS.DOS/NT/06.300	Nom.: SALP-RP-MA-EA-21376-CLS	Issue: 0rev1

3 Data used and processing

3.1 Data used

Envisat Geophysical Data Records (GDRs) from cycle 10 to cycle 51 have been used to derive the results presented in this report. This corresponds to a nearly four-year time period spanning from September 30th 2002 to October 9th 2005. The routine production started on September 2003 with cycle 15. In parallel, a backward reprocessing of cycles 14 to 9 was implemented. With only 7 days of available data, cycle 9 has not been used in this work. 11 GDR cycles have been produced this year: cycles 41 to 51 as part of the current processing.

The Envisat GDR data are generated using two softwares: the IPF, from Level0 to Level1B, and the CMA, from Level1B to Level2. As shown by table 1 several IPF processing chain and CMA Reference Software have been used to produce the 43 cycles of GDR. Tables 2 and 3 describe the main evolutions respectively associated with the IPF and CMA version. The change from IPF 4.54 to IPF 4.56 add an impact on the data. Consequently, from cycle 19 onwards and for the reprocessed cycles 10 to 14, the Automatic Gain Control (AGC) evaluation and the Intermediate Frequency (IF) mask correction (with slight impact on the data) have been modified.

Cycles	IPF version	CMA version
9 to 10	4.58	6.3
11 to 12	4.57	6.3
13 to 14	4.56	6.3
15 to 21	4.54	6.1
22 to 24	4.56	6.2
25 to 26	4.56	6.3
27 to 28	4.57	6.3
29 to 40	4.58	6.3
38 to 40 (reprocessed)	5.02	7.1
41 to 51 until pass 7	5.02	7.1
51	5.03	7.1

Table 1: Processing version

CLS CalVal Envisat	Envisat validation and cross-calibration activities	Page : 4 Date : April 19, 2007
Ref: CLS.DOS/NT/06.300	Nom.: SALP-RP-MA-EA-21376-CLS	Issue: 0rev1

Version	Changes
IPF 4.56	-Extrapolation of AGC value to the Waveform center (49.5) for both Ku- and S-Band -Correction for an error found in the evaluation of S band AGC
IPF 4.57	No impact on data
IPF 4.58	-Addition of a Pass Number Field in FD Level
IPF 5.02	-MWR Side Lobe correction upgrade -USO clock period units correction -Rain Flag tuning to compensate for the increase of the S band Sigma0 -Monthly IF estimation -DORIS Navigator CFI upgrade (RA-2 and MWR) -S-band anomaly flag
IPF 5.03	-Correction for an error found in the Channel 2 brightness temperature -Correction off error in the window delay (for the 80 and 20 MHz bandwidths) -S-band anomaly flag upgrade

Table 2: IPF versions

The change from IPF 4.58/CMA6.3 to IPF 5.02/CMA7.1 strongly impacted the data. The Sea-State bias table has been recomputed ([27]) accounting for the impact of the new orbit and the new geophysical corrections (MOG2D, GOT00 ocean tide correction with the S2 component corrected once only, new wind speed algorithm from Abdalla, 2006 [1]). The new SSB correction is shifted in average by +2.0 cm in comparison with the previous one. New standards are used for the computation of the Envisat Precise Orbit Estimation. One of the main evolutions is the use of the GRACE gravity model EIGEN CG03C. This new model implies a strong reduction of the geographically correlated radial orbit errors. In order to take into account the dynamical effects and wind forcing, a new correction is computed from the MOG2D (Carrere and Lyard, 2003 [4]) barotropic model forced by pressure (without S1 and S2 constituents) and wind. The use of such a correction in the SSH strongly improves the performances. All the corresponding evolutions are detailed in [14].

CLS CalVal Envisat	Envisat validation and cross-calibration activities	Page : 5 Date : April 19, 2007
Ref: CLS.DOS/NT/06.300	Nom.: SALP-RP-MA-EA-21376-CLS	Issue: 0rev1

Version	Changes
CMA 6	<ul style="list-style-type: none"> -MSS CLS01 -Rain flag -Updated OCOG retracker thresholds Ice1/Sea Ice Conf file -Sea State Bias Table file -GOT00.2 Ocean Tide Sol 1 Map file -FES 2002 Ocean Tide Sol 2 Map file -FES 2002 Tidal Loading Coeff Map
CMA 7.1	<ul style="list-style-type: none"> -Improving the mispointing estimation -Addition of square of the SWH in Ku and S band -Addition of GOT2000.2 loading tide -FES2004 tide and loading tide -New DEM AUX file (MACCESS) merge of ACE land elevation data and Smith and Sandwell ocean bathymetry -New orbit -New SSB -new wind table -Mog2D -new S1S2 wave model in dry troposphere -GOT00.2 includes two extra waves, S1 and S2 -GIM model ionospheric correction added in the products

Table 3: CMA versions

3.2 Processing

To perform this quality assessment work, conventional validation tools are used including editing procedures, crossover analysis, collinear differences, and a large number of statistical monitoring and visualization tools. All these tools are integrated and maintained as part of the CNES SSALTO (Segment Sol Altimétrie et Orbitographie) ground segment and F-PAC (French Processing and Archiving Centre) tools operated at CLS premises. Each cycle is carefully routinely analyzed before data release to end users. The main data quality features are reported in a cyclic quality assessment report available on http://www.avisioceanobs.com/html/donnees/calval/validation_report/en/welcome_uk.html. The purpose of this document is to report the major features of the data quality from the Envisat mission.

CLS CalVal Envisat	Envisat validation and cross-calibration activities	Page : 6 Date : April 19, 2007
Ref: CLS.DOS/NT/06.300	Nom.: SALP-RP-MA-EA-21376-CLS	Issue: 0rev1

As for all other existing altimeters, the Envisat GDR data are ingested in the Calval 1-Hz altimeter database maintained by the CLS Spatial Oceanography Division. This allows us to cross-calibrate and cross-compare Envisat data to other missions. In this study data from Jason-1 (GDRs cycles 27 to 174), ERS-2 (OPRs Cycle 78 to 108) are used. Jason-1 is the most suitable for Envisat cross calibration as it is available throughout the Envisat mission and has been extensively calibrated to T/P (Dorandeu et al., 2004b [11]).

Comparisons between Jason-1 and Envisat altimeter and radiometer parameters have been carried out using 10-day dual crossovers for SSH comparison and 3-hour dual crossovers for altimeter and radiometer comparisons. The geographical distribution of the dual crossovers with short time lags strongly changes from one Envisat cycle to another. Indeed, contrary to Envisat which is sun-synchronous, Jason-1 observes the same place at the same local time every 12 cycles (120-day). Following the method detailed in Stum et al. (1998) [51], estimates of the differences are computed using a 120 day running window to keep a constant geographical coverage. ERS-2, flying on same ground track as Envisat only 30 minutes apart, has had a coverage limited to the North Atlantic since the failure of the on-board register in June 2003 (EOHelp message of 4 July 2003). To improve the significance of the Envisat/ERS-2 comparison, long term monitoring of altimeter parameters difference is performed on this restricted area all over the Envisat period using a repeat-track method.

Most of this work has been carried out using parameters available in the GDR products. However, a few updates have been necessary to complete the analyses:

- a method has been developed to detect data corrupted by S-Band anomaly (see 4.3.1)
- a method has been developed to detect data corrupted by sea ice (see 4.3.2)
- filtered dual frequency ionosphere correction: A 300-km low pass filter is applied along track on the dual frequency ionosphere correction to reduce the noise of the correction.
- The new geophysical correction associated with version CMA7 have been updated on the whole dataset in order to have the most homogeneous time series: wind table and SSB, Mog2D, new S1S2 wave model in dry troposphere, GOT00.2 with two extra waves, FES2004, S1 and S2
- A correction to the range is also applied. It is based on the Ultra-Stable Oscillator (USO) clock period variation correction depending on the cycle (see Figure 1):

For cycle 9 to 40, outside of the anomaly periods: The USO clock period, which performs the computation of the Ra-2 window time delay, is affected by a drift due to the ageing of the device. The method to correct the USO clock period is described in Celani (2002 [6]). The correction is regularly updated in the IPF ground processing via an Auxiliary data file. However, due to an anomaly in the ADF format, the correction was not taken into account (Martini, 2003 [36]) in the products for cycles lower or equal 40. ESA supplies auxiliary files to allow users correcting their own database (Martini, 2003 [36]) (<http://earth.esa.int/pcs/envisat/ra2/auxdata/>). The distributed auxiliary correction containing the drift + bias have to be used. The distributed auxiliary correction is smoothed here over a 1-month period to filter peaks and short period variations. The supplied correction has to be subtracted from the original altimetric range (EOP-GOQ and PCF team, 2005) and consequently added to SSH

For cycle 41 to 45, outside of the anomaly periods: The USO drift + bias is taken into account in the products. No additional auxiliary correction has to be used.

CLS CalVal Envisat	Envisat validation and cross-calibration activities	Page : 7 Date : April 19, 2007
Ref: CLS.DOS/NT/06.300	Nom.: SALP-RP-MA-EA-21376-CLS	Issue: 0rev1

Chronology of the USO Correction Computation

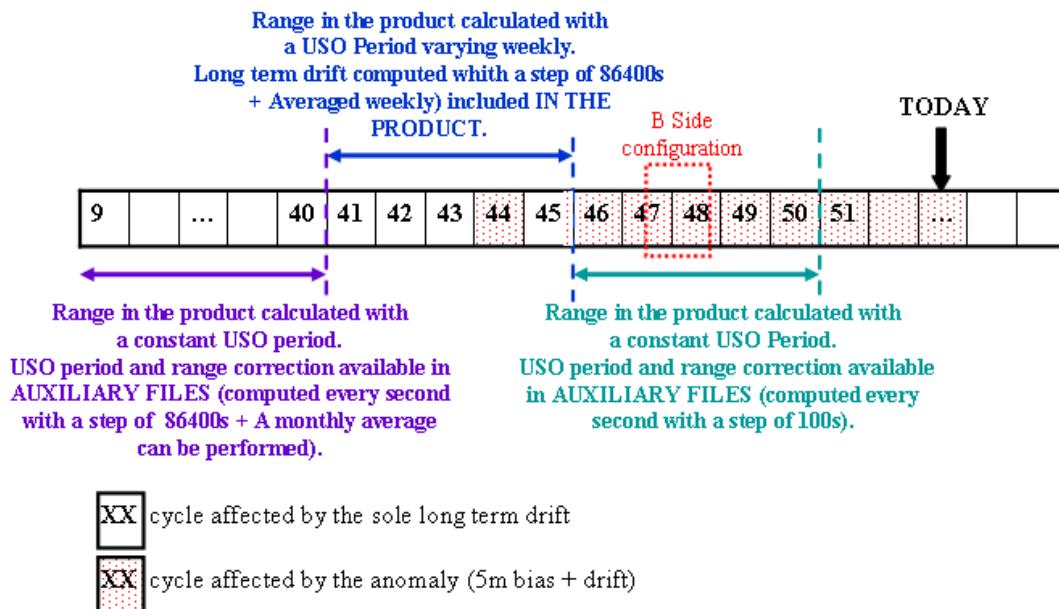


Figure 1: *Chronology of USO Correction computation.*

For cycle 46 onwards, and all the anomaly periods: On the 1st of February 2006 (12:05:36), at the end of cycle 44, for an unknown reason a change of behaviour of the USO device occurred. This anomaly creates a 5.5m jump on the range parameter and oscillations of about 20-30cm of amplitude at the orbital period. The anomaly becomes permanent on cycle 46. The anomaly and associated correction is detailed in 8.1. The quality assessment of these data has been done using the USO temporary correction provided by ESA. Users are strongly advised not to use the range parameter in Ku and S Band without this correction during the anomaly periods.

- pressure values used for computing the inverse barometer and the dry troposphere corrections have been derived from the ECMWF rectangular grids. Indeed, errors due to the bathymetry, up to several centimeters near the coasts, significantly impact the accuracy the so-called gaussian grids used as input of the Envisat (and Jason-1) ground processing (e.g. Dorandeu et al., 2004b [11]).
- Jason-1 doesn't fly at the same altitude as Envisat which means that ionosphere corrections are not comparable (note that this has no impact on the other parameters (wind, waves, ...). Moreover, ERS-2 has a mono-frequency altimeter on-board. Therefore it is not possible to use these satellites to assess the Envisat ionosphere path delay. Thus the JPL GPS-based global Ionospheric Maps (GIM) containing the vertical ionospheric total electron content are used here. Note that since cycle 41 onwards, this GIM ionosphere correction is available in the GDR products. Note that GIM maps contain the vertical ionospheric total electron content in the 0-1400km altitude range. As Envisat flies around 800km, the International Reference Ionosphere (IRI) model is used to estimate the GIM correction at the altitude

CLS CalVal Envisat	Envisat validation and cross-calibration activities	Page : 8 Date : April 19, 2007
Ref: CLS.DOS/NT/06.300	Nom.: SALP-RP-MA-EA-21376-CLS	Issue: 0rev1

of Envisat:

GIM[0-800]=GIM[0-1400].IRI[800]/IRI[1400]

CLS CalVal Envisat	Envisat validation and cross-calibration activities	Page : 9 Date : April 19, 2007
Ref: CLS.DOS/NT/06.300	Nom.: SALP-RP-MA-EA-21376-CLS	Issue: 0rev1

4 Missing and edited measurements

This section mainly intends to analyse the ability of the Envisat altimeter system to correctly sample ocean surfaces. This obviously includes the tracking capabilities, but also the frequency of unavailable data and the ratio of valid measurements likely to be used by applications after the editing process.

4.1 Missing measurements

From a theoretical ground track, a dedicated collocation tool allows determination of missing measurements relative to what is nominally expected. The cycle by cycle percentage of missing measurements over ocean has been plotted in figure 2. The measurement unavailability is more than 9% in average. Ten cycles have more than 10% of unavailability, notably from cycle 13 to cycle 17, and cycle 47 to cycle 48. Passes 1 to 452 of cycle 15 have not been delivered because of a wrong setting of RA-2. Moreover, passes 1 to 790 of cycle 47 and passes 1 to 849 of cycle 48 have not been delivered due to RA2 RFSS configured to side B redundancy. This explains the high ratio of missing measurements for these cycles. Several long RA-2 events occurred during cycles 13, 14, 16, 17, 22, 34 and 51 which resulted in a significant number of missing passes. The significant missing data for cycle 51 is due to an interruption of the Envisat data transmission via the ESA Data Relay Satellite Artemis and a platform incident. The list of instrument and platform events is available in Part 11. Apart from instrumental and platform events, up to 3% of measurements can be missing because of data generation problems at ground segment level: LRAC or PDHS level1 data generation problems or ingestion problems on F-PAC side. Notice however that the situation has been largely improved with a mean data availability of more than 95% from the beginning of 2004 (cycle 23 onwards). Figure 3 shows an example of missing measurements for cycle 50. The measurements which are missing over the Himalayan region are due first to the IF Calibration Mode. Moreover, daily instrument switch-offs (Heater 2 mode) are performed over this region to prevent the S-Band anomaly. Finally, it has been found that some pass segments were quasi-systematically missing. Figure 4 shows the pass segments missing more than 5 times over the 10 last cycles. Apart from that, the data retention rate is very good on every surface observed. This might be due to the tracker used by Envisat Ra-2, the Model Free Tracker (MFT).

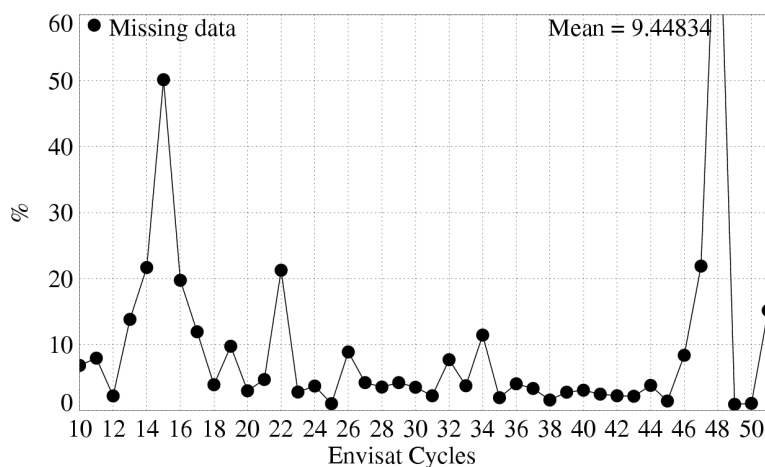


Figure 2: Monitoring of the percentage of missing measurements relative to what is theoretically expected over ocean

<p>CLS CalVal Envisat</p>	<p>Envisat validation and cross-calibration activities</p>	<p>Page : 10 Date : April 19, 2007</p>
<p>Ref: CLS.DOS/NT/06.300</p>	<p>Nom.: SALP-RP-MA-EA-21376-CLS</p>	<p>Issue: 0rev1</p>

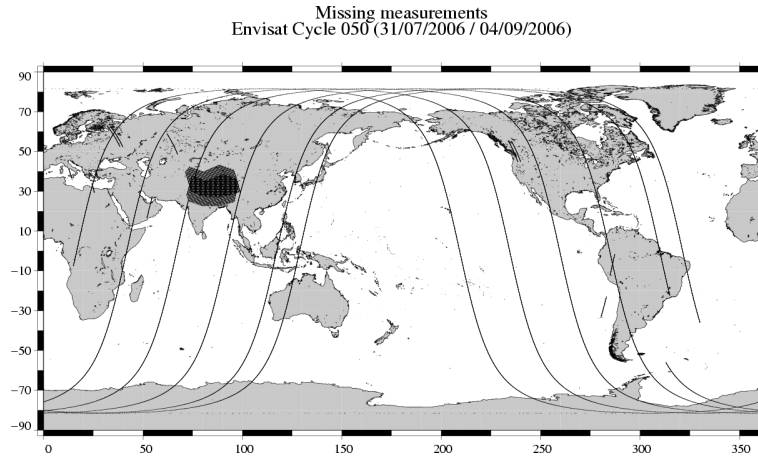


Figure 3: *Envisat missing measurements for cycle 50*

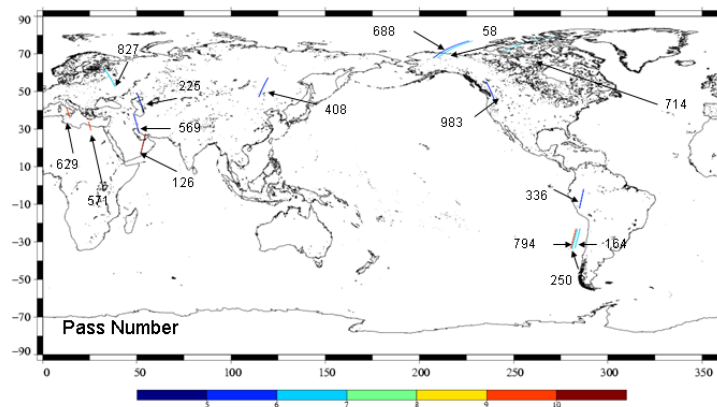


Figure 4: *Pass segments unavailable more than 5 times between cycles 41 and 51. The numbers on the map indicate the pass number. The colour indicates the occurrence of unavailability*

4.2 Missing MWR data

The Envisat MWR exhibits nearly 100% (Dedieu et al., 2005) of availability since the beginning of the mission. However, MWR corrections can be missing in the GDRs due to data generation problems at ground segment level. When the Land/sea radiometer flag is set to land over ocean, it means that the radiometer data is missing. The percentage of missing MWR corrections over ocean has been plotted in figure 5. The mean value is around 2.6% but the radiometer unavailability is not constant. It is greater than 4% for cycles 14 to 19 but lower than 2% from cycle 21 onwards. From cycle 34 onwards the availability of the MWR correction is very good.

CLS CalVal Envisat	Envisat validation and cross-calibration activities	Page : 11 Date : April 19, 2007
Ref: CLS.DOS/NT/06.300	Nom.: SALP-RP-MA-EA-21376-CLS	Issue: 0rev1

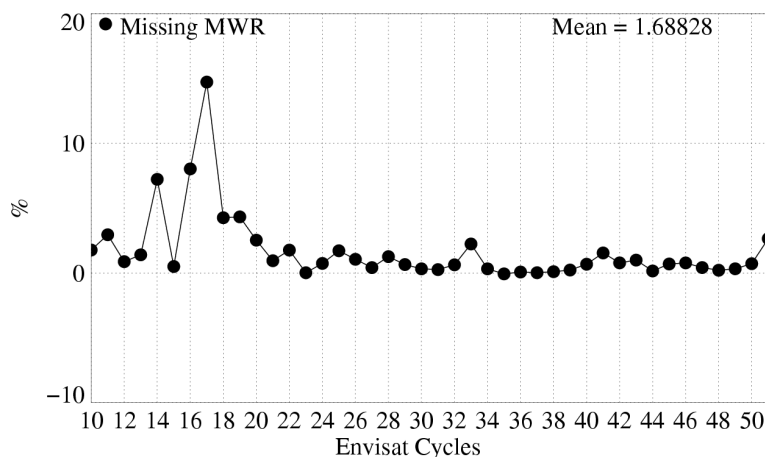


Figure 5: *Cycle per cycle percentages of missing MWR measurements*

4.3 Edited measurements

Data editing is necessary to remove altimeter measurements having lower accuracy. There are 4 steps in the editing procedure. The first step of the editing procedure consists in removing data impacted by the S-Band anomaly or corrupted by sea ice. Then, measurements are edited using thresholds on several parameters. The third step uses cubic splines adjustments to the ENVISAT Sea Surface Height (SSH) to detect remaining spurious measurements. The last step consists in removing entire pass where SSH-MSS mean and standard deviation have unexpected value.

4.3.1 Measurements impacted by S-Band anomaly

During the Commissioning Phase, it has been discovered that the RA-2 data are affected by the so-called S-Band anomaly. The anomaly results in the accumulation of the S-Band echo waveforms (Laxon and Roca, 2002 [29]). It happens randomly after an acquisition sequence and is only stopped by switching the Ra-2 in a Stand-By mode. When this anomaly occurs, the S-Band waveforms are not meaningful. Consequently, all the S-Band parameters and the Dual Frequency ionosphere correction are not reliable. Notably, the S-band Sigma0 is unrealistically high during these events. Thus applying a threshold of 5 dB on the (Ku-S) Sigma0 differences is very efficient for detecting the impacted data over ocean. The ratio of flagged measurements over ocean is plotted in figure 6. Between 0 and 8% of the data are impacted. From cycle 31 onwards, some modifications have been performed by ESA to decrease the duration of these events: instrument switch-offs (Heater 2 mode) are performed twice a day over the Himalayan region. This prevents the S-Band anomaly from lasting more than half a day when it occurs. Thanks to this procedure the ratio of impacted data decreased from 4.2% (cycles 11 to 30) to 2.2% (cycles 31 to 38). A method has been developed to flag the impacted data over all surfaces (Martini et al., 2005 [37]). This method has been implemented in IPF5.02 with an anomaly which has been fixed on IPF5.03. The reconstruction of normal echoes from accumulated waveforms (Martini et al., 2005 [37]) is currently under study.

4.3.2 Measurements impacted by Sea Ice

CLS CalVal Envisat	Envisat validation and cross-calibration activities	Page : 12 Date : April 19, 2007
Ref: CLS.DOS/NT/06.300	Nom.: SALP-RP-MA-EA-21376-CLS	Issue: 0rev1

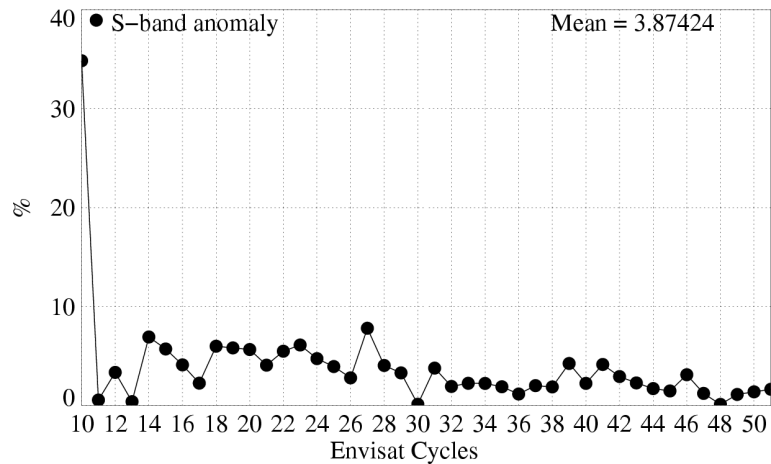


Figure 6: *Cycle per cycle percentages of data impacted by the S-Band anomaly*

Since Envisat operates between 82N and 82S of latitude, sea ice is an important issue for oceanic applications. No ice flag is currently available in the Envisat products, therefore alternate sea ice detection techniques are employed in order to retain only open ocean data. A study performed during the validation phase showed that the combination of altimetric and radiometric criteria was particularly efficient to flag most of the data over ice. The method is described in detail in (Faugere et al, 2003 [18]). We employ the Peakiness parameter (Lillibrige et al, 2005 [33]) in conjunction with the MWR- ECMWF wet troposphere difference which appears to be a good means to complement the Peakiness parameter in all ice conditions. The ratio of flagged measurements over ocean is plotted on 7

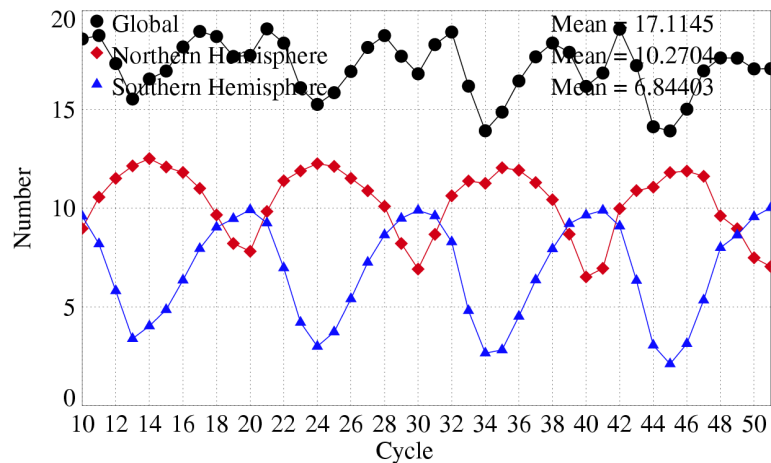


Figure 7: *% of edited points by sea ice flag over ocean*

4.3.3 Editing by thresholds

The second step of the editing procedure consists in using thresholds on several parameters. The minimum and maximum thresholds used in the routine quality assessment are given in table 4.

CLS CalVal Envisat	Envisat validation and cross-calibration activities	Page : 13 Date : April 19, 2007
Ref: CLS.DOS/NT/06.300	Nom.: SALP-RP-MA-EA-21376-CLS	Issue: 0rev1

Parameter	Min thresholds	Max thresholds
Sea surface height (m)	-130	100
Variability relative to MSS (m)	-2	2
Number of 18Hz valid points	10	-
Std deviation of 18Hz range (m)	0	0.25
Off nadir angle from waveform (deg ²)	-0.200	0.160
Dry troposphere correction (m)	-2.500	-1.900
Inverted barometer correction (m)	-2.000	2.000
MWR wet troposphere correction (m)	-0.500	0.001
Dual Ionosphere correction (m)	-0.200	-0.001
Significant waveheight (m)	0.0	11.0
Sea State Bias (m)	-0.5	0
Backscatter coefficient (dB)	7	30
Ocean tide height (m)	-5	5
Long period tide height (m)	-0.500	0.500
Earth tide (m)	-1.000	1.000
Pole tide (m)	-5.000	5.000
RA2 wind speed (m/s)	0.000	30.000

Table 4: *Editing criteria*

The thresholds are expected to remain constant throughout the ENVISAT mission, so that monitoring the number of edited measurements allows a survey of data quality. The percentage of edited measurements over ocean for the main altimeter and radiometer parameters has been plotted in figure 8. These ratios are very stable and surprisingly low over the period if compared to other altimeters. The RMS of elementary measurements has the strongest ratio among the altimeter parameters, more than 1% in average. On cycle 47, a special operation was executed to limit RA-2 Chirp Bandwidth to 80MHz. It has impacted this parameter as well as the dual frequency ratio. A slight seasonal signal is visible on the curve, mostly due to sea state seasonal variations. The number of elementary measurements has a surprisingly low ratio, except for cycles 14 and 20 when wrong configuration files were uploaded onboard after a RA-2 event. The square of the off-nadir angle derived from waveforms leads to very stable editing ratio but with a drop on cycle 41, due to a change of the algorithm in CMA7.1. Variations of this parameter can reveal actual platform mispointing, if any, but can also reveal waveform contamination by rain or by sea-ice. It is indeed computed from the slope of trailing edge when fitting a typical ocean model to the waveforms. No seasonal signal is visible which may prove that the sea-ice detection method is efficient. The dual frequency ratio shows a slight increasing trend between cycles 15 and 28 which cannot be considered as significant, given the scatter of the curve. The Ku-band SWH, sigma0 and MWR ratios are very stable and low, less than 0.2% with no seasonal variations.

<p style="text-align: center;">CLS CalVal Envisat</p>	<p style="text-align: center;">Envisat validation and cross-calibration activities</p>	<p>Page : 14 Date : April 19, 2007</p>
<p>Ref: CLS.DOS/NT/06.300</p>	<p>Nom.: SALP-RP-MA-EA-21376-CLS</p>	<p>Issue: 0rev1</p>

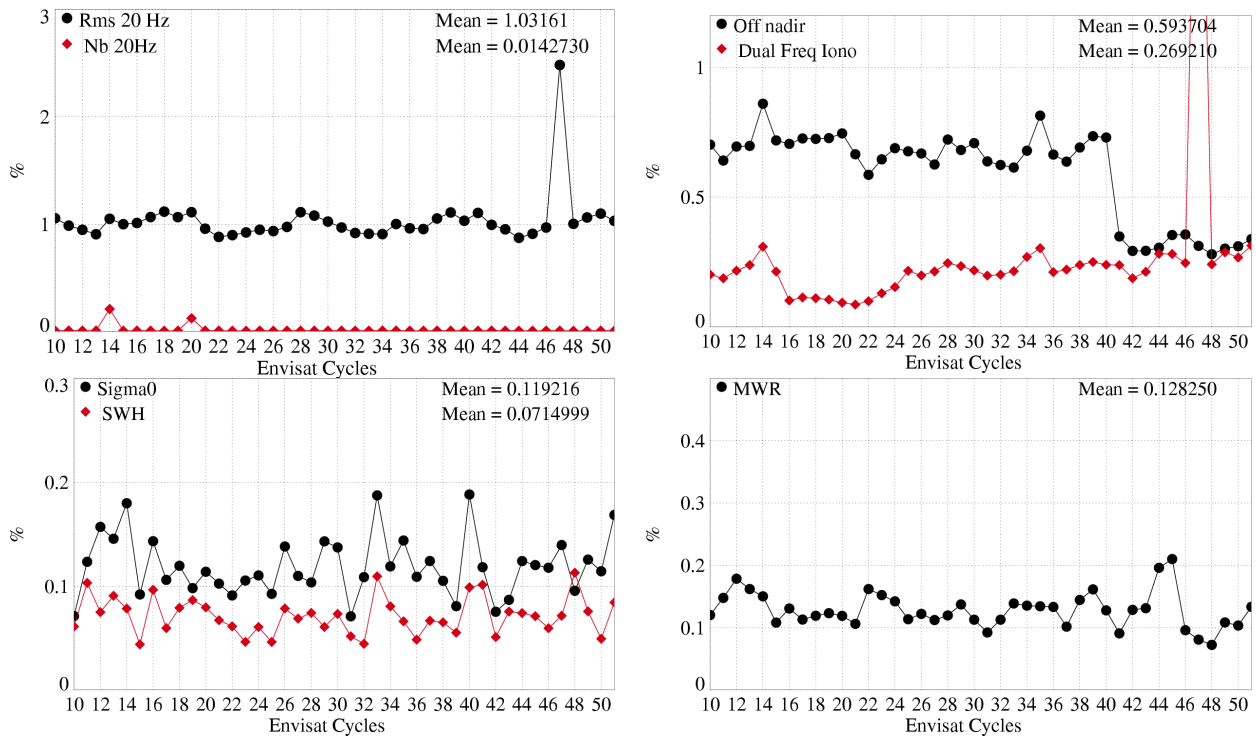


Figure 8: Cycle per cycle percentages of edited measurements by the main Envisat altimeter and radiometer parameters: top-left) Standard deviation of 20 Hz range measurements > 25 cm, Number of 20-Hz range measurements < 10 top-right) Square of off-nadir angle (from waveforms) out of the $[-0.2 \text{ deg}^2, 0.16 \text{ deg}^2]$ range, dual frequency ionosphere correction out of $[-40, 4 \text{ cm}]$ bot-left) Ku-band Significant wave height outside > 11 m, Ku band backscatter coefficient out of the $[7 \text{ dB}, 30 \text{ dB}]$ range bot-right) MWR wet troposphere correction out of the $[-50 \text{ cm}, -0.1 \text{ cm}]$ range.

CLS CalVal Envisat	Envisat validation and cross-calibration activities	Page : 15 Date : April 19, 2007
Ref: CLS.DOS/NT/06.300	Nom.: SALP-RP-MA-EA-21376-CLS	Issue: 0rev1

4.3.4 Editing on SLA

It has been necessary to apply additional editing criteria on SSH-MSS differences in order to remove remaining spurious data. The first criterion consists in removing measurements with SSH-MSS greater than 2m. The strong value on cycle 30 is due to the first occurrence of the USO anomaly. The second criterion was necessary to detect measurements impacted by maneuvers. Maneuvers are necessary to compensate the effect of gravitational forces but can have a strong impact on the orbit quality. Two types of maneuvers are operated to maintain the satellite ground track within the +/-1km deadband around the reference ground track: in-plane maneuvers, every 30-50 days, which only impact the altitude of the satellite and out-of-plane maneuvers, three times a year, to control the inclination of the satellite (Rudolph et al., 2005). The out-of-plane maneuvers are the most problematic for the orbit computation. The second criterion consists in testing the mean and standard deviation of the SSH-MSS over each entire pass. If one of the two values, computed on a selected dataset, is abnormally high, then the entire pass is edited.

A specific study has been performed to determine how to compute the statistics, and what threshold should be applied. The statistics have to be computed on very stable area. The criteria for selecting the area and the thresholds are detailed is:

- The latitude: the range value can be degraded near the ice, despite the use of the ice flag. Moreover, the MSS is less accurate over 66°, as it has been computed without Topex data.
- The oceanic variability: the standard deviation of SLA can be very high because of the mesoscale variability. Areas with high oceanic variability have to be removed to detect the abnormally high standard deviation.
- The bathymetry and distance from the coast: A lot of corrections (tides for example) are less accurate in low bathymetry areas and near the coast (Japan sea).
- The sample: The statistic have to be computed on a significant number of points

All those criteria have been tested and combined. The results are in Annex. The conclusion is that two criteria are needed:

1st criteria: for small portion of pass (less than 200 points) the sample is not big enough to compute reliable statistic. The selection must not be severe:

Selected areas: latitude > 66°, variability < 30cm, bathymetry > 1000m, distance < 100km

Threshold: 30 cm on mean and standard deviation

2nd criteria: for other passes

Selected areas: latitude > 66°, variability < 10cm, bathymetry > 1000m, distance < 100km

Threshold: 15 cm on mean and standard deviation

The percentage of edited measurements over ocean for the main altimeter and radiometer parameters has been plotted in figure 9. On cycles 11, 12, 21 and 26, several full passes have been edited because of bad orbit quality related to out-of-plane manoeuvre or lack of Doris data (cycle 11). The special operation on RA-2 Chirp Bandwidth mentioned previously impacted the SSH editing ratio on cycle 47.

<p style="text-align: center;">CLS CalVal Envisat</p>	<p style="text-align: center;">Envisat validation and cross-calibration activities</p>	<p>Page : 16 Date : April 19, 2007</p>
<p>Ref: CLS.DOS/NT/06.300</p>	<p>Nom.: SALP-RP-MA-EA-21376-CLS</p>	<p>Issue: 0rev1</p>

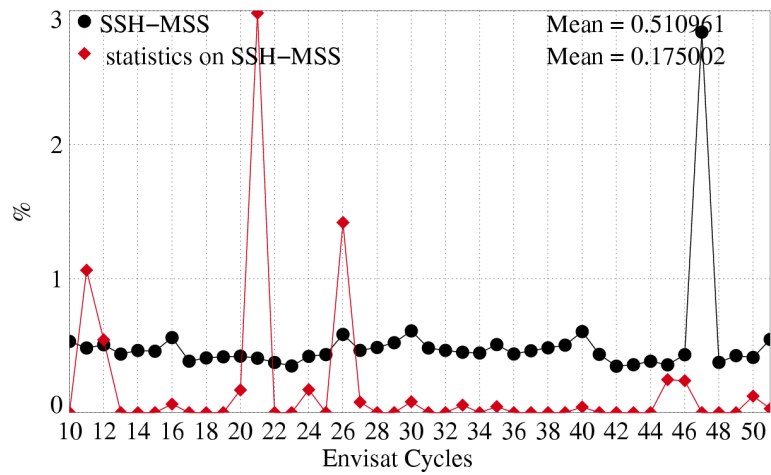


Figure 9: *SSH-MSS out of the $[-2, 2m]$ and edited using thresholds on the mean and standard deviation of SSH-MSS on each pass*

CLS CalVal Envisat	Envisat validation and cross-calibration activities	Page : 17 Date : April 19, 2007
Ref: CLS.DOS/NT/06.300	Nom.: SALP-RP-MA-EA-21376-CLS	Issue: 0rev1

5 Long term monitoring of altimeter and radiometer parameters

All GDR fields are systematically checked and carefully monitored as part of the Envisat routine calibration and validation tasks. However, only the main Ku-band parameters are presented here, as they are the most significant in terms of data quality and instrumental stability. Furthermore, all statistics are computed on valid ocean datasets after the editing procedure.

5.1 Number and standard deviation of 20Hz elementary Ku-band measurements

As part of the ground segment processing, a regression is performed to derive the 1 Hz range from 20 Hz data. Through an iterative regression process, elementary ranges too far from the regression line are discarded until convergence is reached. The mean number and RMS of Ku 20Hz elementary data used to compute the 1Hz average are plotted in figure 10. These two parameters are nearly constant, which provides an indication of the RA-2 altimeter stability. The mean number of Ku 20Hz values over one cycle is about 19.97. This value is very high compared to other altimeters. It is almost not disturbed in wet areas or near the coast. The two drops on the Ku-band on cycles 14 and 20 are due to wrong setting of the RA-2 just after recovery. A slight seasonal signal is visible on the mean RMS of Ku 20Hz. Higher values correspond to higher waves occurring during the austral winter. The mean value is about 9.0 cm. This value represents a rough estimation of the 20 Hz altimeter noise (Zanifé et al. 2003, Vincent et al. 2003a). Assuming that the 20Hz measurements have uncorrelated noise, it corresponds to a noise of about 2 cm at 1Hz. It is consistent with the expected noise values.

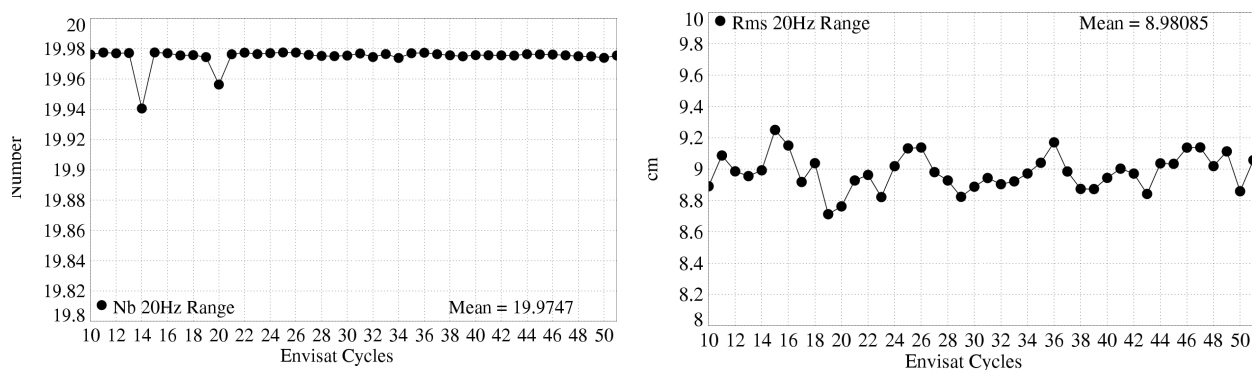


Figure 10: left) Cycle mean of the number of 20 Hz elementary range measurements used to compute 1 Hz range. right) Cycle mean of the standard deviation of 20 Hz measurements.

Histograms of RMS of Ku and S-band Range on cycle 51 are plotted in figure 11.

CLS CalVal Envisat	Envisat validation and cross-calibration activities	Page : 18 Date : April 19, 2007
Ref: CLS.DOS/NT/06.300	Nom.: SALP-RP-MA-EA-21376-CLS	Issue: 0rev1

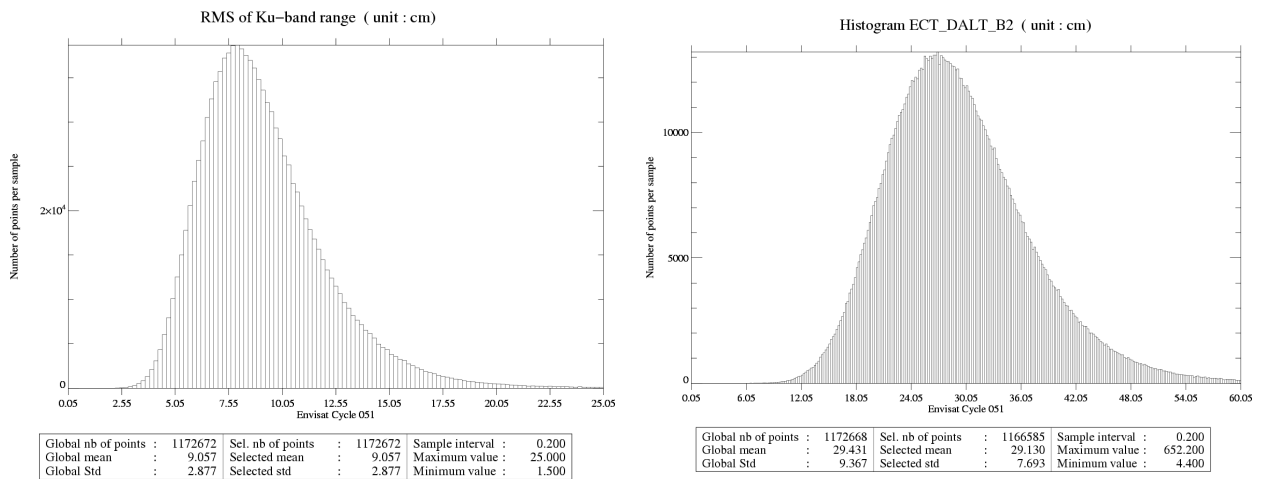


Figure 11: *Histogram of RMS of Ku and S range (cm)*

CLS CalVal Envisat	Envisat validation and cross-calibration activities	Page : 19 Date : April 19, 2007
Ref: CLS.DOS/NT/06.300	Nom.: SALP-RP-MA-EA-21376-CLS	Issue: 0rev1

5.2 Off-nadir angle from waveforms

The off-nadir angle is estimated from the waveform shape during the altimeter processing. The square of the off-nadir angle is plotted in figure 12. The mean value is between 0.02 deg² and 0.03deg² before cycle 41. There is a slight rising trend over this period and a 0.005 deg² jump between cycles 21 and 22 which is due to the upgrade of the IF mask filter auxiliary data file. The mean value observed during this period is not significant in terms of actual platform mispointing. This is due to the way the slope of the waveform trailing edge is computed. On cycle 41, a 0.02 deg² drop occurs, due to an improvement of the mispointing estimation in IPF 5.02. The mispointing was estimated through the waveform trailing edge slope using an adaptative window that defines the beginning and the end of the slope. To avoid the filter bump effect that leads to high value of the mispointing, an optimum and fixed gate was estimated and implemented. Note that the rising trend observed previously disappeared. This is probably an effect of the regular update of the IF filter since cycle 41.

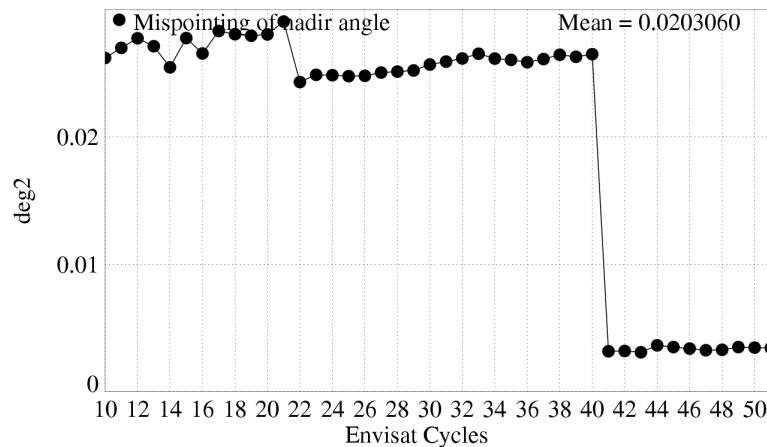


Figure 12: Cycle mean of the square of the off-nadir angle deduced from waveforms (deg²).

The histogram of the squared mispointing is plotted in figure 13.

<p style="text-align: center;">CLS CalVal Envisat</p>	<p style="text-align: center;">Envisat validation and cross-calibration activities</p>	<p>Page : 20 Date : April 19, 2007</p>
<p>Ref: CLS.DOS/NT/06.300</p>	<p>Nom.: SALP-RP-MA-EA-21376-CLS</p>	<p>Issue: 0rev1</p>

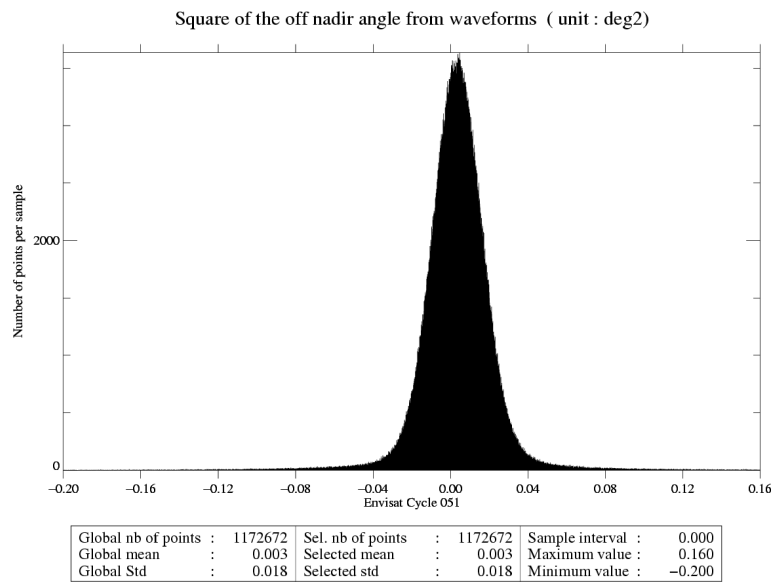


Figure 13: *Histogram of off-nadir angle from waveforms (deg²)*

CLS CalVal Envisat	Envisat validation and cross-calibration activities	Page : 21 Date : April 19, 2007
Ref: CLS.DOS/NT/06.300	Nom.: SALP-RP-MA-EA-21376-CLS	Issue: 0rev1

5.3 Significant Wave Height

The cycle by cycle mean and standard deviation of Ku and S-band SWH are plotted in figure 14. The curve reflects sea state variations. The mean value of Ku SWH is 2.66 m. The S-band mean SWH is very close, less than 10 cm apart. The cycle by cycle mean of Envisat-Jason-1 differences and ERS-2-Envisat differences are plotted in figure 14. These differences are quite stable. Envisat SWH is respectively 15 cm and 22 cm higher than Jason-1 and ERS-2 SWH.

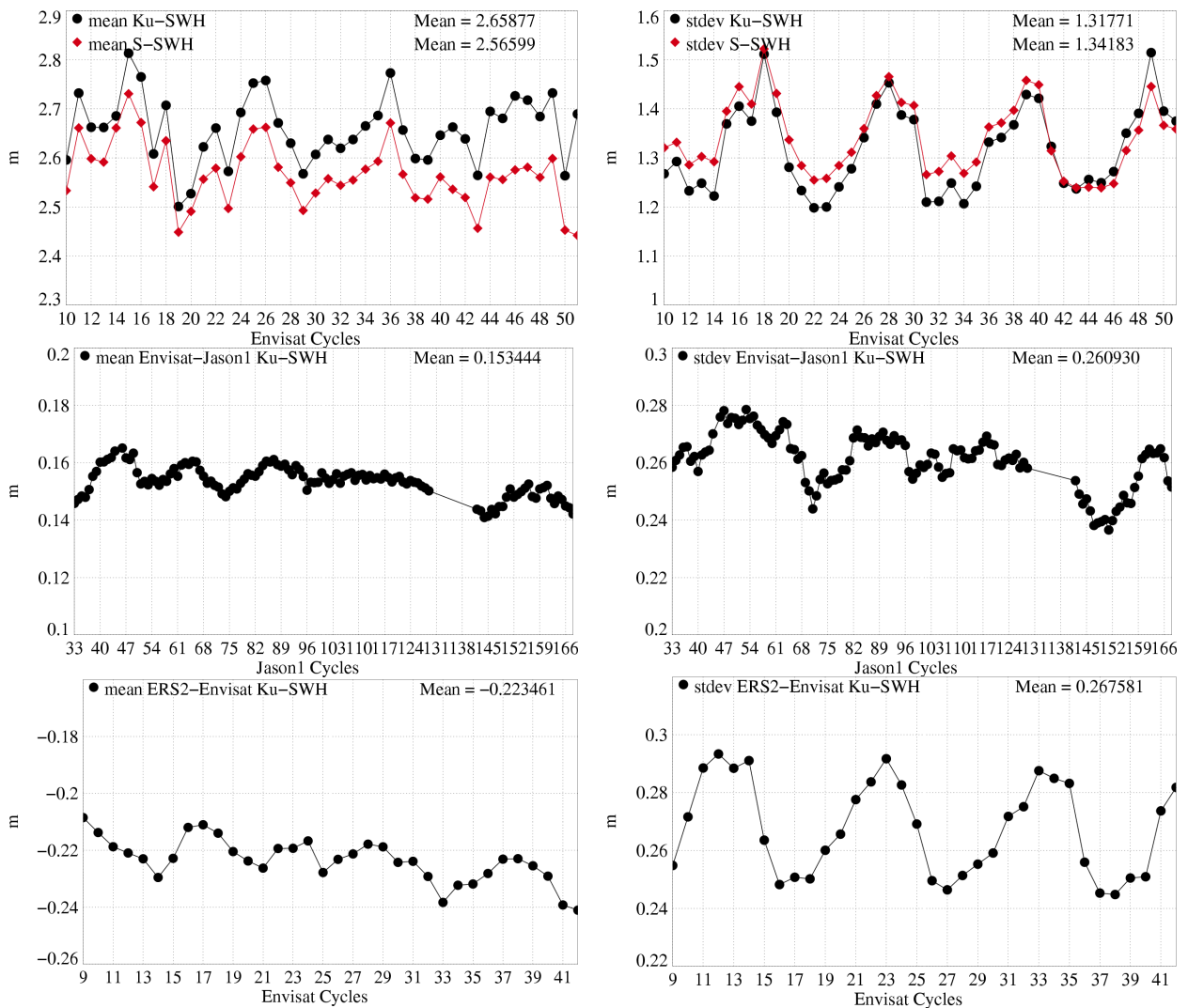


Figure 14: Global statistics (m) of Envisat Ku and S SWH top-right) Mean and top-left) Standard deviation. bot-right) Mean Envisat-Jason-1 Ku SWH differences at 3h EN/J1 crossovers computed with 120 days running means. bot-left) Mean. ERS-2-Envisat Ku SWH collinear differences over the Atlantic Ocean.

Histograms of Ku and S-band SWH are plotted in figure 15. The Ku SWH histogram has a good shape.

CLS CalVal Envisat	Envisat validation and cross-calibration activities	Page : 22 Date : April 19, 2007
Ref: CLS.DOS/NT/06.300	Nom.: SALP-RP-MA-EA-21376-CLS	Issue: 0rev1

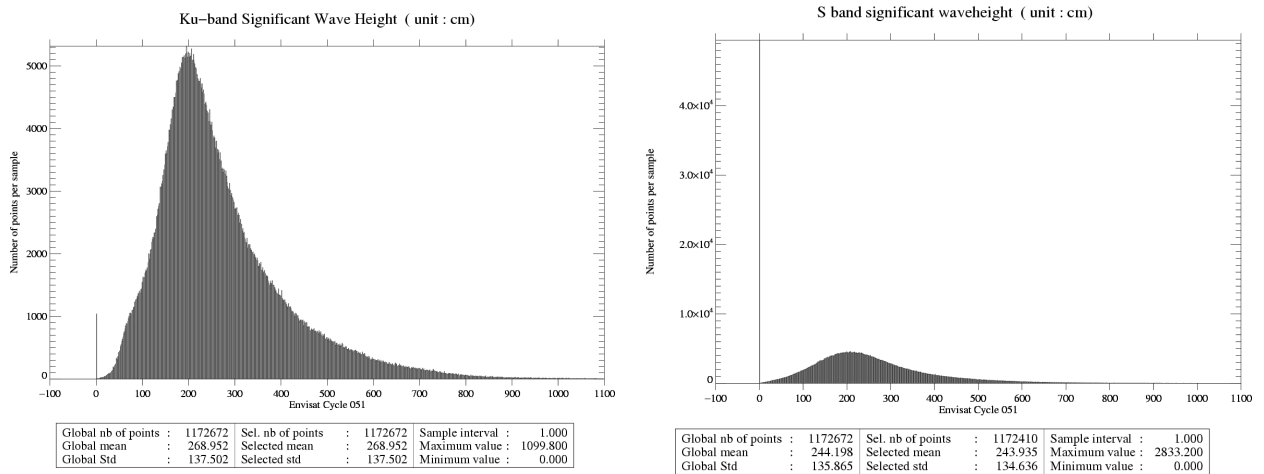


Figure 15: *Histogram of Ku and S SWH (m)*

CLS CalVal Envisat	Envisat validation and cross-calibration activities	Page : 23 Date : April 19, 2007
Ref: CLS.DOS/NT/06.300	Nom.: SALP-RP-MA-EA-21376-CLS	Issue: 0rev1

5.4 Backscatter coefficient

The cycle by cycle mean and standard deviation Ku and S-band Sigma0 are plotted in figure 16. Note that a -3.5 dB bias has been applied (Roca et al., 2003 [44]) on the Ku-band Sigma0 in order to be compliant with the wind speed model (Witter and Chelton, 1991 [56]). The mean values in Ku band are stable, around 11.1 dB. Two 0.66 dB jumps are visible on the S-Band on cycles 14 and 22. They are due to a correction of the AGC evaluation. This modification has been included in IPF version 4.56, used from cycle 22 onwards for the current processing and for all the reprocessed cycles. The cycle by cycle mean of Envisat-Jason-1 differences and ERS-2-Envisat differences are plotted in figure 16. The mean difference between Envisat and Jason-1 Ku-band Sigma0 is -2.9 dB. This high value is explained by the fact that, Envisat Sigma0 value has been biased and not Jason-1. This mean difference has increased by 0.07dB between cycles 48 and 118 which corresponds to 0.04 dB/year. From cycle 136 onwards, a new retracking algorithm (MLE4) has been implemented on Jason-1. This change induced a -0.08dB drop on the [Envisat-Jason-1] difference. Moreover a decreasing trend is visible after the jump. This trend, though not really significant, has to be monitored in the next cycles. The mean ERS-2-Envisat Ku-band Sigma0 difference is 0.05 dB. However, this mean value accounts for the calibration correction applied in the ground processing to be compliant with the wind speed algorithm (Witter and Chelton, 1991 [56]). The monitoring of (ERS-2 - Envisat) Sigma0 differences exhibits a 0.1 dB jump between cycles 38 and 39. This jump occurs at the end of cycle 38, on the 4th July 2005 11:29 UTC. Since no jump is observed on the Envisat/Jason-1 differences, it may be attributed to ERS-2. This jump is still under investigation.

Histograms of Ku and S-band Sigma0 are plotted in figure 17. The Ku Sigma0 histogram has a good shape.

<p align="center">CLS CalVal Envisat</p>	<p align="center">Envisat validation and cross-calibration activities</p>	<p>Page : 24 Date : April 19, 2007</p>
<p>Ref: CLS.DOS/NT/06.300</p>	<p>Nom.: SALP-RP-MA-EA-21376-CLS</p>	<p>Issue: 0rev1</p>

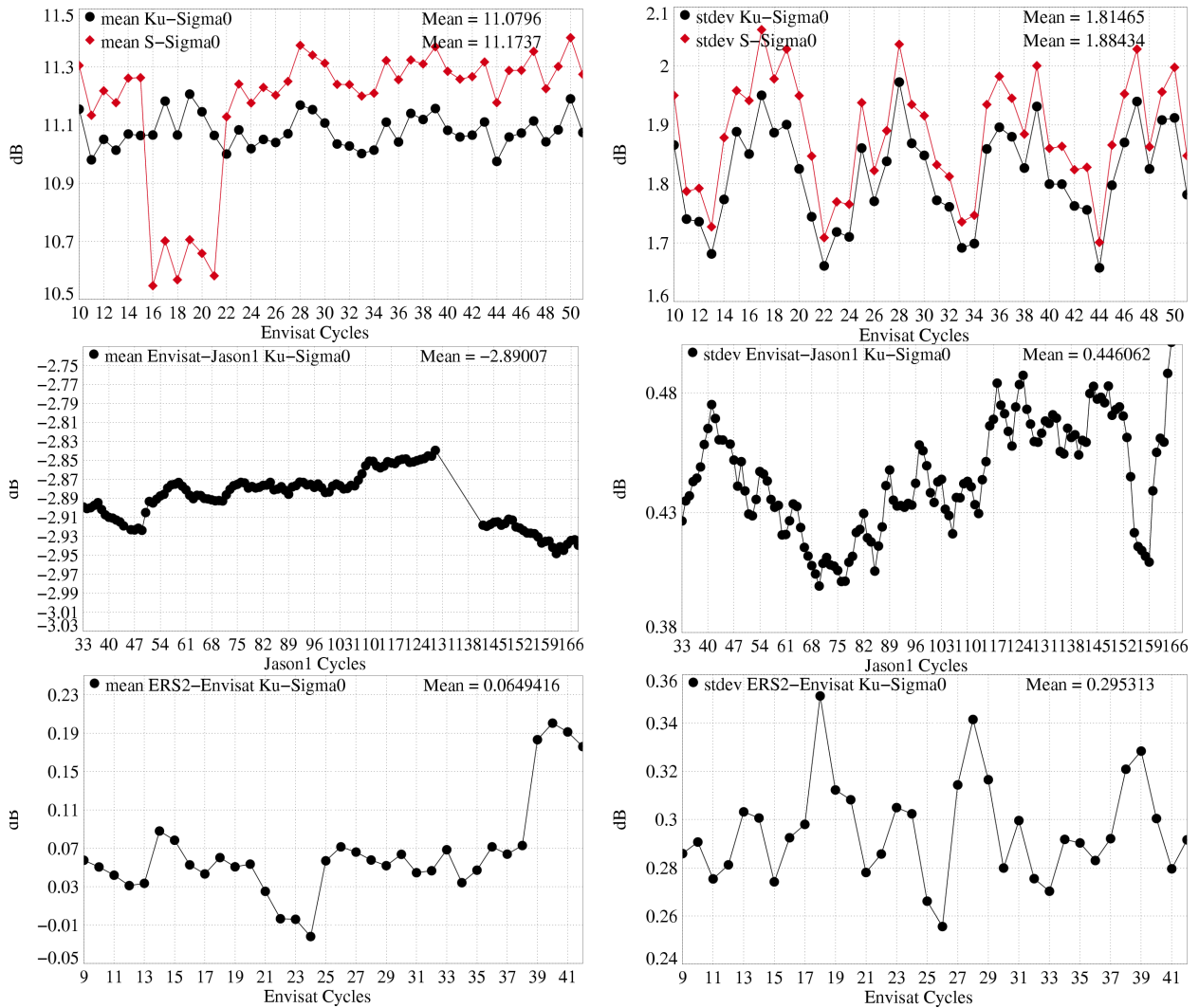


Figure 16: Global statistics (dB) of top) Envisat Ku and S Sigma0 Mean and Standard deviation. middle) Mean Envisat-Jason-1 Ku Sigma0 differences at 3h EN/J1 crossovers computed with 120 days running means. bottom) Mean and Standard of ERS-2-Envisat Ku Sigma0 collinear differences over the Atlantic Ocean.

CLS CalVal Envisat	Envisat validation and cross-calibration activities	Page : 25 Date : April 19, 2007
Ref: CLS.DOS/NT/06.300	Nom.: SALP-RP-MA-EA-21376-CLS	Issue: 0rev1

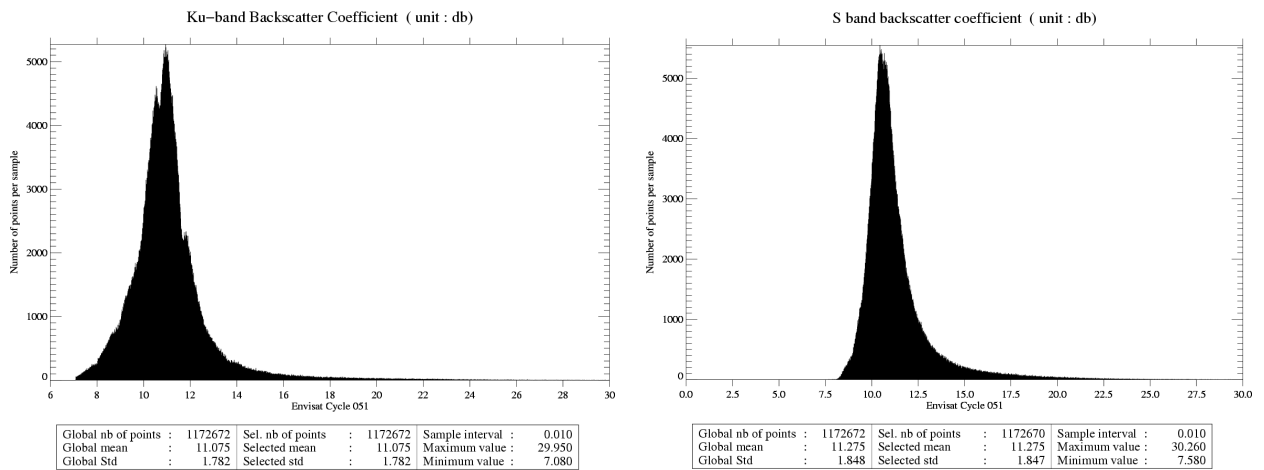


Figure 17: *Histogram of Ku and S Sigma0 (dB)*

CLS CalVal Envisat	Envisat validation and cross-calibration activities	Page : 26 Date : April 19, 2007
Ref: CLS.DOS/NT/06.300	Nom.: SALP-RP-MA-EA-21376-CLS	Issue: 0rev1

5.5 Dual frequency ionosphere correction

As performed on TOPEX (Le Traon et al. 1994 [30]) and Jason-1 (Chambers et al. 2002 [7]) it is recommended to filter dual frequency ionosphere correction on each altimeter dataset to reduce noise. A 300-km low pass filter is thus applied along track on the dual frequency ionosphere correction. As previously mentioned, the JPL GIM ionosphere corrections are computed to assess the dual frequency altimeter based ionosphere correction. The cycle by cycle mean of dual frequency and JPL GIM ionosphere correction are plotted in figure 18. The mean value of the two corrections is clearly decreasing since the beginning of Envisat mission due to inter-annual reduction of the solar activity. The mean differences (GIM-Dual frequency), plotted in figure 18, is very stable around -0.7 cm. It is stronger in absolute value for high ionosphere corrections, for descending passes (in the daytime). The standard deviation of the difference is plotted in figure 18. Low values, less than 2 cm, indicate a good correlation between dual-frequency and GIM corrections. Notice that, in this analysis, the same sea state bias (SSB) has been used to correct the Ku and S-Band Ranges for cycles 9-40, as it is done so far in the GDR processing. Since cycle 41, a suitable Ku and S-band SSB correction is used on the two bands before computing the dual frequency ionosphere correction from Ku and S-band ranges (Labroue (2004 [26])). The differences with the GDR correction are very small with no impact on the global statistics and only small geographic variations between -1 mm and +1.5 mm (Labroue 2004 [26]).

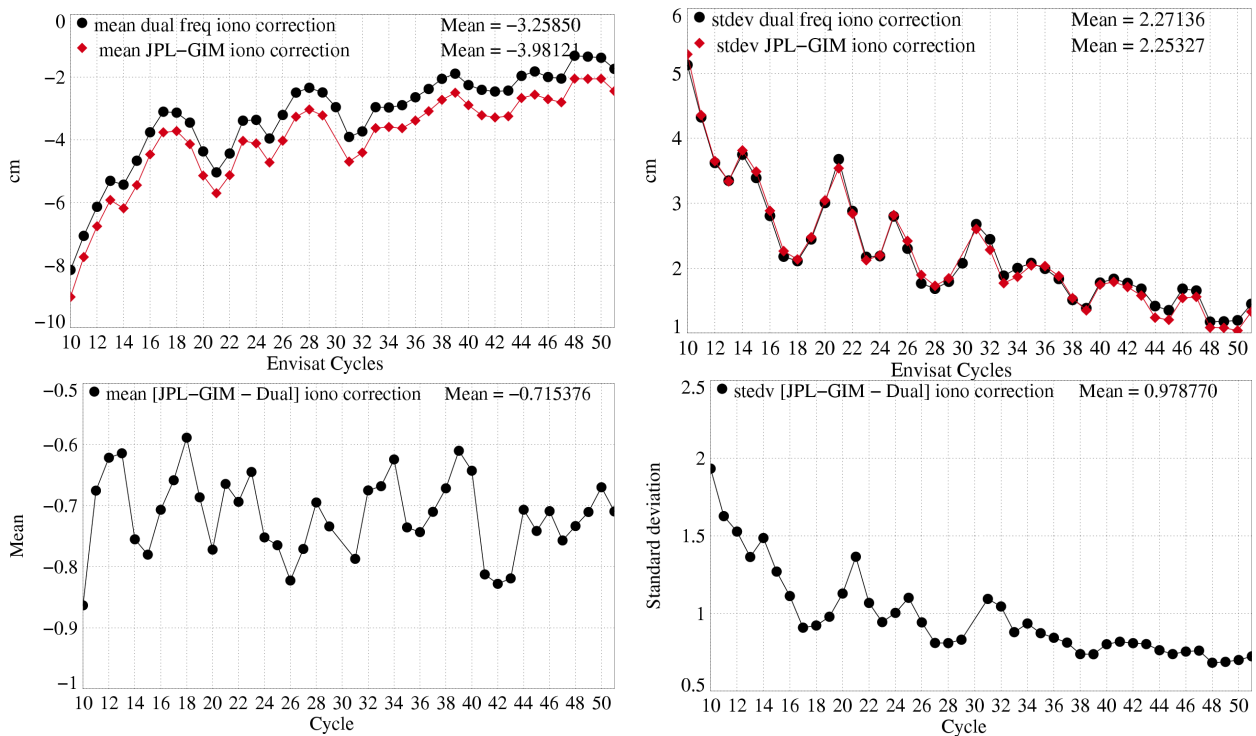


Figure 18: Comparison of global statistics of Envisat dual-frequency and JPL-GIM ionosphere corrections (cm). top) Cycle mean and standard deviation of Dual Frequency and GIM correction. bot) Mean and standard deviation of the differences

CLS CalVal Envisat	Envisat validation and cross-calibration activities	Page : 27 Date : April 19, 2007
Ref: CLS.DOS/NT/06.300	Nom.: SALP-RP-MA-EA-21376-CLS	Issue: 0rev1

5.6 MWR wet troposphere correction

A neural network formulation has been used in the inversion algorithm retrieving the wet troposphere correction from the measured brightness temperatures (Obligis et al., 2005 [42]). As an example, the scatter plot of MWR correction according to ECMWF model for cycle 51 is given in figure 19.

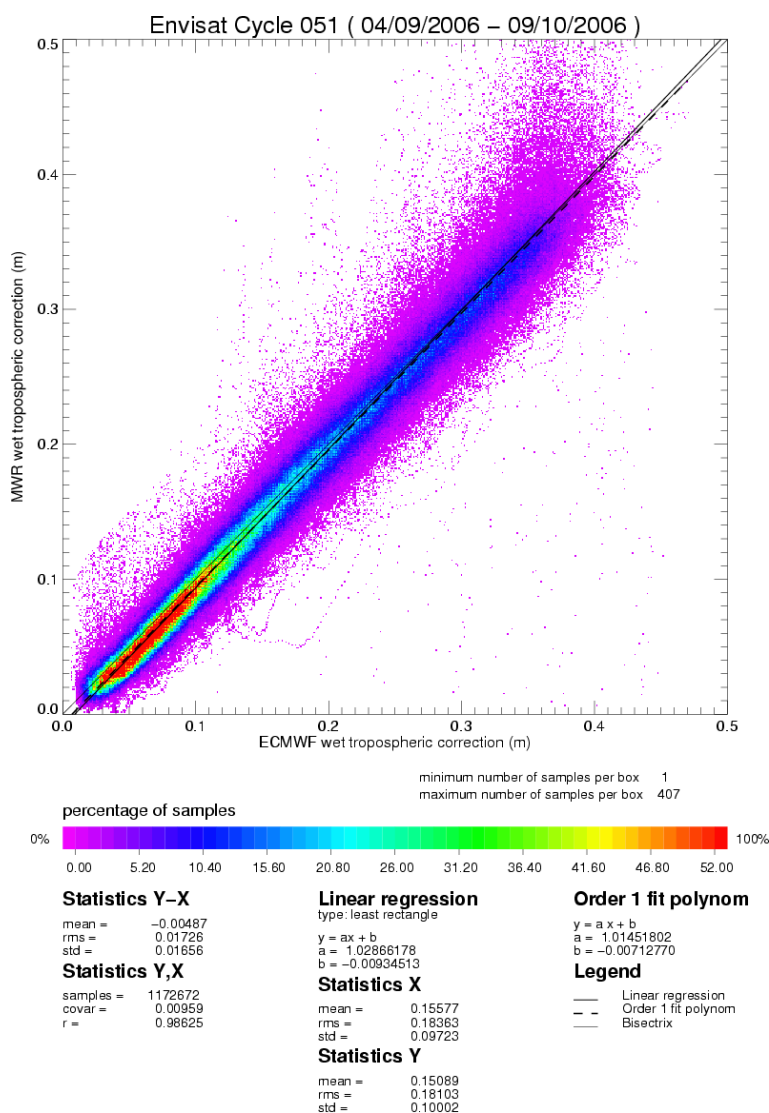


Figure 19: Scatter plot of MWR correction according to ECMWF model (m)

Since the beginning of the mission, the instrumental parameters at 36.5 GHz have been drifting and investigations are in progress to identify the source for these drifts. A correction of the TB36.8 GHz has been proposed in Tran et al., 2006 [54] (not applied here). In particular, different behavior is observed depending on the brightness temperature values. Mean and standard deviation of (MWR-ECMWF model) differences are plotted in figure 20. The difference is not really stable, though the global mean remains small. It rises by 3mm between cycles 11 and 27, which corresponds to 1.8 mm/year. Then, it decreases by 2mm between cycle 27 and 46. Finally, between cycle 47 and 51 a strong increase followed by an equivalent decrease is

CLS CalVal Envisat	Envisat validation and cross-calibration activities	Page : 28 Date : April 19, 2007
Ref: CLS.DOS/NT/06.300	Nom.: SALP-RP-MA-EA-21376-CLS	Issue: 0rev1

observed. This strange behaviour has not been explained so far. The standard deviation drops down by 2 mm from cycle 13. This is due to a change in the ECMWF model on the 14th of January 2003 [13]. The impact of these changes has been found to be meteorologically positive, and it is confirmed by the improved consistency with the MWR. Note that this change did not impact the MWR-ECMWF mean differences. Similar results are visible on Jason-1 mission. A specific analysis of the MRW/ECMWF model comparison is available in 8.6. Moreover, a complete monitoring of all the radiometer parameters is available in the cyclic Envisat Microwave Radiometer Assessment (Dedieu et al., 2005 [8]).

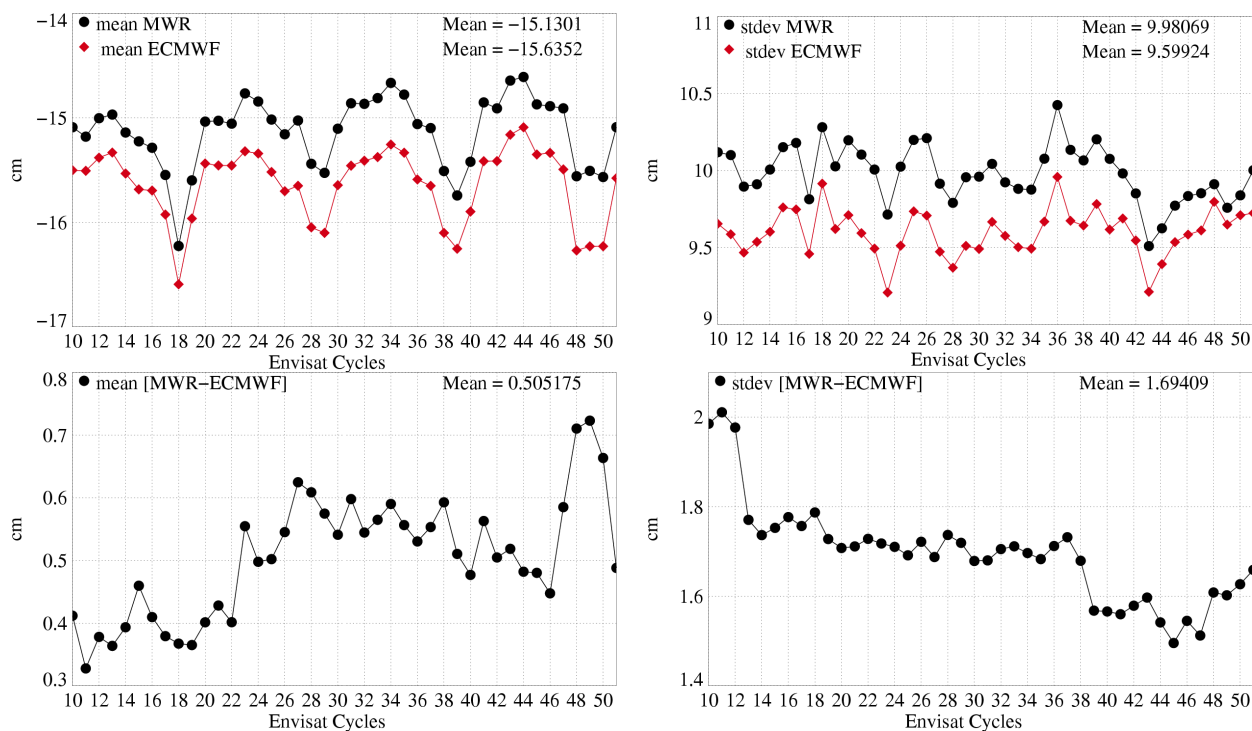


Figure 20: Comparison of global statistics of Envisat MWR and ECMWF wet troposphere corrections (cm). top) Cycle mean and standard deviation of MWR and ECMWF corrections bot) Mean and standard deviation of the differences.

The (ERS-2 -Envisat) cyclic 23.8 GHz brightness temperatures differences over the Atlantic area are plotted on figure 21. The ERS-2 drift proposed by Eymard et al., 2003 [16] is applied. The correction of the drift proposed by Scharroo et al., 2004 [49], should decrease the mean difference by 0.8K as described in Mertz et al., 2004 [39]. Nevertheless, the mean difference variations are more steady for the period after cycle 21. The (ERS-2 -Envisat) TB36.5 GHz values are also reported in figure 21. The differences before and after cycle 18 have a different behaviour: one observes a great decrease from -2 to -4 K between cycles 13 and 17 whereas the curve seems to be steadier after cycle 18. This is not an impact of the coverage of the data since in the restricted area, the statistics reveals the same features. Tran et al., 2006 [54], propose a correction for the drift of the 36.5 GHz TB on Envisat (not used here). They also show an unusual behaviour of the TB values during that period. Note that this behaviour is not visible on hottest or coldest values but mainly on the mean values. The impact of the drift of the TB36.5 on (ERS-2 -Envisat) wet troposphere correction differences is visible in figure 22.

<p>CLS CalVal Envisat</p>	<p>Envisat validation and cross-calibration activities</p>	<p>Page : 29 Date : April 19, 2007</p>
<p>Ref: CLS.DOS/NT/06.300</p>	<p>Nom.: SALP-RP-MA-EA-21376-CLS</p>	<p>Issue: 0rev1</p>

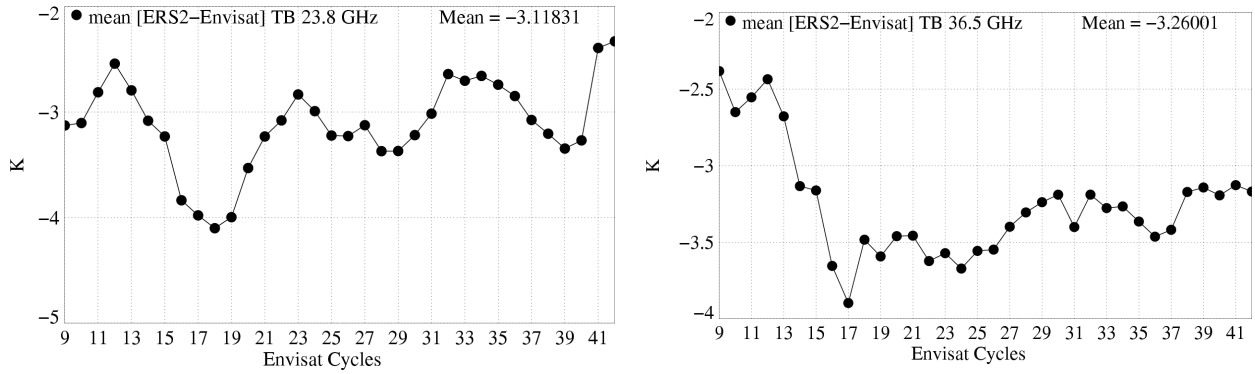


Figure 21: Monitoring of the (ERS-2 - Envisat) brightness temperatures

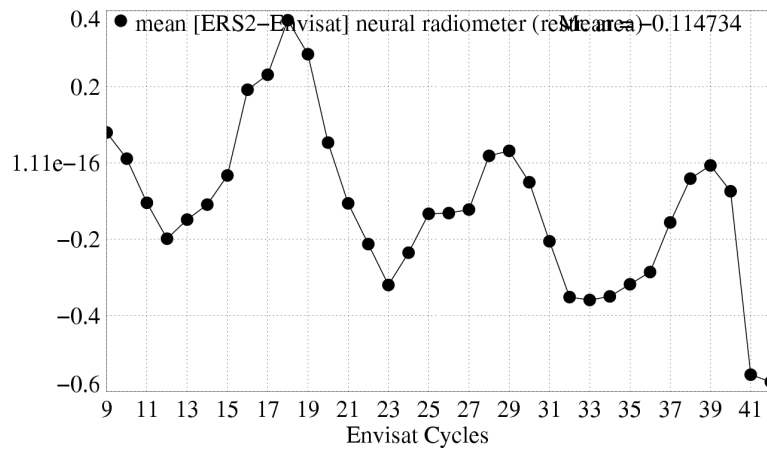


Figure 22: Monitoring of the (ERS-2 - Envisat) wet troposphere correction

CLS CalVal Envisat	Envisat validation and cross-calibration activities	Page : 30 Date : April 19, 2007
Ref: CLS.DOS/NT/06.300	Nom.: SALP-RP-MA-EA-21376-CLS	Issue: 0rev1

6 Sea Surface Height performance assessment

One of the main objectives of the Calibration and Validation activities is to assess the performance of the whole altimeter system. This means that the quality of each parameter of the product is evaluated, in particular if it is likely to be used in the Sea Surface Height (SSH) computations. Conventional tools like crossover differences and repeat-track analyses are systematically used in order to monitor the quality of the system.

6.1 SSH definition

The standard SSH calculation for Envisat is defined below.

$$SSH = Orbit - Altimeter Range - \sum_{i=1}^n Correction_i$$

$$\sum_{i=1}^n Correction_i = \text{Dry troposphere correction : new S1 and S2 atmospheric tides applied}$$

+ Combined atmospheric correction : MOG2D and inverse barometer

+ Radiometer wet troposphere correction

+ Filtered dual frequency ionospheric correction

+ Non parametric sea state bias correction

+ Geocentric ocean tide height, GOT 2000 : S1 atmospheric tide is applied

+ Solid earth tide height

+ Geocentric pole tide height

As said in 3.2, the new geophysical correction associated with version CMA7 have been updated on the whole data-set in order to have the most homogeneous time series. For Envisat, the only discontinuities existing in our dataset are between cycle 40 and 41 due to:

- the orbit: Envisat orbit is computed using GRIM5 gravity model for cycles 9 to 40 and EIGEN-CG03C from cycle 41 onwards.

- the retracking (IF monthly estimations from cycle 41 onwards)

The USO auxiliary correction distributed by ESA are used in Envisat SSH computation.

6.2 Single crossover mean

SSH crossover differences are computed on a one-cycle basis, with a maximum time lag of 10 days, in order to reduce the impact of ocean variability which is a source of error in the performance estimation. The mean of crossover differences represents the average of SSH differences between ascending and descending passes. This difference can reflect orbit errors or errors in geophysical corrections. The fact that Envisat is Sun-synchronous can play a role since the ascending passes and descending passes respectively cross the equator at 10pm local time and 10am local time. Thus all the parameters with a daily cycle can induce errors resulting in ascending/descending differences. The error observed at crossovers can be split into two types:

CLS CalVal Envisat	Envisat validation and cross-calibration activities	Page : 31 Date : April 19, 2007
Ref: CLS.DOS/NT/06.300	Nom.: SALP-RP-MA-EA-21376-CLS	Issue: 0rev1

the time invariant errors and the time varying errors.

To analyse the time invariant errors, we have computed local averages of crossover differences over cycles 10 to 40 and 41 to 51. The maps of the mean differences at crossovers are shown in figure 23. On the 10-40 map, systematic differences between ascending and descending passes are observed in some areas. Mean ascending/descending differences are locally higher than 4 cm (Southern Pacific and Southern Atlantic). These patterns, called geographically correlated radial orbit errors, are induced by errors in the gravity models currently used in the orbit computation. Notice that the signal visible around the equator on ERS-2 (Scharroo, 2002 [47]), related to poor quality of the ionosphere correction, is not present for Envisat thanks to a good correction of the dual frequency correction. On the 41-51 map the geographically correlated orbit errors are almost fully removed thanks to the use of EIGEN-CG03C gravity model. Small signals remain in Indian and Pacific Oceans.

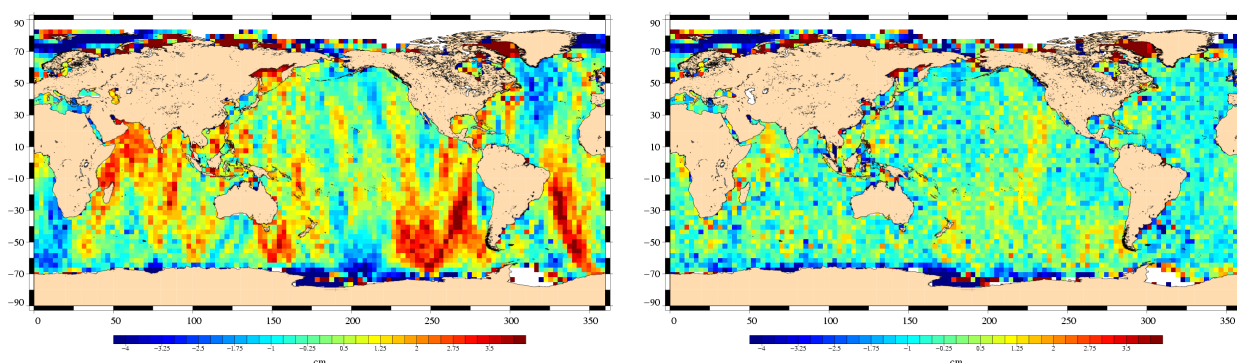


Figure 23: Maps of the time invariant 35-day crossover mean differences (cm) for Envisat averaged in ($3^\circ \times 3^\circ$) geographical bins over cycles 10 to 40 (left) and over cycles 41 to 51 using the new POE orbit using a new gravity model (right).

Besides the systematic ascending-descending errors, a time varying error can also be observed at crossovers. The cyclic mean ascending-descending SSH differences at crossovers shows this error in figure 24. The cyclic mean crossover differences have been plotted in three different configurations: full data set, deep ocean data, and deep ocean data with low variability, and excluding high latitudes. A strong annual signal is evidenced on the 3 curves. Its amplitude is approximately 1 cm.

A specific study has been carried out in order to analyse deeply this signal. The results of this study are available in section 8.3. The main results of this study is first that the amplitude is geographically dependent, and then that the geographical patterns depend on the oceanic tide model used in the SSH.

6.3 Variance at crossovers

The variance of crossover differences conventionally gives an estimate of the overall altimeter system performance. Indeed, it gathers error sources coming from orbit, geophysical corrections, instrumental noise, and part of the ocean variability. The standard deviation of the Envisat SSH crossover differences has been plotted in figure 25, depending on three data selection criteria. Without any selection, a seasonal signal is observed because variations in sea ice coverage induce changes in ocean sampling by altimeter measurements. When only retaining deep ocean areas, excluding high latitudes (higher than 50 deg.) and high ocean variability areas, the standard deviation then gives reliable estimate of the altimeter system performances. In that case most of the cycles have a standard deviation between 7.5 and 7.7 cm. But there are

CLS CalVal Envisat	Envisat validation and cross-calibration activities	Page : 32 Date : April 19, 2007
Ref: CLS.DOS/NT/06.300	Nom.: SALP-RP-MA-EA-21376-CLS	Issue: 0rev1

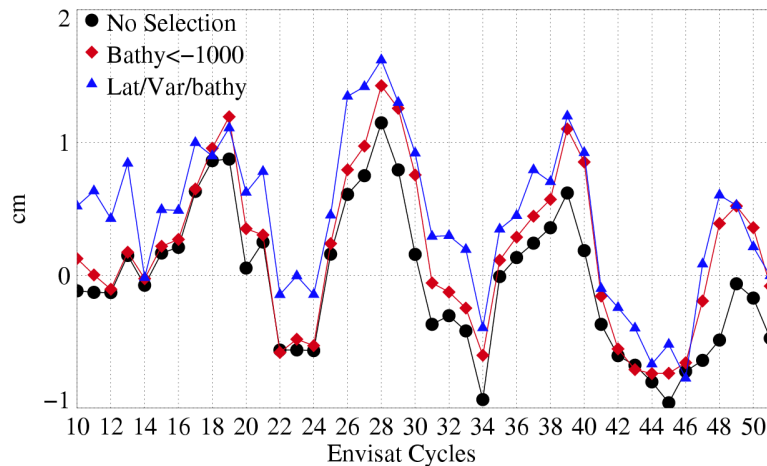


Figure 24: *Time varying 35-day crossover mean differences (cm). Cycle per cycle Envisat crossover mean differences. An annual cycle is clearly visible. Diamonds: shallow waters (1000 m) are excluded. Triangles: shallow waters excluded, latitude within [-50S, +50N], high ocean variability areas excluded*

some exceptions that can be explained. Cycles 15 and 48 are strongly different because of the low number of crossover points. There are less than 10000 crossovers whereas other cycles lead to more than 20000. Cycles 21 and 26 have higher values because of bad orbit quality over a few passes related to out-of-plane maneuvers. Cycle 21 has a strong value (8.5 cm) because of the combined effect of 2 maneuvers, intense solar activity between these 2 maneuvers, and lack of laser measurements between these two maneuvers. Cycle 11 has a relative high value because of missing Doris data. No degradation of the performances have been noticed since the beginning of the USO anomaly on cycle 46. This shows that the correction provided by ESA allows Envisat Ra2 data to maintain the same level of quality.

In order to compare Envisat and Jason-1 performances at crossovers, Envisat and Jason-1 crossovers have been computed on the same area excluding latitude higher than 50 degree, shallow waters and using exactly the same interpolation scheme to compute SSH values at crossover locations. Performances at crossovers are compared, for the two satellites on figure 26. The standard deviation of Envisat/Envisat and Jason-1/Jason-1 SSH crossover differences are respectively 6.1 cm and 6.2 cm. Performances are slightly better for Envisat over cycles 1 to 40 except for cycles 21 and 26. Note that the number of crossover points is considerably greater for Jason-1 between cycles 13 and 19 and for cycle 22 where a lot of passes are missing on Envisat. From cycle 41 onwards, the effect of the new retracking on Jason-1 data is visible. Indeed, the MLE4 induced a lower high frequency energy on the Jason-1 signal. The Jason-1 performances are now slightly better than Envisat ones.

CLS CalVal Envisat	Envisat validation and cross-calibration activities	Page : 33 Date : April 19, 2007
Ref: CLS.DOS/NT/06.300	Nom.: SALP-RP-MA-EA-21376-CLS	Issue: 0rev1

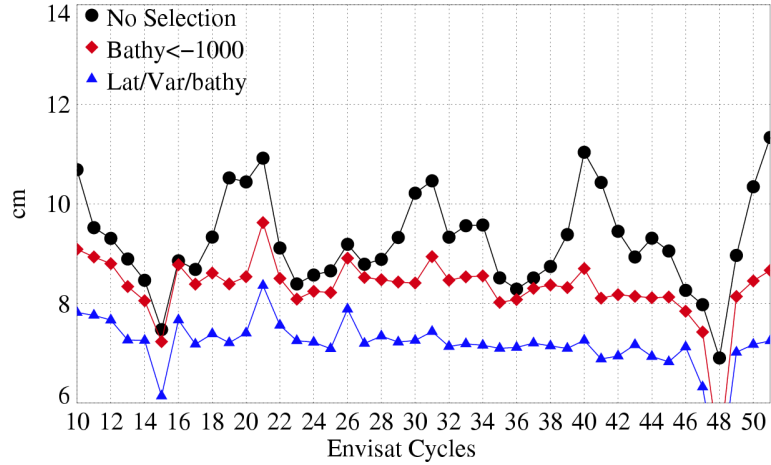


Figure 25: Standard deviation (cm) of Envisat 35-day SSH crossover differences depending on data selection. Dots: without any selection. Diamonds: shallow waters (1000 m) are excluded. Triangles: shallow waters excluded, latitude within $[-50S, +50N]$, high ocean variability areas excluded.

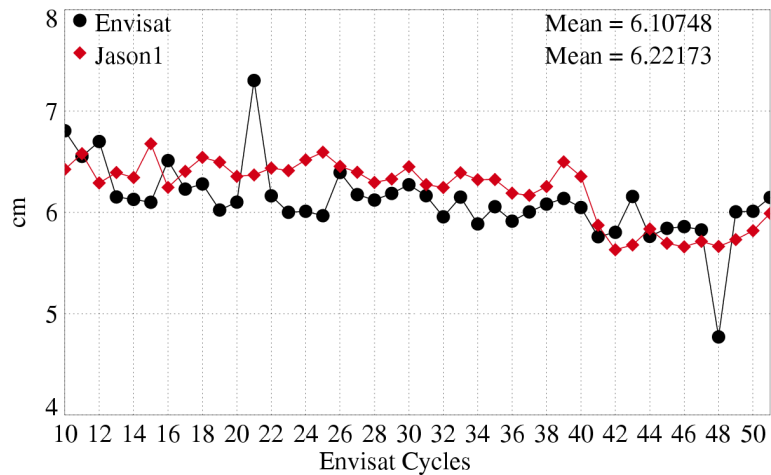


Figure 26: Comparison of the Standard deviation (cm) of Envisat (dot) and Jason-1 (diamond) 10-day SSH crossover differences

CLS CalVal Envisat	Envisat validation and cross-calibration activities	Page : 34 Date : April 19, 2007
Ref: CLS.DOS/NT/06.300	Nom.: SALP-RP-MA-EA-21376-CLS	Issue: 0rev1

7 Envisat SSH bias and Mean Sea Level trends

7.1 SSH definition

As previously mentioned, a drift is suspected on the MWR correction. Consequently, the ECMWF wet troposphere correction is used, as no major change in the model has impacted the data since the beginning of the Envisat mission (ECMWF web page). A part from that the same SSH as for 6.1 is used.

7.2 Envisat Bias

Envisat Mean Sea Level (MSL) estimations are plotted in figure 27 for three different editing criteria in order to estimate the impact of shallow waters and high latitudes. The mean SSH bias relative to the CLS01 MSS is about 49.5 cm over this period. Seasonal signals are observed on the three curves, though the annual cycle is more pronounced on the full data-set.

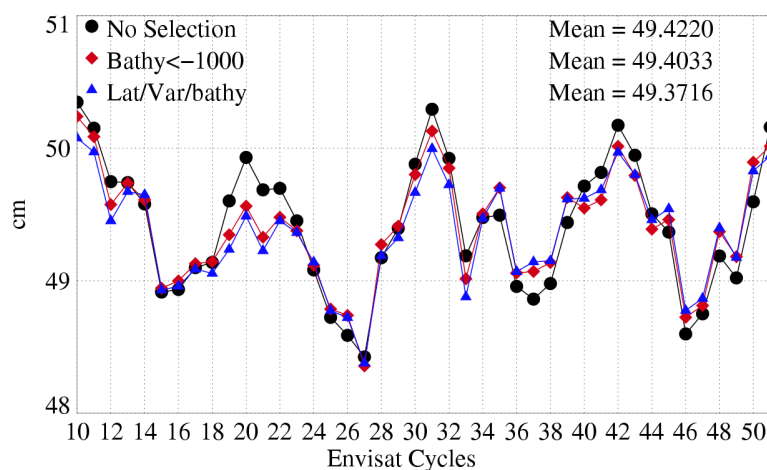


Figure 27: Mean of Envisat Sea Level depending on data selection. Dots: without any selection. Diamonds: shallow waters (1000 m) are excluded. Triangles: shallow waters excluded, latitude within $[-50S, +50N]$, high ocean variability areas excluded.

In order to compare Envisat and Jason-1 SSH estimations, 10-day dual crossovers have been computed for each Envisat cycle. The same ECMWF correction has been used for both Jason-1 and Envisat to avoid potential radiometer errors. Figure 28 shows the mean Envisat-Jason-1 differences at global and hemispheric scales. The global mean is about 33.6 cm over the period. There is a decreasing trend on the difference between cycles 10 and 20 then the differences seem to stabilize. This behavior remains unexplained. The hemispheric differences seem consistent from one cycle to another. From cycles 10 to 16, no hemispheric difference is observed, while after Cycle 16, high hemispheric biases are evidenced. The differences are periodically strongly reduced with a period of 6-8 Envisat cycles (200-300 days). The same kind of observation had been made on Jason-1 T/P differences (Dorandeu, 2004b). These differences might be attributed to residual orbit errors on at least one of the satellites.

CLS CalVal Envisat	Envisat validation and cross-calibration activities	Page : 35 Date : April 19, 2007
Ref: CLS.DOS/NT/06.300	Nom.: SALP-RP-MA-EA-21376-CLS	Issue: 0rev1

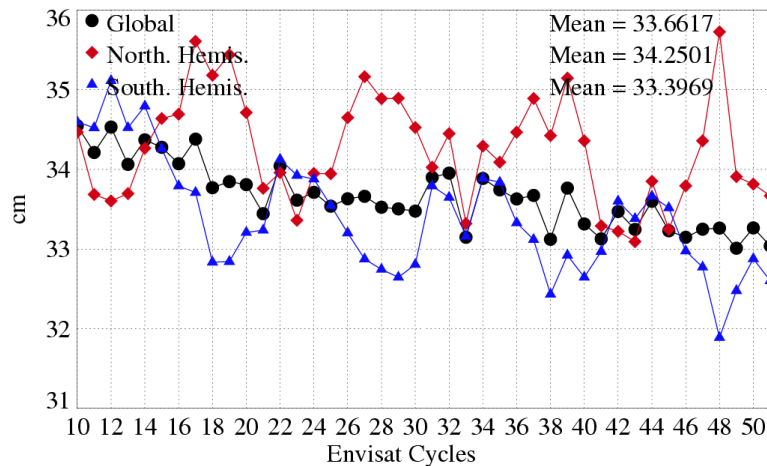


Figure 28: Mean of Envisat -Jason-1 differences at 10-day dual crossovers. Dots: Global. Diamonds: Northern Hemisphere. Triangle: Southern Hemisphere.

7.3 MSL trends

Finally MSL estimations from Envisat and Jason-1 have been compared. The results are obtained after area weighting (Dorandeu and Le Traon 1999). The same corrections are used for the 3 satellites. Annual and semi-annual signals have been removed. An additional 60-day period sinusoid has been fitted and removed on Jason to remove residual orbit errors (Luthcke et al. 2003). Biases relative to MSS have been removed for each mission to ease the comparison. Figure 29 shows the global MSL trend for the two satellites on the whole Envisat period (2003-2006). The Envisat curve shows a quasi null trend while Jason-1 leads to an increasing trend of about 3 mm/year. This difference is partly due to the unexplained behavior of Envisat MSL estimations on the first cycles. Indeed the MSL has a decreasing trend until the last months of 2003, around cycle 20. This is consistent with the Envisat-Jason-1 trend observed at dual crossovers. Figure 30 shows the global MSL trend for three different periods (2003-2004, 2004-2005, 2005-2006). A consistent increasing trend is visible for the three periods on Jason-1. On the contrary, Envisat trend is decreasing over 2003-2004, which confirm what has been said bellow. Then, Envisat trend is consistent with Jason-1 trend only on 2004-2005. Finally, on the last two years, Envisat trend is about 0.

A complete study on the MSL seen by all the operational altimeter missions and its comparison to the Reynolds SST is available in Appendix 2.

CLS CalVal Envisat	Envisat validation and cross-calibration activities	Page : 36 Date : April 19, 2007
Ref: CLS.DOS/NT/06.300	Nom.: SALP-RP-MA-EA-21376-CLS	Issue: 0rev1

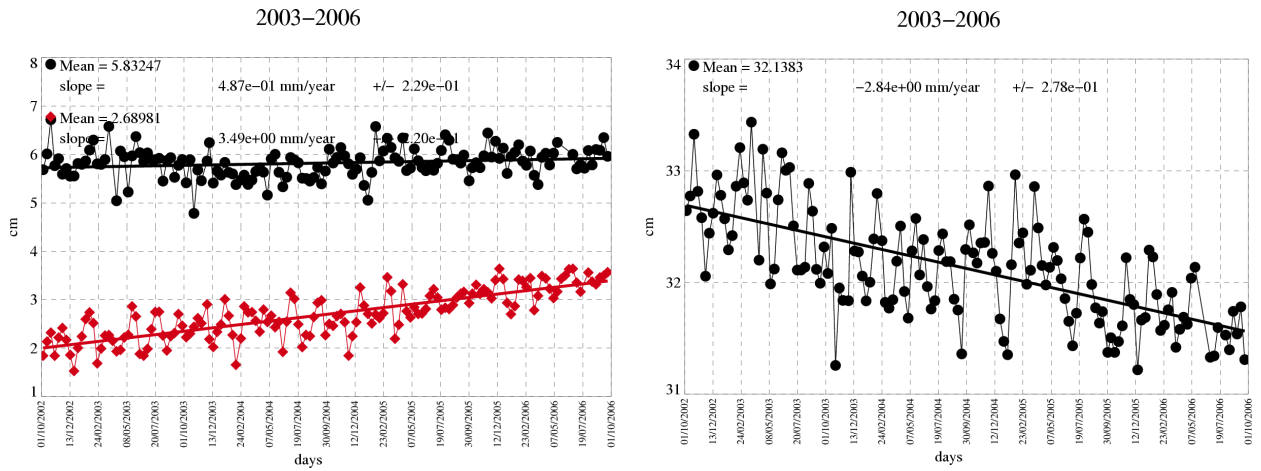


Figure 29: Envisat and Jason-1 MSL trend over the period 2003-2006 (left), Envisat - Jason-1 MSL trend (right)

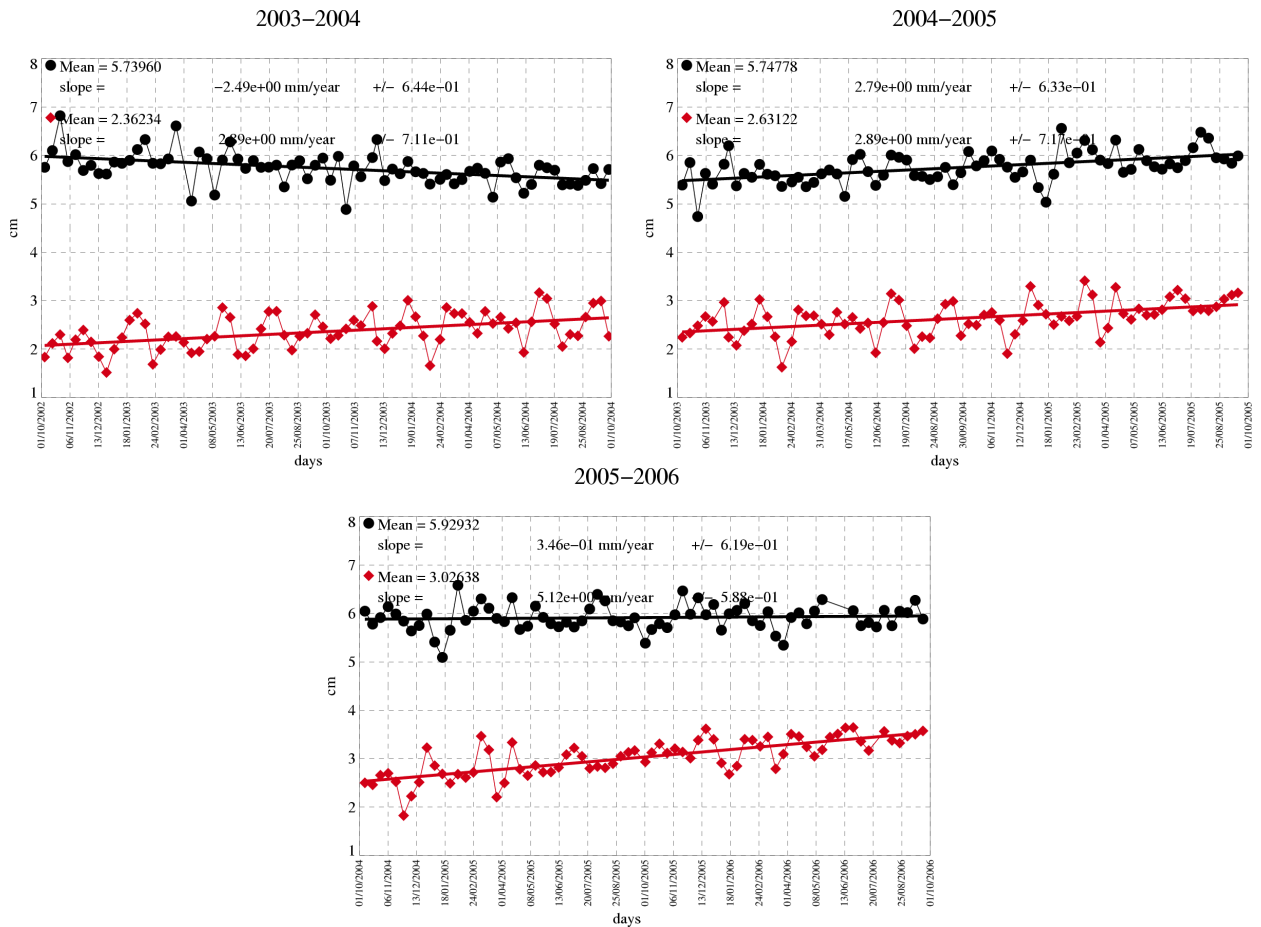


Figure 30: Envisat and Jason-1 MSL trend over the period 2003-2004 (top left), 2004-2005 (top right), 2005-2006 (bot)

CLS CalVal Envisat	Envisat validation and cross-calibration activities	Page : 37 Date : April 19, 2007
Ref: CLS.DOS/NT/06.300	Nom.: SALP-RP-MA-EA-21376-CLS	Issue: 0rev1

8 Particular investigation

8.1 The Ra-2 USO anomaly and its associated correction

8.1.1 Introduction

In February 2006, the RA-2 Ultra Stable Oscillator (USO) clock frequency underwent, for an unknown reason, a strong change of behaviour. The anomaly consists in a bias, superposed with an oscillating signal with an orbital period. Translated into range, the mean bias reaches 5.6m and the oscillating signal has an amplitude of about 30cm. In order to overcome this brutal change of behaviour, a method was developed to correct anomalous data. The daily mean values of this correction is shown in figure 31.

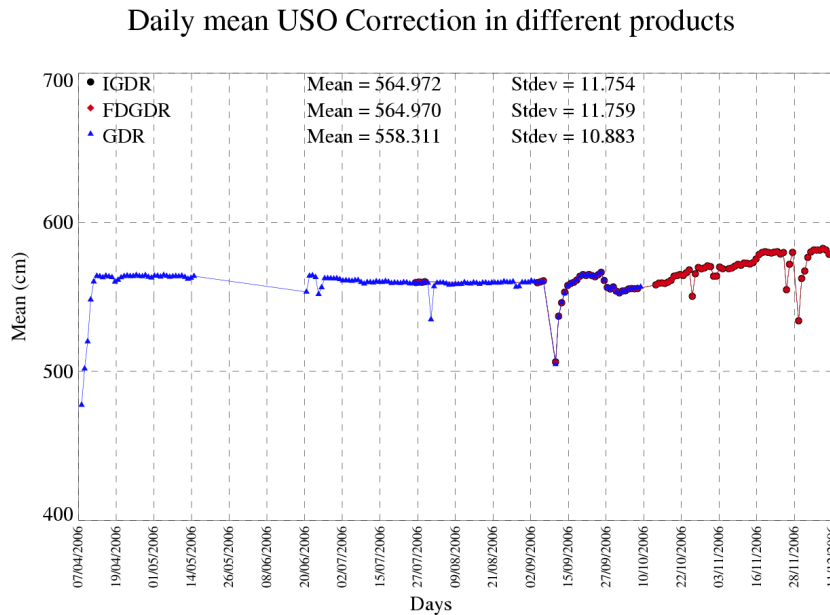


Figure 31: Mean per day of the correction since the beginning of the USO anomaly.

8.1.2 USO correction method

The proposed method, detailed in [22], to calculate the USO period is based on a reference to the time given by the platform clock, the On-Board Datation Handling (OBDH):

$$Period(t) = \frac{OBDH_{count}(t - step/2) - OBDH_{count}(t + step/2)}{USO_{count}(t - step/2) - USO_{count}(t + step/2)} \quad (1)$$

Once the raw period is calculated, it is noticeable in Figure 32 (left), that a quantification noise appears. In order to smooth it, a filter is applied on the raw period 32 (top right) before converting it to a smooth

CLS CalVal Envisat	Envisat validation and cross-calibration activities	Page : 38 Date : April 19, 2007
Ref: CLS.DOS/NT/06.300	Nom.: SALP-RP-MA-EA-21376-CLS	Issue: 0rev1

range correction 32 (bottom right).

The filter chosen is a spline regression filter because it presents the strong advantage of interpolating small gaps of data. It is shown to give better results than a classical low pass simple filter (Lanczos Filter) near gaps and similar results elsewhere.

To translate the period into a range correction, the following equation is used:

$$Corr_{USO} = Range. \frac{Period(t) - Period_{used}}{Period(t)} \quad (2)$$

Period_used is the period used for the clock period in the ground segment and equal to 12500ps for IPF versions up to V4.58. Since the 11/03/2006, the clock period used in the ground segment has been set to 12499.999726000 ps.

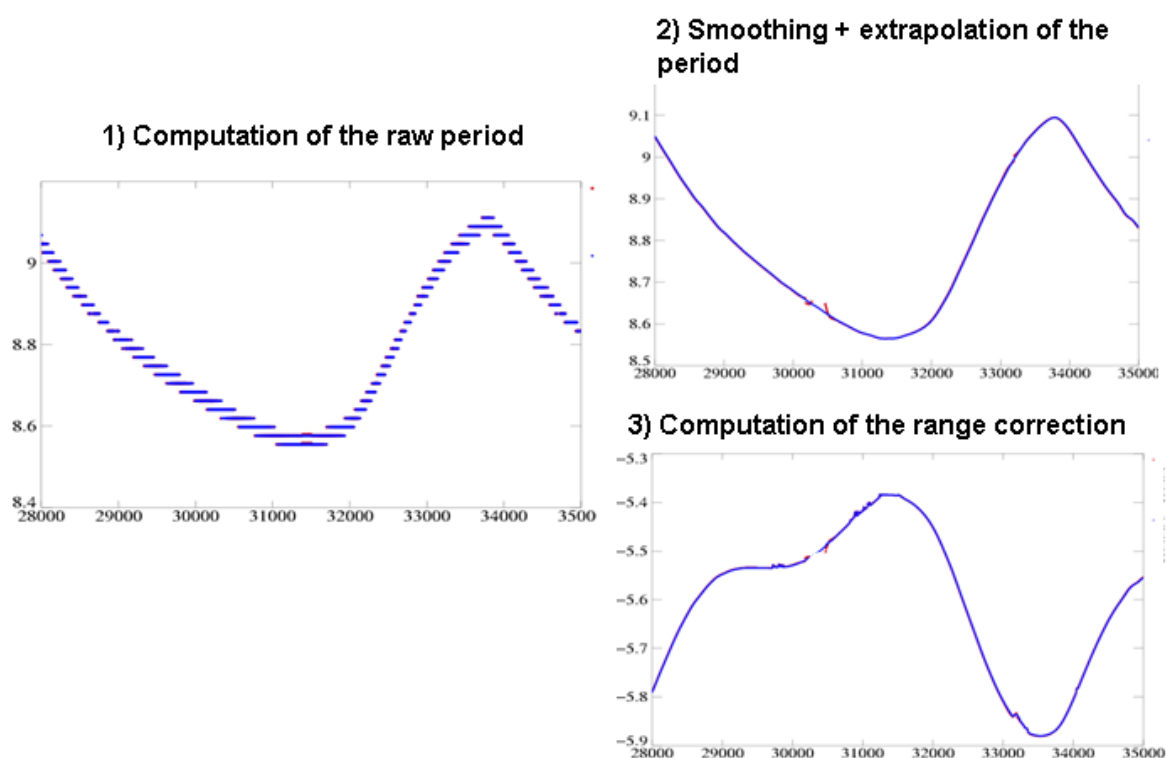


Figure 32: Raw period (left). Spline filtered period (top right). Associated correction (bottom right)

- Minimum standard deviation between the two filtered periods and
- Absence of strong non physical divergence for the spline Period filtered on short data sets (product per product).

CLS CalVal Envisat	Envisat validation and cross-calibration activities	Page : 39 Date : April 19, 2007
Ref: CLS.DOS/NT/06.300	Nom.: SALP-RP-MA-EA-21376-CLS	Issue: 0rev1

- Absence of local oscillations (this could be detected thanks to a relative comparison with a model method (see chapter on the comparison with the correction proposed by R Scharroo).

8.1.3 Correction availability

This correction has been computed and delivered operationally to the users since August 2006, see Figure 1). The correction concerning previous anomalies (Cycles 30, 44 and 45) were computed with the same method and also delivered to the users.

The description of the auxiliary files is available at the following address:

<http://earth.esa.int/pcs/envisat/ra2/auxdata/NewCorrection.html>

A software can be used to include the correction fields in the product themselves. It is available at the following address:

<http://earth.esa.int/pcs/envisat/ra2/auxdata/software/>

This device is available under SUN and LINUX versions.

8.1.4 Validation over ocean

8.1.4.1 Quality assessment of the corrected GDR

The quality assessment is presented in the previous chapters through the SSH performance analysis. The fact that no particular degradation are noticed on the monitoring of the performances assess the quality of the correction. Figure 33 shows an example of the SLA without and with correction. Obviously, without the correction, all the oceanic structures would be drowned by the USO clock signal.

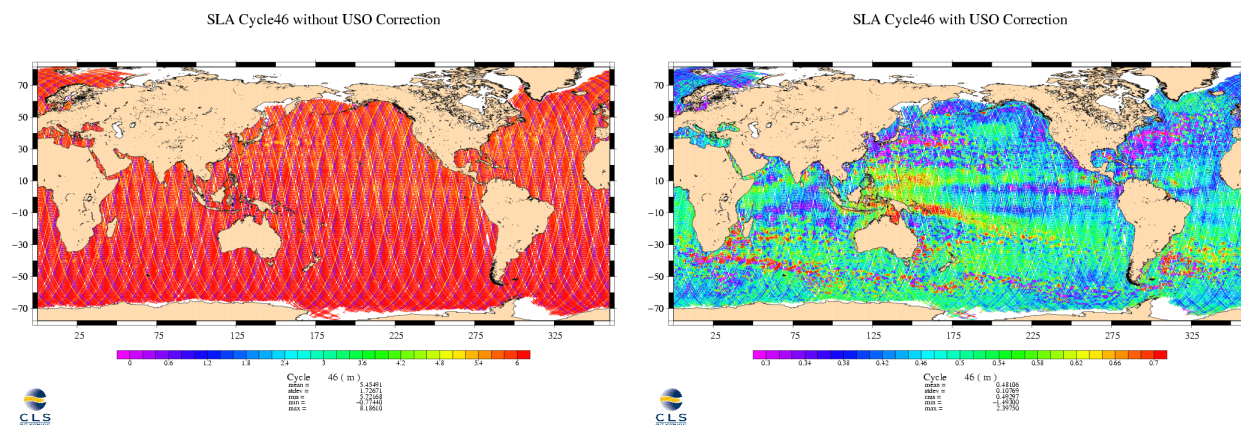


Figure 33: *SLA without (left) and with (right) the USO Correction on cycle 46 affected by the anomaly.*

Another way of validating the correction consists in analysing relative performances of different corrections. The following part deals with a comparison between two possible approaches of correction.

CLS CalVal Envisat	Envisat validation and cross-calibration activities	Page : 40 Date : April 19, 2007
Ref: CLS.DOS/NT/06.300	Nom.: SALP-RP-MA-EA-21376-CLS	Issue: 0rev1

8.1.4.2 Comparison to the correction proposed by R Scharroo

Another approach was proposed (Scharroo, 2006,[50])to compute the Ultra Stable Oscillator (USO) clock frequency on ENVISAT altimeter RA-2 based on a modelling of the USO period oscillation which was found to be strongly linked to the diurnal alternation. Because those methods are completely different, this relative comparison is a good way for assessing the performance of the corrections.

The performances are compared over the same data set over ocean using GDR data and associated USO correction of Cycles 46 and 47.

Thanks to either correction, it is shown that the previously unusable altimetric data now have satisfactory performances. However, some fine differences were evidenced during this analysis. The major conclusions of this analysis are:

- The global mean and standard deviation of the difference between both corrections are 0.1 cm and 9 cm.
- The standard deviation of the difference depends on the evolution of the mean USO value: when the mean USO value changes slowly (long term drift), the standard deviation of the difference is lower than 1 cm whereas when the mean USO value change rapidly (after a switch off/on for example) this value reaches 10 cm.

Figure 34 shows the mean differences averaged over the Cycles 46 and 47.

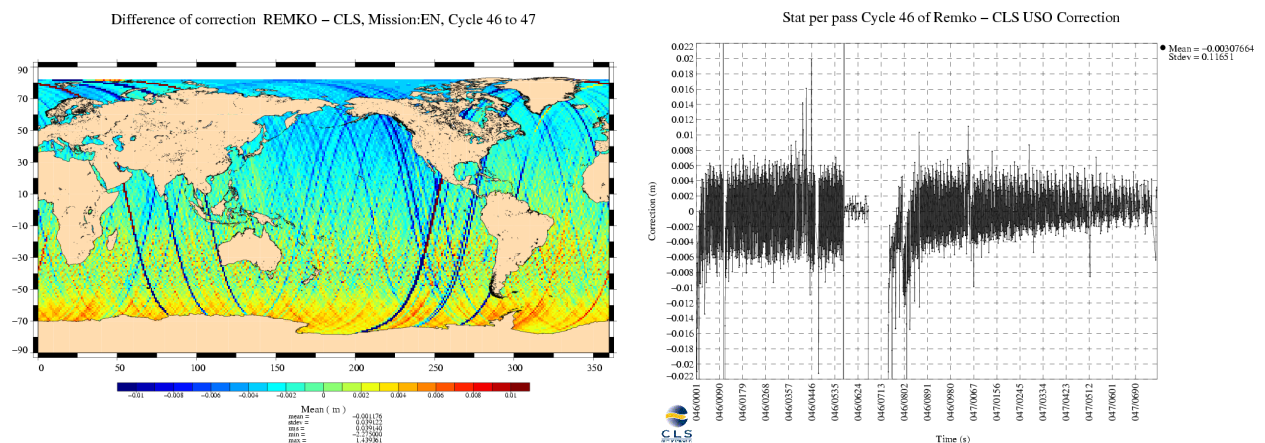


Figure 34: (Predictive model USO Correction - Operational USO Correction) mean differences (left). Average USO Correction differences per pass for Cycle 46 and 47(right).

CLS CalVal Envisat	Envisat validation and cross-calibration activities	Page : 41 Date : April 19, 2007
Ref: CLS.DOS/NT/06.300	Nom.: SALP-RP-MA-EA-21376-CLS	Issue: 0rev1

Several observations can be made:

- The global mean differences are rather small.
- The geographical distribution of the difference between the two corrections is not homogeneous: the operational correction is slightly higher (of about 2-3 mm) than the predictive model's in the northern hemisphere whereas the situation is inverted in the Southern hemisphere.
- The patterns of the difference are different on ascending and descending passes.
- In case of slow change of the mean USO value, the shape of the orbital oscillations are very similar (cf Figure 35 (left)) .
- In case of quick change of the mean USO value, high discontinuities (jumps) are noticed on the predictable model correction and the performances of the SSH on these passes are strongly degraded (cf Figure 35 (right))

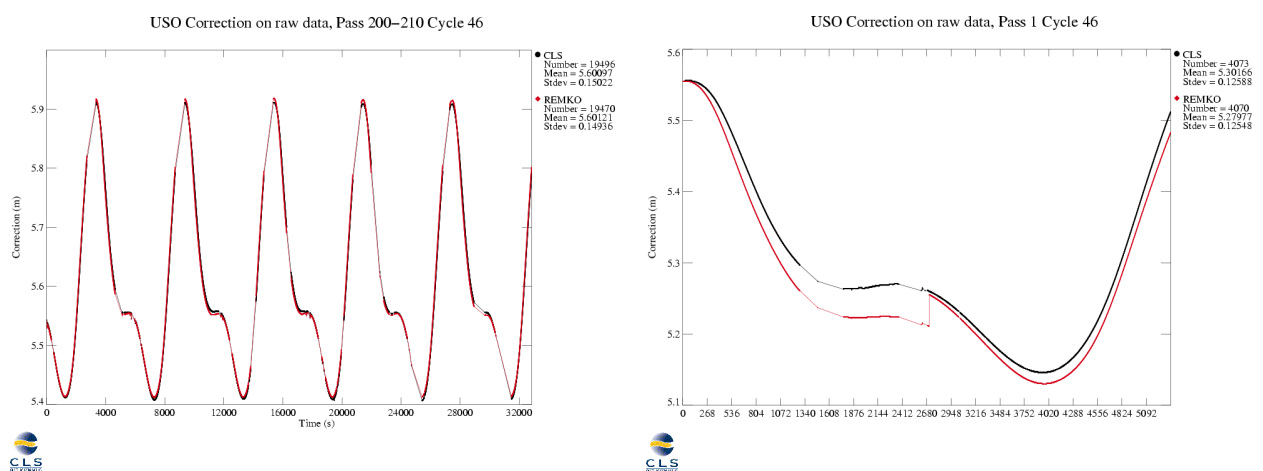


Figure 35: Predictive model USO Correction (Red) and Operational USO Correction (Black) for tracks 200 to 210 of cycle 46 (slow change of the mean USO value) (left) and for track 1 of cycle 46 (quick change of the mean USO value) (right).

- The Mean SSH differences at crossovers has a strong bias when using the predictable model correction whereas the statistics are close to usual values when using the operational correction (see table hereafter). Furthermore, some geographically correlated errors are visible on the mean at crossovers map using the predictable model correction.
- The performances of SSH at crossovers and along track are very close. There is a 1cm rms gain when using the operational correction instead of the predictable model correction. Most of this gain is likely be due to several passes where high differences are observed (see table hereafter).

CLS CalVal Envisat	Envisat validation and cross-calibration activities	Page : 42 Date : April 19, 2007
Ref: CLS.DOS/NT/06.300	Nom.: SALP-RP-MA-EA-21376-CLS	Issue: 0rev1

Performance of SSH at crossovers		Operational Correction	Predictive model Correc- tion
Cycle 46	Number of Points	39406	39406
	Mean	-0.74 cm	-1.55 cm
	Standard Deviation	8.28 cm	8.41 cm
	Mean Quadratic Error	8.31 cm	8.55 cm
Cycle 47	Number of Points	26723	26723
	Mean	-0.67 cm	-1.23 cm
	Standard Deviation	7.93 cm	7.90 cm
	Mean Quadratic Error	7.96 cm	8.00 cm

Although the two corrections studied seemed to have similar behaviours and to both provide a good correction of the data oscillations, the analyse presented here enables to lighten some differences. The predictive model, seems to need further tunings in order to better take into account rapid changes of the mean USO value in order to avoid the jumps between consecutive tracks. In addition to that, the bias it introduces between ascending and descending tracks should be further investigated and could probably be over turned with a different tuning of the model.

Concerning the operational method, this study enabled to evidence very weak oscillations which drove to a refinement of the spline smoothing factor. After this refinement, the local oscillations are removed.

8.1.4.3 Analysis of the validity of the long term drift component of the new correction

From Cycle 9 to Cycle 45, outside of the anomaly periods, the USO period was computed with a step of 86400 seconds (one day) and averaged monthly in order to follow the long term drift of the on board clock. The aim of this study was to compare, on a non anomalous period, two methods of computing the USO corrections: the new method using a step of 100s with a spline filter and the old one, using a step of 86400s averaged monthly.

As expected, the first one is shown to follow more precisely the short terms variations such as recoveries after instrumental events. The other one is very much smoothed and only gives information on the long term drift. As seen in Figure 36, for the analysed couple of cycles, the drift can be approached by a linear increasing. The slopes of both methods are almost equal.

Thanks to this study, it is therefore shown that the global long term drift is the same in both cases and that the short step method enables to recover the long term drift as well as the short term ones.

This validates that the short step method does not loose long term information.

8.1.5 Conclusion

The USO anomaly is a major anomaly which strongly impacts the RA-2 quality data quality. The correction proposed by ESA allowed Ra-2 data to recover their quality thanks to the temporary (but operational) procedure. An extensive validation was performed and enabled to show that the corrected data now had a nominal quality.

<p>CLS CalVal Envisat</p>	<p>Envisat validation and cross-calibration activities</p>	<p>Page : 43 Date : April 19, 2007</p>
<p>Ref: CLS.DOS/NT/06.300</p>	<p>Nom.: SALP-RP-MA-EA-21376-CLS</p>	<p>Issue: 0rev1</p>

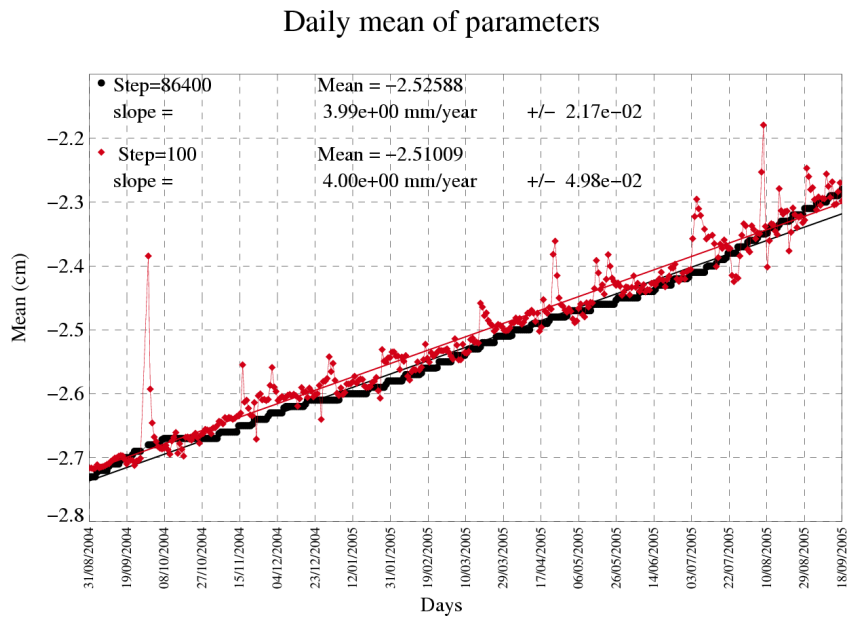


Figure 36: Mean per day of Correction Step=100s and Correction Step=86400s.

CLS CalVal Envisat	Envisat validation and cross-calibration activities	Page : 44 Date : April 19, 2007
Ref: CLS.DOS/NT/06.300	Nom.: SALP-RP-MA-EA-21376-CLS	Issue: 0rev1

8.2 Analysis of the geographical feature of EN/J1 SSH Differences

8.2.1 Introduction

The purpose of this analysis is to describe the geographical feature of EN/J1 SSH Differences at 10-day crossovers. In particular the impact of the version change is described. First, the Envisat and Jason-1 changes are presented. Then, the EN/J1 SSH differences are shown in the two versions of GDR and discussed. The analysis has been done from two periods of one year, cycles 31 to 40 and 41 to 50.

8.2.2 Main data product changes on Envisat and Jason-1

A new configuration of Envisat and Jason have been operational since September 2005. Several improvements in terms of data quality are included in these news versions of GDR product.

SSH1 (used over cycle 31 to 40)	SSH2 (used over cycle 31 to 40)	SSH3 (used over cycle 41 to 50)	SSH4 (used over cycle 41 to 50)
Old orbit configuration (GRIM5 for Envisat, JGM3 For Jason-1)	Old orbit configuration (GRIM5 for Envisat, JGM3 For Jason-1)	New orbit configuration (EIGEN-CG03C)	New orbit configuration (EIGEN-CG03C)
MLE3 retracking for Jason-1	MLE3 retracking for Jason-1	MLE4 retracking for Jason-1	New Retracking for Jason-1 (MLE4)
USO correction (For Envisat)	same as SSH1	same as SSH1	same as SSH1
ECMWF wet troposphere correction	same as SSH1	same as SSH1	same as SSH1
ECMWF dry tropospheric correction	same as SSH1	same as SSH1	same as SSH1
Filtered dual frequency ionospheric correction	same as SSH1	same as SSH1	same as SSH1
Non parametric SSB from product (CMA6)	Non parametric SSB from product (CMA6)	Non parametric SSB from product (CMA7)	non parametric SSB MLE4 for Jason-1 ([28])
Inverse barometer	MOG2D	MOG2D	MOG2D
pole tide correction	same as SSH1	same as SSH1	same as SSH1
earth tide correction	same as SSH1	same as SSH1	same as SSH1
Geocentric ocean tide height, GOT 2000	same as SSH1	same as SSH1	same as SSH1

Table 5: SSH definition

CLS CalVal Envisat	Envisat validation and cross-calibration activities	Page : 45 Date : April 19, 2007
Ref: CLS.DOS/NT/06.300	Nom.: SALP-RP-MA-EA-21376-CLS	Issue: 0rev1

8.2.3 Comparison of SSH performance

The map of the mean differences at crossovers is shown in Figure 37. The global mean difference has been removed in order to have differences centered around zero. The map on the top left side shows 1 year (cycles 30-40) of data using SSH1. Differences up to +/-3 cm are observed on several areas. A part of these differences are clearly due to orbit errors (SouthWest of Chile, ...). The gravity models used in the orbits are GRIM5 and JGM3 respectively for Envisat and Jason-1. Using SSH2, no difference is observed. The map on the bottom shows 1 year of data (cycles 41-51) using SSH3. The differences have strongly changed. The differences related to the gravity model errors have disappeared. The differences is now latitudinal. Envisat is slightly higher (up to 2cm) than Jason-1 at low latitudes, and slightly lower at high latitudes, especially in the Southern hemisphere. So the difference obtained with the new version of GDR is not satisfactory, and the cause of these latitude dependant features has to be explained.

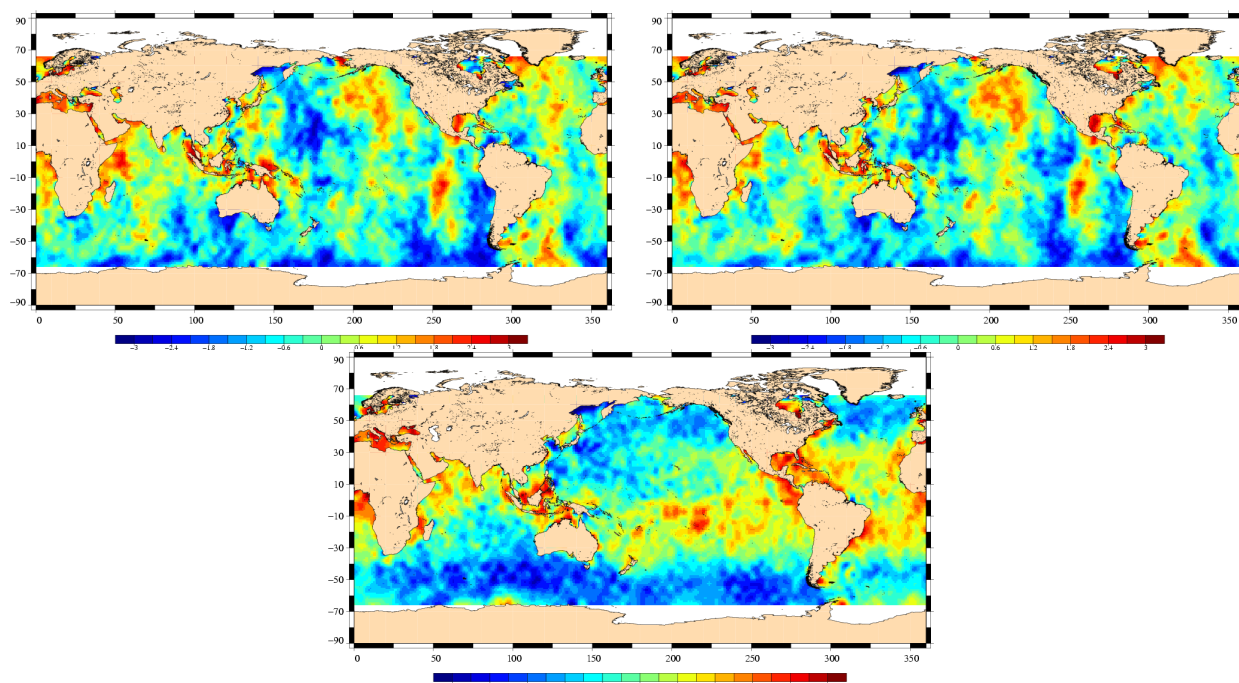


Figure 37: *SSH Crossover mean difference, using SSH1 over cycles 31 to 40 (top left), using SSH2 over cycles 31 to 40 (top right), and using SSH3 over 41 to 50 (bottom)*

Figure 38 shows that there is a strong correlation between the differences of SSH and the SWH. Envisat is higher than Jason-1 in low SWH conditions, and lower than Jason-1 in strong SWH conditions.

8.2.4 Comparison of SSH performance with new SSB for Jason-1

A new version of SSB has been developed for Jason-1 MLE4 data ([28]). Figure 38 (right) shows the impact of the new SSB on the correlation between the SSH difference and the SWH. The strong trend observed with SSH3 has been largely reduced.

The geographical distribution confirm this better consistency between the two satellites (see Figure 39) shows the crossover mean difference centred of SSH over 1 year of data with new product. On the right map, data with new product and new SSB for Jason-1. Some slight differences remain in the equatorial

CLS CalVal Envisat	Envisat validation and cross-calibration activities	Page : 46 Date : April 19, 2007
Ref: CLS.DOS/NT/06.300	Nom.: SALP-RP-MA-EA-21376-CLS	Issue: 0rev1

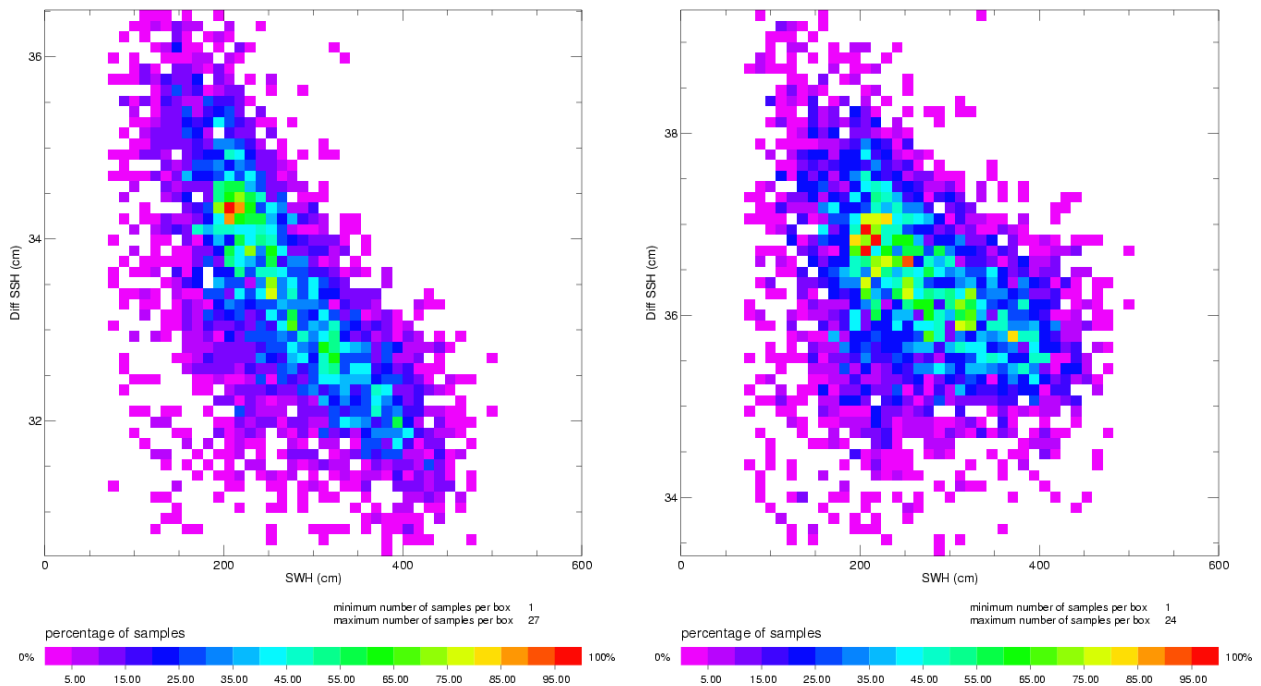


Figure 38: Scatter plot of SSH crossover mean difference (cm) according to Significant wave height (cm) using SSH3 (left) and using SSH4 (right) over cycles 41 to 50

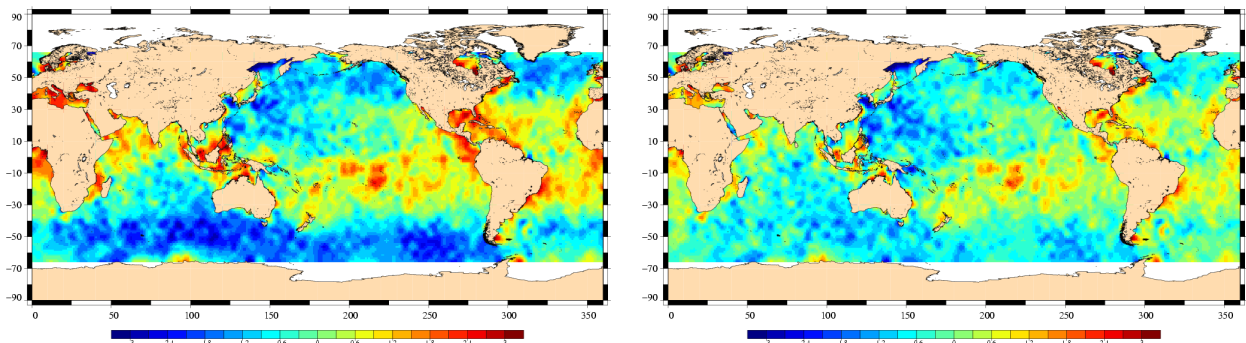


Figure 39: Crossover mean difference using SSH3 (left) and using SSH4 (right) over cycles 41 to 50

pacific and in the Atlantic at mid-latitude.

8.2.5 Impact of GIM

Using GIM inospheric correction (instead of the dual frequency correction) on Jason-1 and Envisat in SSH4 changes the map of differences. Large patterns remain in the equatorial pacific (see figure 40).

8.2.6 Conclusion

The new configuration (SSH3) allows to reduce the geographically correlated differences thanks to the improvement of the orbits. Using a SSB consistent with the new retracking on Jason-1 allows to remove the differences correlated with SWH.

<p style="text-align: center;">CLS CalVal Envisat</p>	<p style="text-align: center;">Envisat validation and cross-calibration activities</p>	<p>Page : 47 Date : April 19, 2007</p>
<p>Ref: CLS.DOS/NT/06.300</p>	<p>Nom.: SALP-RP-MA-EA-21376-CLS</p>	<p>Issue: 0rev1</p>

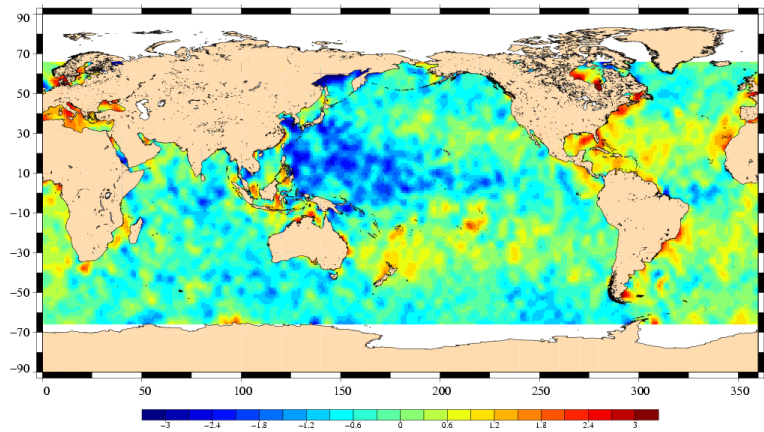


Figure 40: *Crossover mean difference using SS4 + GIM ionosphere correction over cycles 41 to 50*

CLS CalVal Envisat	Envisat validation and cross-calibration activities	Page : 48 Date : April 19, 2007
Ref: CLS.DOS/NT/06.300	Nom.: SALP-RP-MA-EA-21376-CLS	Issue: 0rev1

8.3 Analysis of the annual signal at EN SSH crossover

8.3.1 Introduction

In order to better analyse the annual signal shown in figure 24 a temporal sinusoidal function with a 365 day period has been fitted to mean crossover differences averaged into 10°x 10° bins. For each bin, the following sinusoidal signal is fitted:

$$S(t) = A \cos\left(\frac{2\omega t}{365} + \phi\right)$$

Where t is the time in days, A the amplitude and ϕ the phase.

Only open ocean data are used in this analysis. Latitudes higher than 60 degree are also removed because the seasonal data unavailability at high latitudes corrupts the estimation of the annual signal. Regions of high mesoscale variability are also removed to reduce the noise.

8.3.2 Estimation using the reference SSH

The amplitude A of the estimated sinusoidal signal has been plotted in figure 41, after smoothing in figure 42. The amplitude of the annual signal is not homogeneous. High amplitudes, greater than 2 cm, are visible in two types of regions: some deep sea regions, in the Southern Pacific (longitude 220) and Southern Atlantic, and some coastal regions: Asia an Oceania coasts, Gulf of Mexico. The GOT00 tide is used for this map.

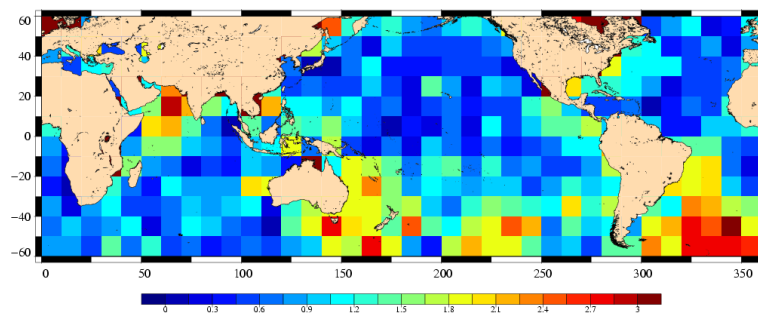


Figure 41: Amplitude (cm) of the annual signal on the mean at crossovers estimated in 10x10 deg boxes (using GOT00 tide model)

8.3.3 Impact of tide on the annual signal

The impact of using FES 2004, FES 2002 and FES 99 is analysed here.

8.3.3.1 Change of tide correction

Using FES04 tide model instead of GOT00 strongly changes the map of amplitude as observed in figure 43. For example the feature in the southern pacific has disappeared but others, still stronger have appeared

<p>CLS CalVal Envisat</p>	<p>Envisat validation and cross-calibration activities</p>	<p>Page : 49 Date : April 19, 2007</p>
<p>Ref: CLS.DOS/NT/06.300</p>	<p>Nom.: SALP-RP-MA-EA-21376-CLS</p>	<p>Issue: 0rev1</p>

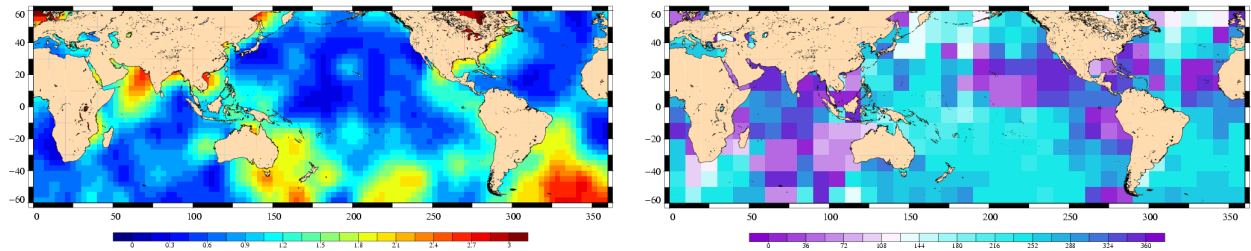


Figure 42: Amplitude (cm) and phase (deg) of the annual signal on the mean at crossovers estimated in 10x10 deg boxes

(East Australia and East Indonesia). These differences are shown in figure 46. This indicates that this annual signal geographically dependant might be linked to errors in oceanic tide models. Note that the phase obtained with FES04 (figure 44) is similar to the one obtained previously with GOT00. Using FES02 gives approximately the same results as with FES04. On the contrary, using FES99, (figure 45) the same results as with GOT00 are found.

To sum up, on the one hand, using FES99 gives similar results as using GOT00, and on the other hand FES02 gives similar results as FES04. A possible cause of this observation is the method used to assimilate ERS2 data. Indeed, the use of ERS-2 data might have introduced an error in the tide models. ERS-2 data have been assimilated in both FES02 and FES04 in coastal regions, but not in FES99 and GOT00. Note that the strongest differences are located in coastal zones.

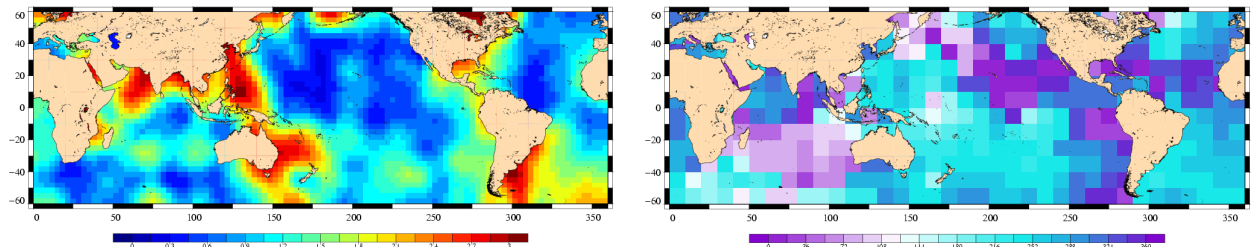


Figure 43: Amplitude (cm) and phase (deg) of the annual signal on the mean at crossovers estimated in 10x10 deg boxes using FES04

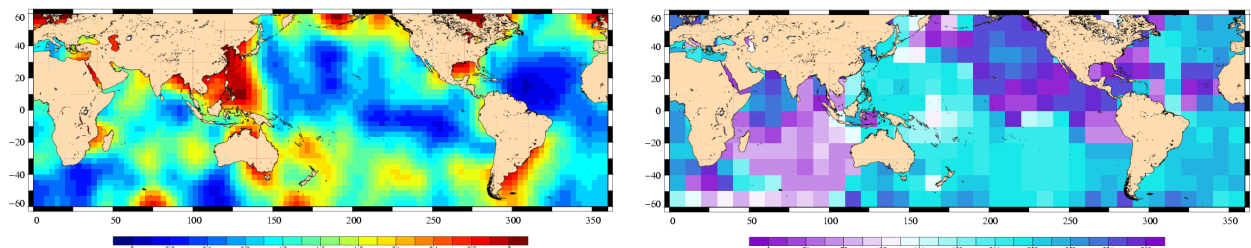


Figure 44: Amplitude (cm) and phase (deg) of the annual signal on the mean at crossovers estimated in 10x10 deg boxes using FES02

<p>CLS CalVal Envisat</p>	<p>Envisat validation and cross-calibration activities</p>	<p>Page : 50 Date : April 19, 2007</p>
<p>Ref: CLS.DOS/NT/06.300</p>	<p>Nom.: SALP-RP-MA-EA-21376-CLS</p>	<p>Issue: 0rev1</p>

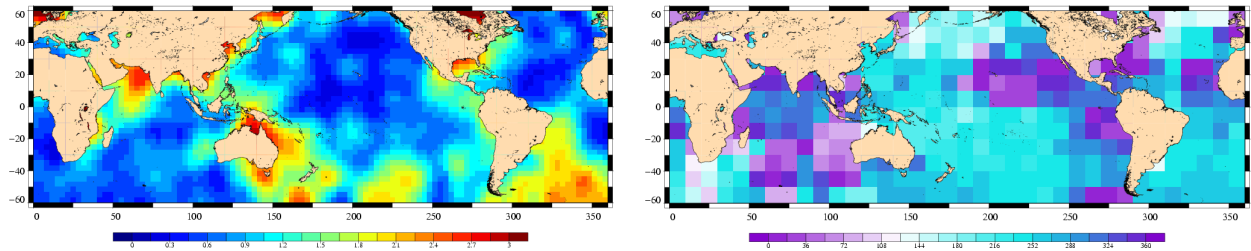


Figure 45: Amplitude (cm) and phase (deg) of the annual signal on the mean at crossovers estimated in 10x10 deg boxes using FES99

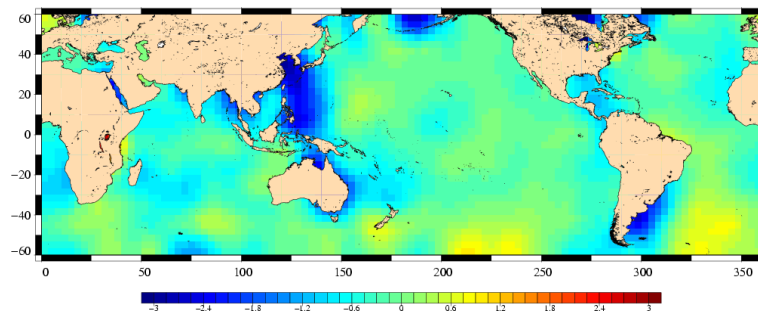


Figure 46: Difference of the amplitude (cm) of the annual signal estimated using GOT00 and FES04 tide

8.3.3.2 Comparison between GOT00 and FES04 tidal waves

As expected, in figure 47, the amplitude of the annual signal with a SSH including no tide corrections shows the same geographical as diurnal tidal waves (see figure 51).

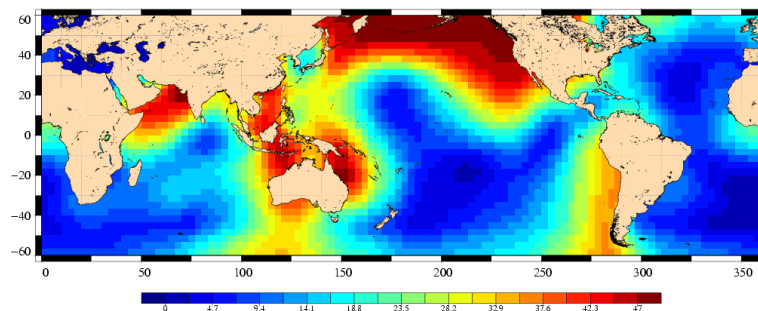


Figure 47: Amplitude (cm) of the annual signal on the mean at crossovers estimated in 10x10 deg boxes using no tide correction

In order to identify the differences between the two tide models, the main components of the oceanic tides are compared here (figure 48 to 55)

<p>CLS CalVal Envisat</p>	<p>Envisat validation and cross-calibration activities</p>	<p>Page : 51 Date : April 19, 2007</p>
<p>Ref: CLS.DOS/NT/06.300</p>	<p>Nom.: SALP-RP-MA-EA-21376-CLS</p>	<p>Issue: 0rev1</p>

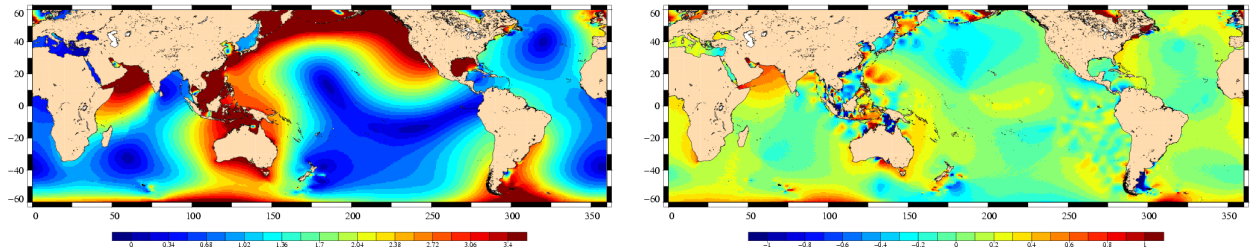


Figure 48: *Q1 oceanic tide component of Fes04 and difference between Q1 component of FES04 and GOT00*

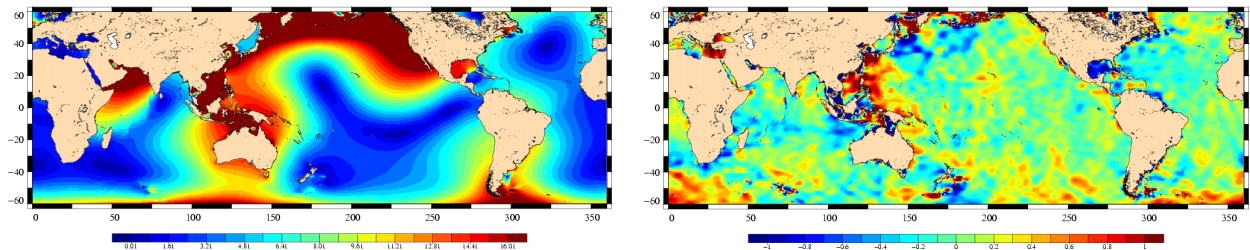


Figure 49: *O1 oceanic tide component of Fes04 and difference between O1 component of FES04 and GOT00*

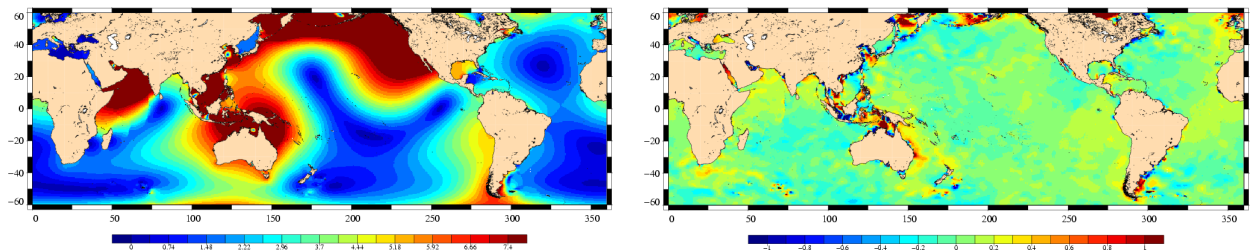


Figure 50: *P1 oceanic tide component of Fes04 and difference between P1 component of FES04 and GOT00*

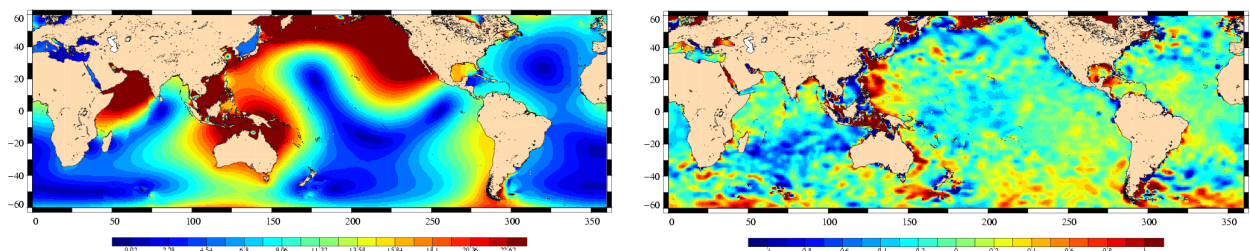


Figure 51: *K1 oceanic tide component of Fes04 and difference between K1 component of FES04 and GOT00*

<p>CLS CalVal Envisat</p>	<p>Envisat validation and cross-calibration activities</p>	<p>Page : 52 Date : April 19, 2007</p>
<p>Ref: CLS.DOS/NT/06.300</p>	<p>Nom.: SALP-RP-MA-EA-21376-CLS</p>	<p>Issue: 0rev1</p>

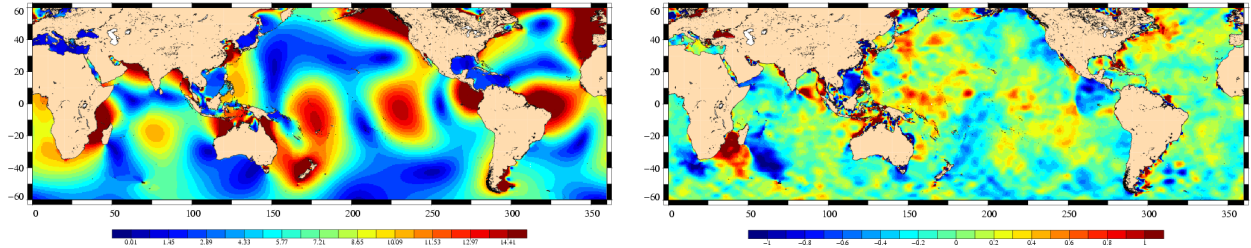


Figure 52: *N2 oceanic tide component of Fes04 and difference between N2 component of FES04 and GOT00*

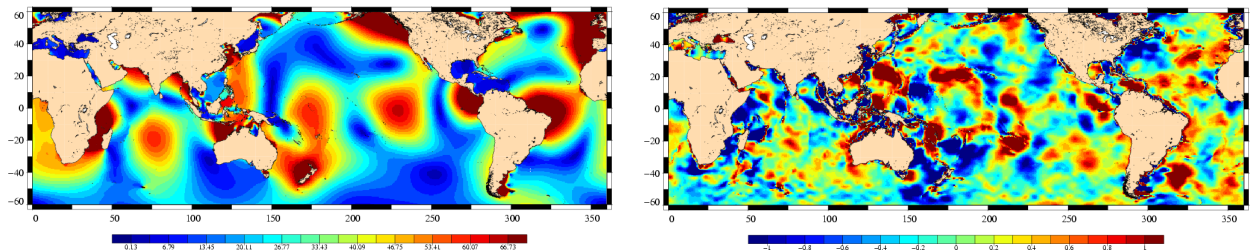


Figure 53: *M2 oceanic tide component of Fes04 and difference between M2 component of FES04 and GOT00*

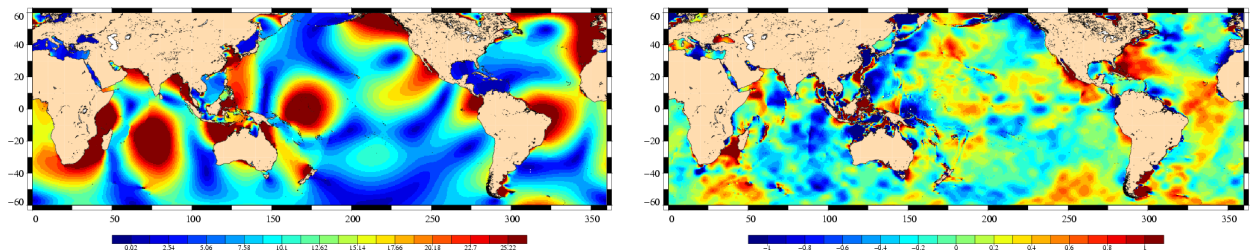


Figure 54: *S2 oceanic tide component of Fes04 and difference between S2 component of FES04 and GOT00*

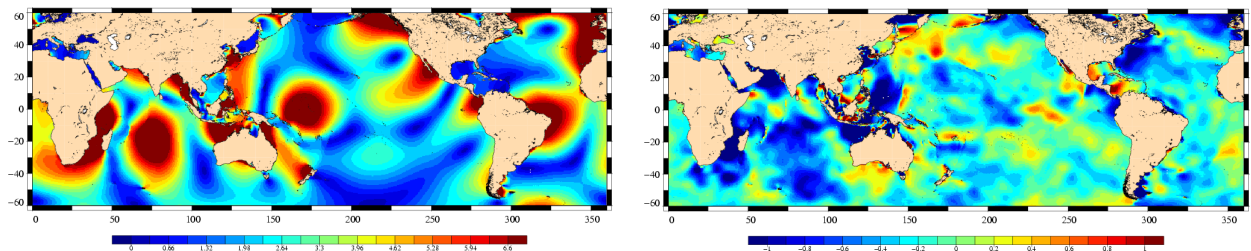


Figure 55: *K2 oceanic tide component of Fes04 and difference between K2 component of FES04 and GOT00*

CLS CalVal Envisat	Envisat validation and cross-calibration activities	Page : 53 Date : April 19, 2007
Ref: CLS.DOS/NT/06.300	Nom.: SALP-RP-MA-EA-21376-CLS	Issue: 0rev1

8.3.4 Impact of orbit on the annual signal

It is also interesting to evaluate the impact of the orbit on the annual signal, as the oceanic tide is also used in the orbit computation. The DEOS Institute at Delft University produces a POE orbit with standards different from the CNES POE orbit (Doornbos et al., 2005 [10]). Notably, the Delft orbit has been computed using the Grace gravity model EIGEN-GRACE01S since the cycle 10. The tide used in the computation of this orbit is PGS7751E (GSFC). The patterns obtained are similar as those observed for the CNES orbit but the amplitude is in general lower, in particular in South Atlantic.

The map of the estimated amplitude using the Delft POE with tide GOT00 and FES04 is plotted in figure 57. The map are similar from those using the CNES POE, figure 42 and figure 43, though the amplitude of the signal is slightly lower.

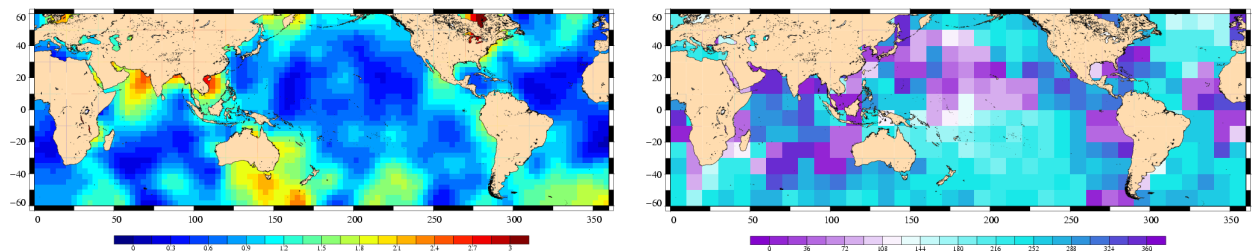


Figure 56: *Amplitude (cm) and phase (deg) of the annual signal on the mean at crossovers estimated in 10x10 deg boxes using Delft orbit*

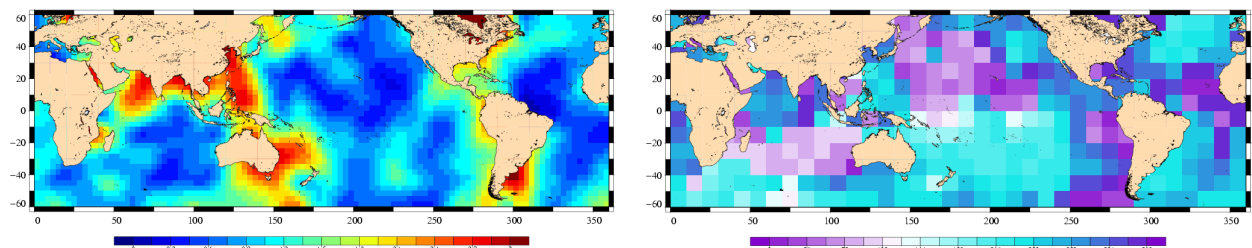


Figure 57: *Amplitude (cm) and phase (deg) of the annual signal on the mean at crossovers estimated in 10x10 deg boxes using Delft orbit and FES04 tide*

CLS CalVal Envisat	Envisat validation and cross-calibration activities	Page : 54 Date : April 19, 2007
Ref: CLS.DOS/NT/06.300	Nom.: SALP-RP-MA-EA-21376-CLS	Issue: 0rev1

8.4 Comparison Orbit POE and Delft

The aim of this study is to compare the orbit included in the product, the CNES POE orbit, to the other available POE orbit, the Delft orbit. The Delft university computes routinely a precise orbit for Envisat. The Eigen-Grace01S orbits are available at <http://www.deos.tudelft.nl/ers/precorbs/orbits/> (Doornbos et al, 2004). The Delft orbit has been updated in our database for cycles 10 to 47.

8.4.1 Orbit differences

Figure 58 shows the mean differences over the period 31-37 and 41-47.

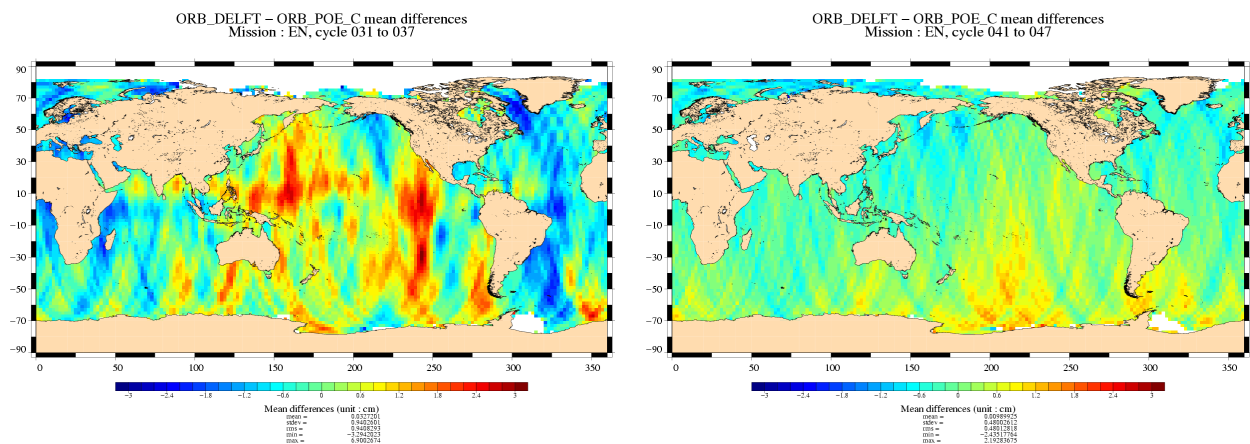


Figure 58: *Delft - CNES (GRIM5) mean differences (left), Delft - CNES (EIGEN-CG03C) mean differences (right).*

The differences observed between the 2 maps shows that the mean differences decrease with the new CNES orbit configuration. Both orbits use the Grace gravity models, over cycle 41 to 47. The differences are quite small, lower than 1 cm. Delft orbit is slightly higher than the CNES orbit in Southern Pacific Ocean and in the high latitudes in the Southern Hemisphere.

8.4.2 Performance at crossovers

In figure 59 the mean ascending/descending differences are small using the two orbits. However, using the Delft orbit, some geographically correlated biases are still visible, notably in West Pacific and West Indian Ocean. This might be due to the fact that the gravity model used in the Delft computation is an early version of Grace gravity model.

Figure 60 shows the difference between the variance of the Delft SSH and the CNES SSH. Before cycle 40, the difference is negative which mean that the performances of the Delft SSH are better than the CNES SSH. On cycle 41 onwards, the opposite observation can be made. The gain in variance using the CNES SSH is about 2cm^2 .

<p>CLS CalVal Envisat</p>	<p>Envisat validation and cross-calibration activities</p>	<p>Page : 55 Date : April 19, 2007</p>
<p>Ref: CLS.DOS/NT/06.300</p>	<p>Nom.: SALP-RP-MA-EA-21376-CLS</p>	<p>Issue: 0rev1</p>

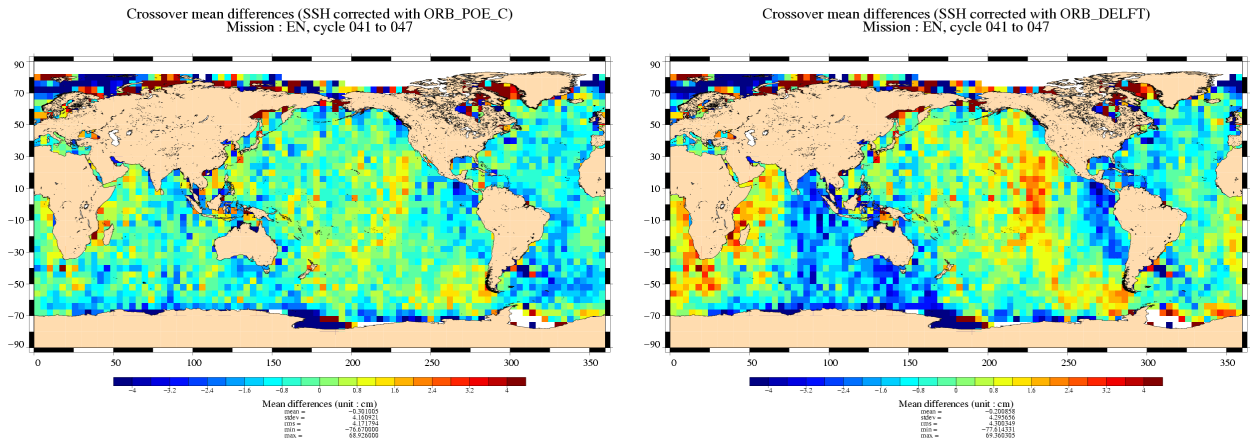


Figure 59: Crossover mean differences over cycles 41 to 47. SSH using the Delft orbit (right) and CNES orbit (left).

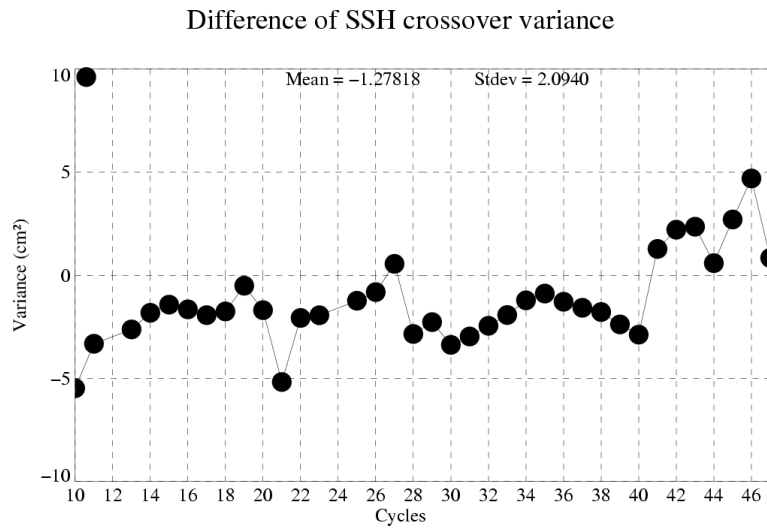


Figure 60: Difference of variance $[Var(SSH(POE Delft)) - Var(SSH(POE CNES))]$ (cm²)

CLS CalVal Envisat	Envisat validation and cross-calibration activities	Page : 56 Date : April 19, 2007
Ref: CLS.DOS/NT/06.300	Nom.: SALP-RP-MA-EA-21376-CLS	Issue: 0rev1

8.5 The B Side configuration performances

Preliminary results on Envisat RA-2 Side B behaviour over ocean

Y. Faugère (CLS)
A. Olivier (CLS)



ENVISAT Altimetry Quality Working Group Meeting (#7)



- 1 -

Introduction

WARNING 1 : Data Side B exist BUT they are computed with Side A configuration of the Ground Segment Chain !

- Aim of the study: complementary diagnostic on the Side B data: Real data DO exist.
 - Are they absolutely unusable?
 - Can they be use while waiting for the re processing?

WARNING 2: S Band power drop on Side B

- Study focused on Ku band parameters
- SSH and SLA assessments are performed with the GIM Ionospheric correction (Bifrequency Iono correction absent)



ENVISAT Altimetry Quality Working Group Meeting (#7)



- 2 -

CLS CalVal Envisat	Envisat validation and cross-calibration activities	Page : 57 Date : April 19, 2007
Ref: CLS.DOS/NT/06.300	Nom.: SALP-RP-MA-EA-21376-CLS	Issue: 0rev1

OverView

- Availability of measurements
- Altimeter parameters monitoring
- Sea Level Anomaly
- SSH performance assessment
- Recommendation for USO acquisition rhythm to reprocess Side B data in the good configuration of the Ground Segment Chain
- Conclusions

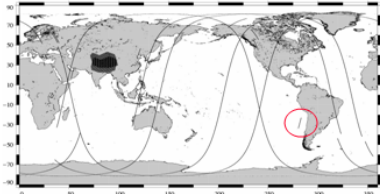


ENVISAT Altimetry Quality Working Group Meeting (#7)
- 3 -

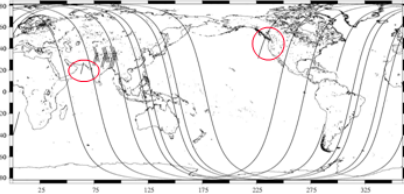


Missing measurements

Cycle 49 : Side A



Cycle 47-48 : Side B (without 25-29 May)



Mean number of 20Hz measurements	Side A	Side B
Range	19.97 / 20	19.98 / 20
Significant Wave Heigh	19.91 / 20	19.92 / 20
Sigma 0	19.99 / 20	19.99 / 20

- No major difference in the availability of measurements.



ENVISAT Altimetry Quality Working Group Meeting (#7)
- 4 -



CLS CalVal Envisat	Envisat validation and cross-calibration activities	Page : 58 Date : April 19, 2007
Ref: CLS.DOS/NT/06.300	Nom.: SALP-RP-MA-EA-21376-CLS	Issue: 0rev1

Altimeter parameters and comparison points

Altimeter parameters Side A Compared to Side B:

- Altimeter Range
- Significant Wave Height
- Sigma 0
- Peakiness of the waveform + Off nadir angle

} Estimated with MLE3

Comparison points:

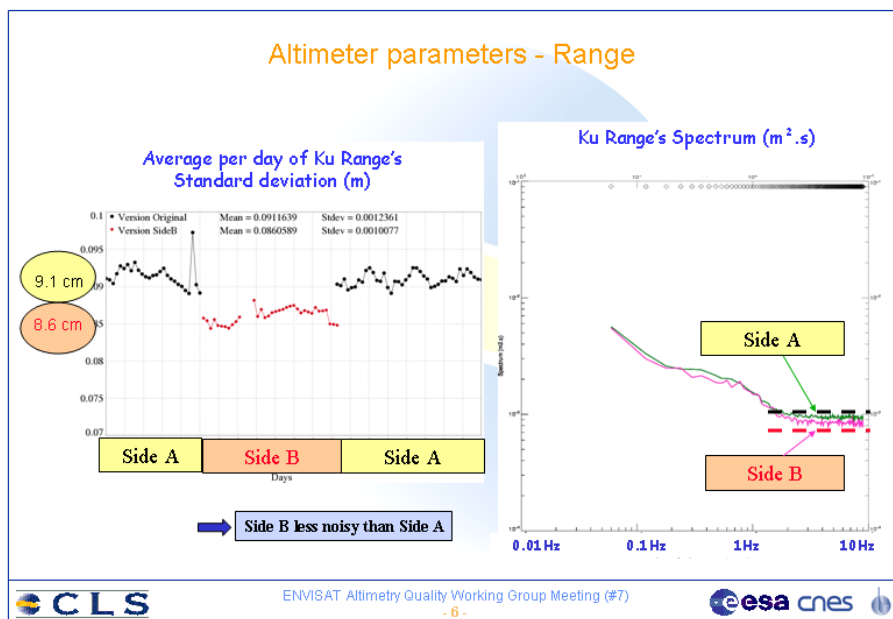
- Cycle Monitoring from the beginning of the mission
- Daily monitoring on the whole cycles 47-48-49
 - Cycle 47 from pass 790 to 1002 (from April 17th to July 31th)
 - Cycle 48 from pass 1 to 89 and 233 to 847 (from May 15th to June 21th)
- Histogram of parameters on Cycle 49 (Side A) compared to the 37 days of side B (Mixed Cycles 47 and 48)



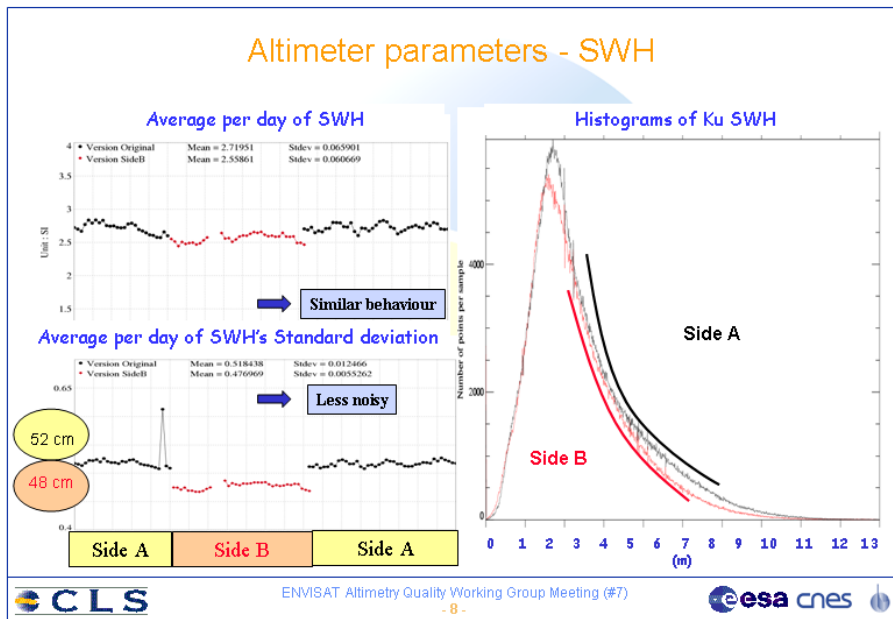
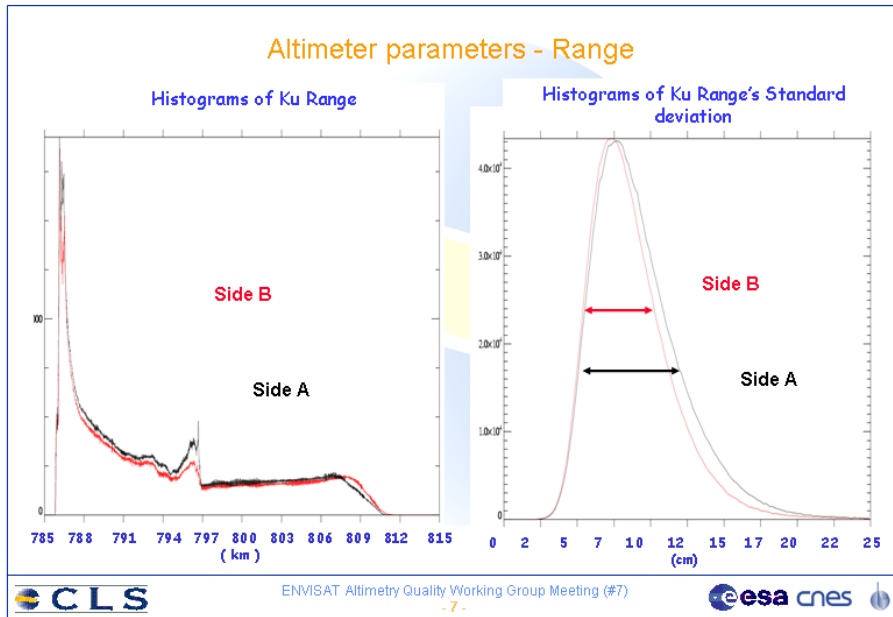
ENVISAT Altimetry Quality Working Group Meeting (#7)



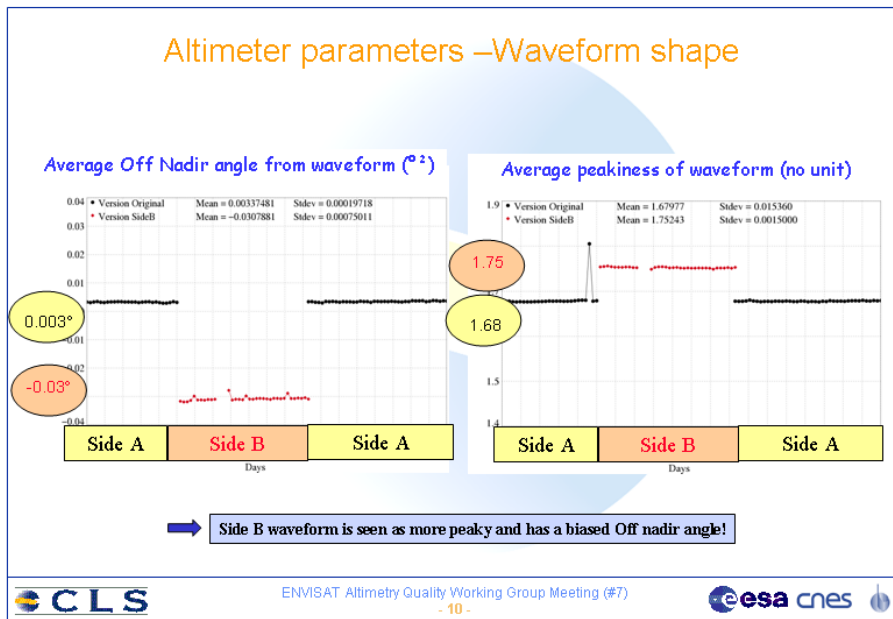
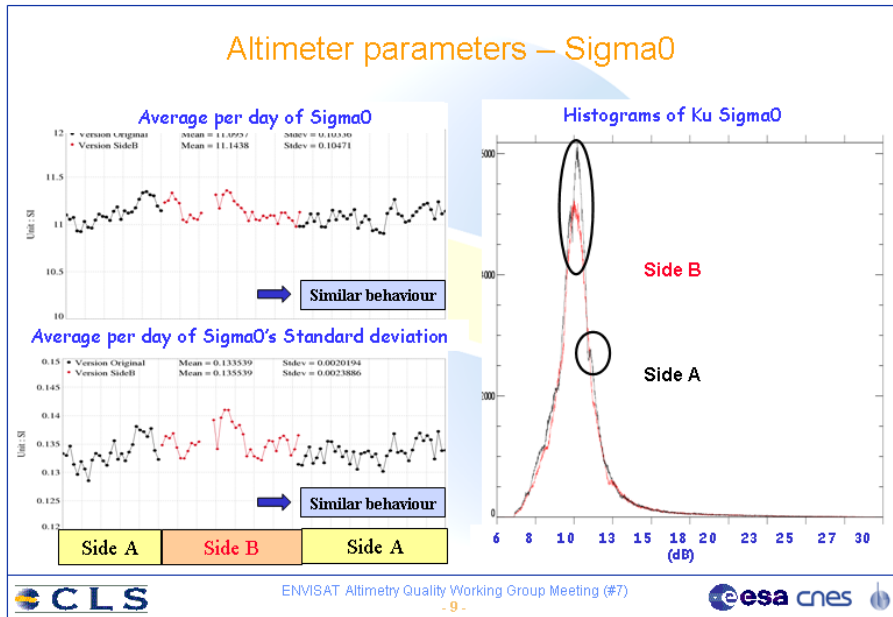
- 5 -



<p>CLS CalVal Envisat</p>	<p>Envisat validation and cross-calibration activities</p>	<p>Page : 59 Date : April 19, 2007</p>
<p>Ref: CLS.DOS/NT/06.300</p>	<p>Nom.: SALP-RP-MA-EA-21376-CLS</p>	<p>Issue: 0rev1</p>



CLS CalVal Envisat	Envisat validation and cross-calibration activities	Page : 60 Date : April 19, 2007
Ref: CLS.DOS/NT/06.300	Nom.: SALP-RP-MA-EA-21376-CLS	Issue: 0rev1



CLS CalVal Envisat	Envisat validation and cross-calibration activities	Page : 61 Date : April 19, 2007
Ref: CLS.DOS/NT/06.300	Nom.: SALP-RP-MA-EA-21376-CLS	Issue: 0rev1

Synthesis on the altimetric parameters estimations

- Altimetric **range** and **SWH** unbiased between Side A and B but Side B standard deviation is significantly lower.
- For **sigma0**, no major difference where noticed except that Side B histogram seems less chaotic.
- Side B **waveform shape parameters** are strongly biased : probably due to a bad instrumental parameters (+Filter).

This preliminary results show that :

- Shape of the waveform not properly taken into account in the retracking: real need to reprocess data with good configuration of the Ground Segment.

BUT!!!

- No major problems are observed, Side B data seem usable.



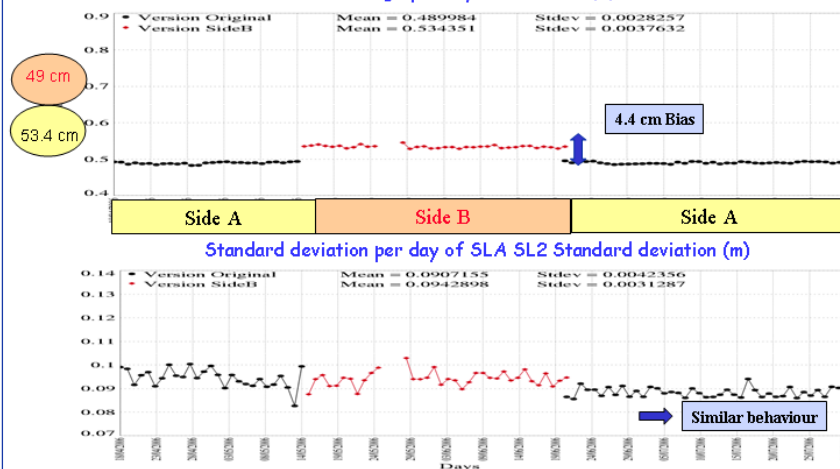
ENVISAT Altimetry Quality Working Group Meeting (#7)

- 11 -



Sea Level Anomaly monitoring

Average per day of SLA SL2 (m)

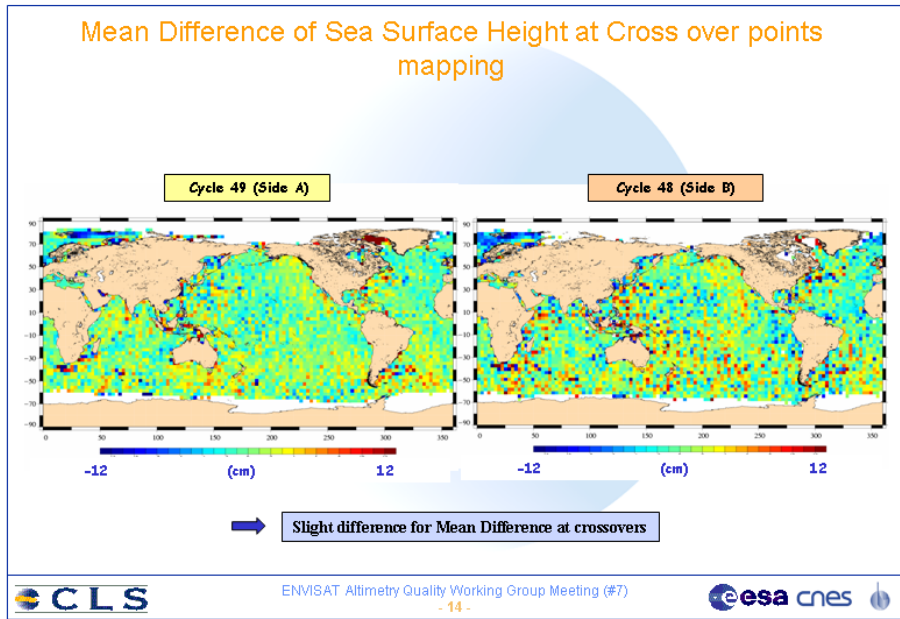
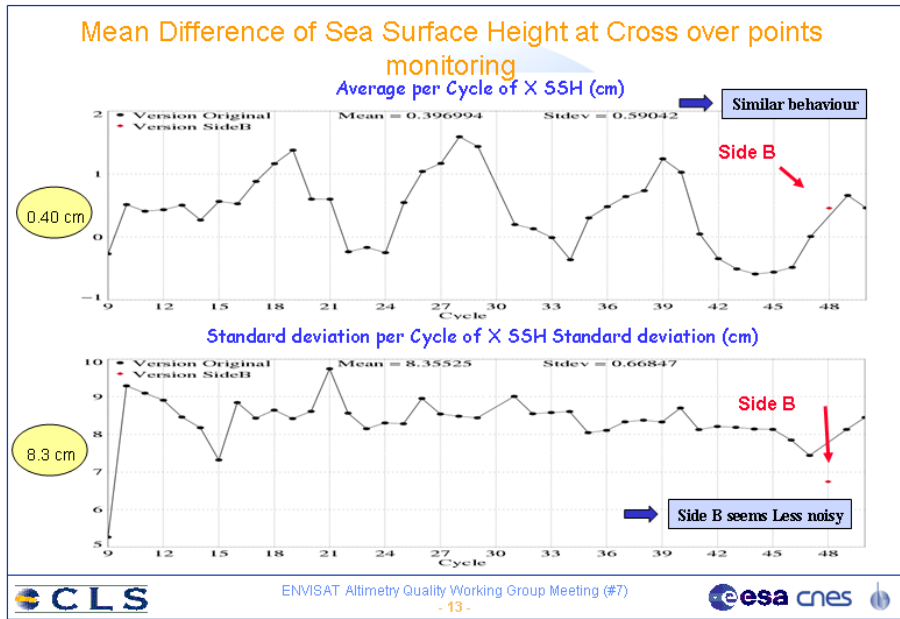


ENVISAT Altimetry Quality Working Group Meeting (#7)

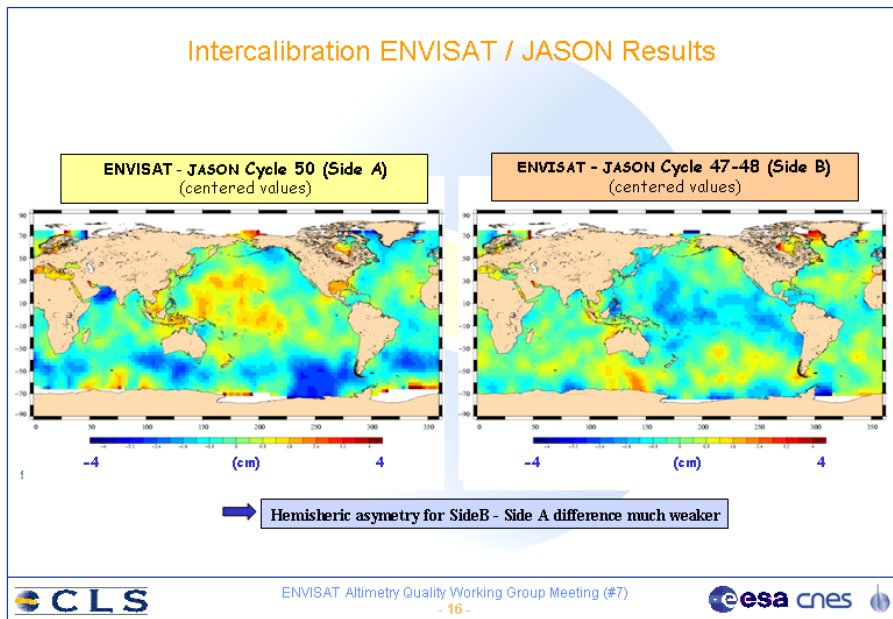
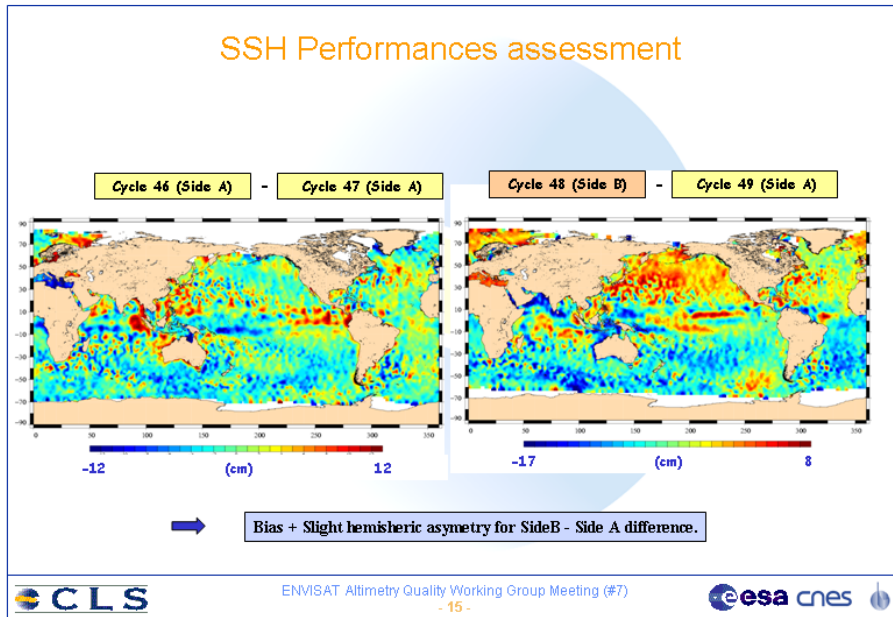
- 12 -



<p>CLS CalVal Envisat</p>	<p>Envisat validation and cross-calibration activities</p>	<p>Page : 62 Date : April 19, 2007</p>
<p>Ref: CLS.DOS/NT/06.300</p>	<p>Nom.: SALP-RP-MA-EA-21376-CLS</p>	<p>Issue: 0rev1</p>



CLS CalVal Envisat	Envisat validation and cross-calibration activities	Page : 63 Date : April 19, 2007
Ref: CLS.DOS/NT/06.300	Nom.: SALP-RP-MA-EA-21376-CLS	Issue: 0rev1



CLS CalVal Envisat	Envisat validation and cross-calibration activities	Page : 64 Date : April 19, 2007
Ref: CLS.DOS/NT/06.300	Nom.: SALP-RP-MA-EA-21376-CLS	Issue: 0rev1

Synthesis on the oceanic parameters

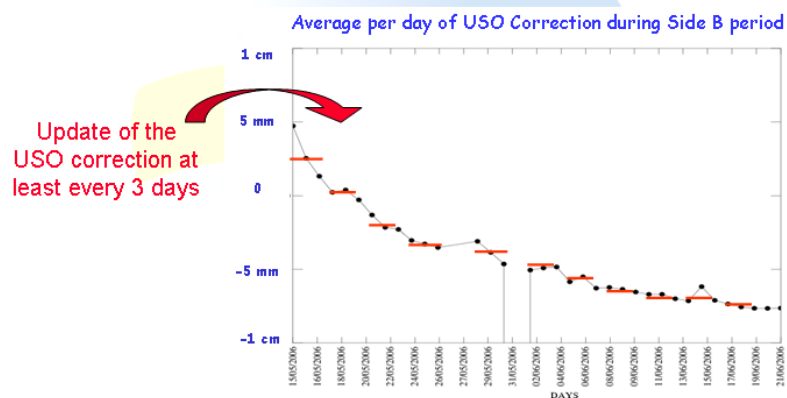
- Apparently no bias on altimetric parameters
BUT
- Bias on SLA of 4.4cm with asymetry between N and S hemispheres less visible on the J1/ENVISAT Intercalibration on Side B period.
- If it persists after the re-processing, reasons will still have to be investigated:
 - Probably not datation problem (0.385ms for Cycle 48, 0.205ms for Cycle 47)
 - Wave estimation or SSB?
 - First order SSB = -0.043 for Cycles 46 and 49 (Side A)
 - First order SSB = -0.030 for Cycles 47 and 48 (Side B)
 - Other reasons?



ENVISAT Altimetry Quality Working Group Meeting (#7)
- 17 -



USO period to be used for the reprocessing of Side B data in the good configuration of the Ground Segment Chain



ENVISAT Altimetry Quality Working Group Meeting (#7)
- 18 -



CLS CalVal Envisat	Envisat validation and cross-calibration activities	Page : 65 Date : April 19, 2007
Ref: CLS.DOS/NT/06.300	Nom.: SALP-RP-MA-EA-21376-CLS	Issue: 0rev1

General Conclusions

- These results are very preliminary : bad configuration of Ground segment. Need to be done again with good configuration (USO rhythm of acquisition proposed).
- However, give good indication of the quality of the data and performances.
 - Good availability of data in Side B configuration
 - Some bias and difference of noise on Altimetric parameters (mainly waveform shape parameters).
 - Low differences on Histograms.
 - On SLA and performances: no difference in average but some geographically correlated differences. Asymetry N/S hemispheres.



**We DO NOT recommend to use Side B data (in this bad configuration)
HOWEVER, they are not TOTALLY crazy:
For a transition period (before re-processing) those data could be used with VERY
MUCH care!**



CLS CalVal Envisat	Envisat validation and cross-calibration activities	Page : 66 Date : April 19, 2007
Ref: CLS.DOS/NT/06.300	Nom.: SALP-RP-MA-EA-21376-CLS	Issue: 0rev1

8.6 Wet tropospheric correction

In 2005, a change of the CMA version was implemented and among other evolutions, radiometric wet tropospheric correction was corrected. The modification mainly consists in a better accounting of the side lobes effect. In order to validate this evolution, a multi mission study was performed through a quantification of the differences between the new radiometer correction and the model correction. The differences between both corrections are analysed, then, the impact of the computation evolution (better accounting of the side lobes effect) is analysed in terms of data pollution by land emissivity.

For all the results shown hereafter, the reference is the ECMWF model correction. For the moment, it is known to be less accurate than the radiometric measurement one, but it presents the advantage of being very stable and independent from all the missions. The radiometric measurement correction studied here concerns more specifically the ENVISAT radiometer (MWR) correction for the last CMA version (V7).

8.6.1 Monitoring per day of the wet troposphere correction differences (radiometer - model) and long term monitoring

Figure 61 shows the differences between the radiometric correction and the ECMWF model one for 4 altimetric missions.

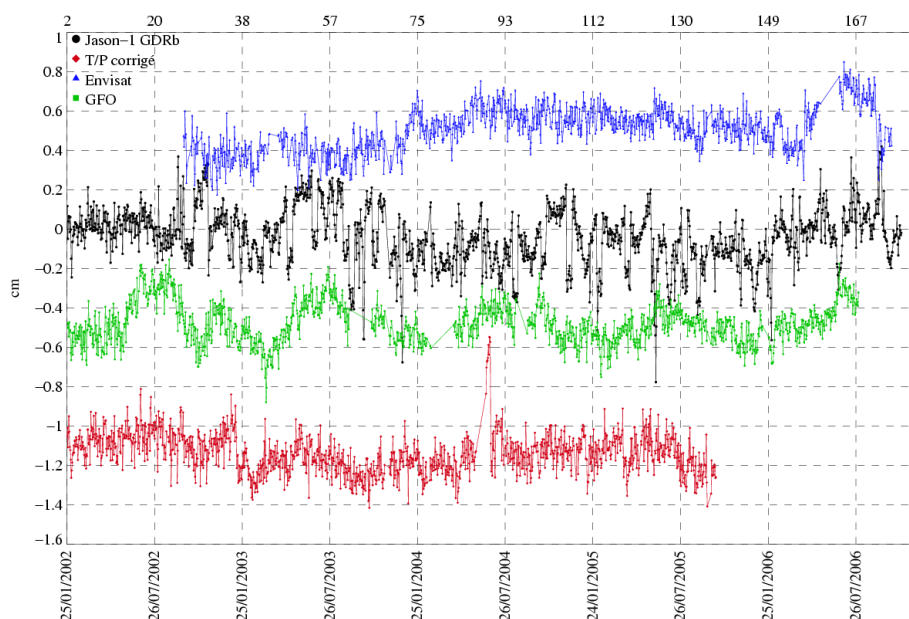


Figure 61: Mean per day of the difference between the radiometric corrections and the ECMWF model: Jason-1, T/P, GFO, et ENVISAT.

Different behaviours can be noticed on ENVISAT's correction compared to the other missions:

- The global mean has an amplitude of about 3mm, similarly to the others but the local drifts are not quite the same.
- The noise level is relatively smaller than the others mainly JASON's which noise seems higher probably because of the several yaw manoeuvres it is affected by.

CLS CalVal Envisat	Envisat validation and cross-calibration activities	Page : 67 Date : April 19, 2007
Ref: CLS.DOS/NT/06.300	Nom.: SALP-RP-MA-EA-21376-CLS	Issue: 0rev1

- Like for JASON and GFO, the difference tends to present a 4mm oscillation at the end of 2006
- But, unlike the other missions, ENVISAT correction undergoes a 2 to 3 mm drift in the middle of the period. Furthermore, ENVISAT correction presents 2 small jumps around cycle 48 and 49 which are not seen on other missions.
- ENVISAT's correction is also the only one not to present a 2 to 3 mm oscillation at the end of 2002.

When comparing the different radiometric corrections, local drifts are observed and the oscillations can not be attributed to a geophysical signal as it is not consistent for all mission. The long term signals are not as stable as the model and it is not possible to conclude if one of the radiometric correction is better than the other with only these sole observations. For the moment, it is therefore strongly recommended to keep on using the ECMWF model correction for any long term monitoring such as the mean sea level drift.

8.6.2 Geographical correlations of the wet troposphere correction differences (radiometer - model)

Figure 62 (left) shows the difference in term of bias and standard deviation between ENVISAT radiometric corrections and the ECMWF model for a period of one year from December the 2nd of 2003 to December the 2nd of 2004. It shows that although the average difference is weak (millimetric), the geographical repartition is not homogeneous.

In dry zones (high latitudes) the model has globally smaller values than the radiometric measures. Conversely in the inter-tropical zones the model correction is higher.

A difference is also noticeable on the ice shores where a blue line (radiometric correction smaller than the model's) limits the zone of glaciations. Indeed, both correction do not behave the same way on ice. This is traduced by a bias on the annual average.

Concerning the energy repartition (standard deviation) (see figure 62 (right)), the differences are weaker. However they are still situated on wet zones between tropics and close to ice shelves.

The difference between the model and the bi-frequency radiometer correction is indeed a good indication of ice zones localisation and Y. Faugère showed (in [R-2]) that it enables to flag the ice precisely.

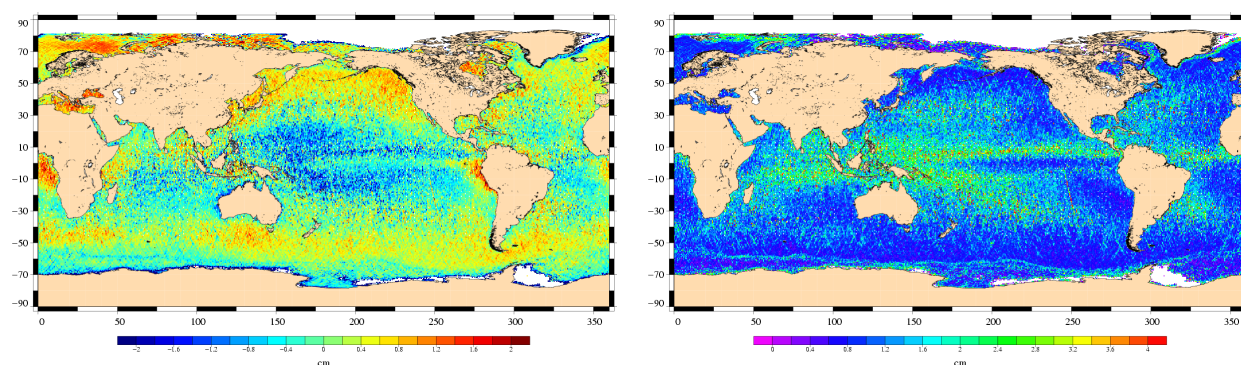


Figure 62: Map of the difference between ENVISAT radiometric corrections and the ECMWF model. Left hand map shows the average on one year (02/12/2003 to 02/12/2004). Right hand map shows the associated standard deviation.

These maps are completed by a diagramme representing the differences between both wet tropospheric

CLS CalVal Envisat	Envisat validation and cross-calibration activities	Page : 68 Date : April 19, 2007
Ref: CLS.DOS/NT/06.300	Nom.: SALP-RP-MA-EA-21376-CLS	Issue: 0rev1

corrections calculated on a period of 1 year (December the 2nd of 2003 to December the 2nd of 2004) and averaged by classes of latitude presented in Figure 63.

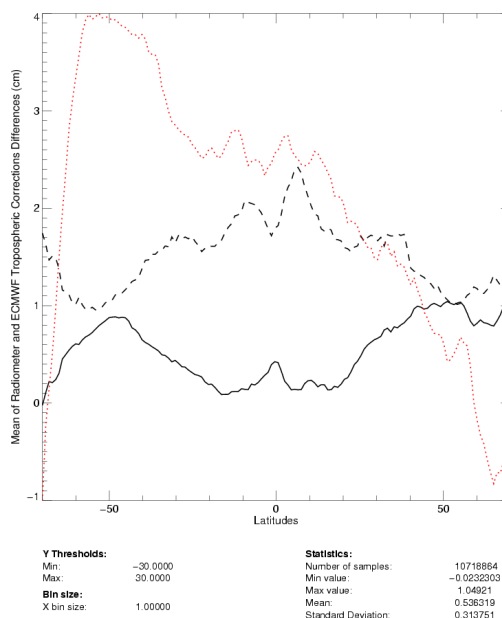


Figure 63: *Difference between ENVISAT radiometric and the ECMWF model corrections as a function of latitude. Black plain curves (-) represent the mean difference, black dotted lines (- - -) represent the standard deviation and the red curves (-) represent the number of valid measurements repartition.*

The mean bias between both corrections changes with latitude: radiometric correction has lower values for wet zones than for dry ones (as seen in Figure 62 (right)). A similar behaviour can be observed on the other missions which would indicate that the model over estimates the correction in these zones.

It is recalled that MWR is a dual-frequency radiometer. Conversely, JASON JMR is a tri-frequency one. The number of frequencies has a direct impact on the correction (for instance concerning the stability of the correction near coasts, and for extreme (very wet or very dry) atmospheric conditions). The differences between the model and the radiometer are therefore much weaker when the instrument has 3 frequencies.

CLS CalVal Envisat	Envisat validation and cross-calibration activities	Page : 69 Date : April 19, 2007
Ref: CLS.DOS/NT/06.300	Nom.: SALP-RP-MA-EA-21376-CLS	Issue: 0rev1

8.6.3 Stability of the corrections when approaching coasts

The main evolution of the radiometric correction consists in a better accounting of the side lobes. This was expected to decrease the impact of data pollution by land emissivity. The evolution consists in tabulating the effect of the earth in the secondary lobes on a global grid at a resolution of 1° instead of using a constant correction. Eight tables are used, one for each frequency and each season.

Differences between wet troposphere are calculated on a period of 1 year (between December the 2nd of 2003 to December the 2nd of 2004) and averaged by classes of distance to the coast as presented in Figure 64.

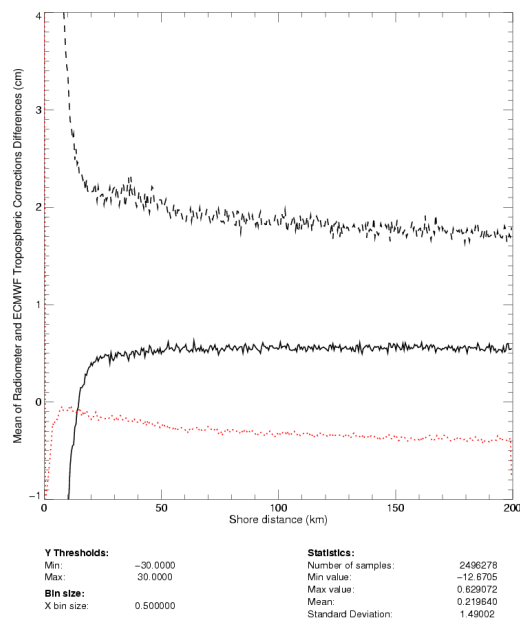


Figure 64: *Difference between ENVISAT radiometric and the ECMWF model corrections as a function of distance to coast. Black plain curves (-) represent the mean difference, black dotted lines (- - -) represent the standard deviation and the red curves (-) represent the number of valid measurements repartition.*

When approaching from the coast, the average bias decreases and the standard deviation increases exponentially. This shows a very strong instability near coasts which could be due to the pollution of the radiometric footprint by the land emissivity.

However, figure 65 shows that this instability is very much closer from the coast with the new V7 CMA version than with the previous one. The pollution of land is visible at around 30km from the coast instead of more than 180km with the former version. The pollution of data by coasts is therefore very minimized now thanks to the better accounting of the side lobe effect on the new V7 CMA version.

<p style="text-align: center;">CLS CalVal Envisat</p>	<p style="text-align: center;">Envisat validation and cross-calibration activities</p>	<p>Page : 70 Date : April 19, 2007</p>
<p>Ref: CLS.DOS/NT/06.300</p>	<p>Nom.: SALP-RP-MA-EA-21376-CLS</p>	<p>Issue: 0rev1</p>

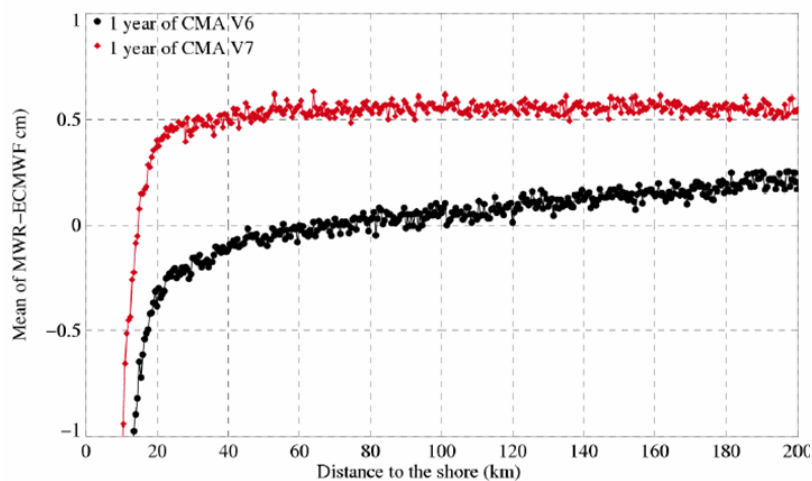


Figure 65: *Difference between ENVISAT radiometric and the ECMWF model corrections as a function of distance to coast. Better accounting of Side Lobe effect for the new V7 version compared to V6 version.*

CLS CalVal Envisat	Envisat validation and cross-calibration activities	Page : 71 Date : April 19, 2007
Ref: CLS.DOS/NT/06.300	Nom.: SALP-RP-MA-EA-21376-CLS	Issue: 0rev1

8.6.4 Conclusion

The comparison between two corrections of wet troposphere was performed: one calculated from the radiometer measurement and the other calculated from the ECMWF model. Both correction show different behaviours which enabled us to draw several conclusions.

First, the monitoring of the correction based on the radiometer measurement presents some instabilities and local drifts. These variabilities do not seem to be due to geophysical signals as they are different for all altimetric missions. Therefore, it is strongly recommended to keep on using the ECMWF model correction for any long term monitoring such as the mean sea level drift.

ENVISAT bi-frequency radiometer is shown to be very instable near ice zones and as a consequence, the standard deviation of the radiometer correction compared to the model one is a very robust way of flagging ice shelves.

The representation of the correction mean difference and variability as a function of latitude showed that the model seemed to be over-estimated for wet zones. A very strong instability of the radiometric correction was also shown for measures when approaching the coasts. The new version of CMA is shown to decrease significantly the distance of data pollution by the land. Indeed, the limit distance of land emissivity impact on the data was previously more than 180km. It is now situated at less than 30km from the coast.

CLS CalVal Envisat	Envisat validation and cross-calibration activities	Page : 72 Date : April 19, 2007
Ref: CLS.DOS/NT/06.300	Nom.: SALP-RP-MA-EA-21376-CLS	Issue: 0rev1

8.7 High frequency analysis

A new configuration of Envisat and Jason GDR has been operational since september 2005. In particular, a new retracking (MLE4) has been implemented on Jason-1. The purpose of this analysis is to describe the impact of this new retracking on the high frequency signal of Jason-1 data. Two methods have been used in this analysis, a spectral analysis and filtering technique. These two methods are described in [18]. The data corresponding to cycles 128-135 Jason-1 have been used here.

8.7.1 Spectral analysis

Figure 66 shows the Envisat and Jason-1 spectra using 20Hz and 1Hz data over cycle 131. On 20Hz data, at frequencies higher than 3Hz, the Envisat signal is hidden by a plateau at $10^{-3}m^2.s$. This plateau is the signature of a 9.2 cm white noise. On Jason-1 MLE3 data, the plateau is lower and the behaviour of the spectrum is different from Envisat one between 0.1 and 1Hz. The use of MLE4 data strongly changes the shape of the spectra in this range of frequency. Now Envisat and Jason-1 are much more consistent both at 20Hz and 1Hz.

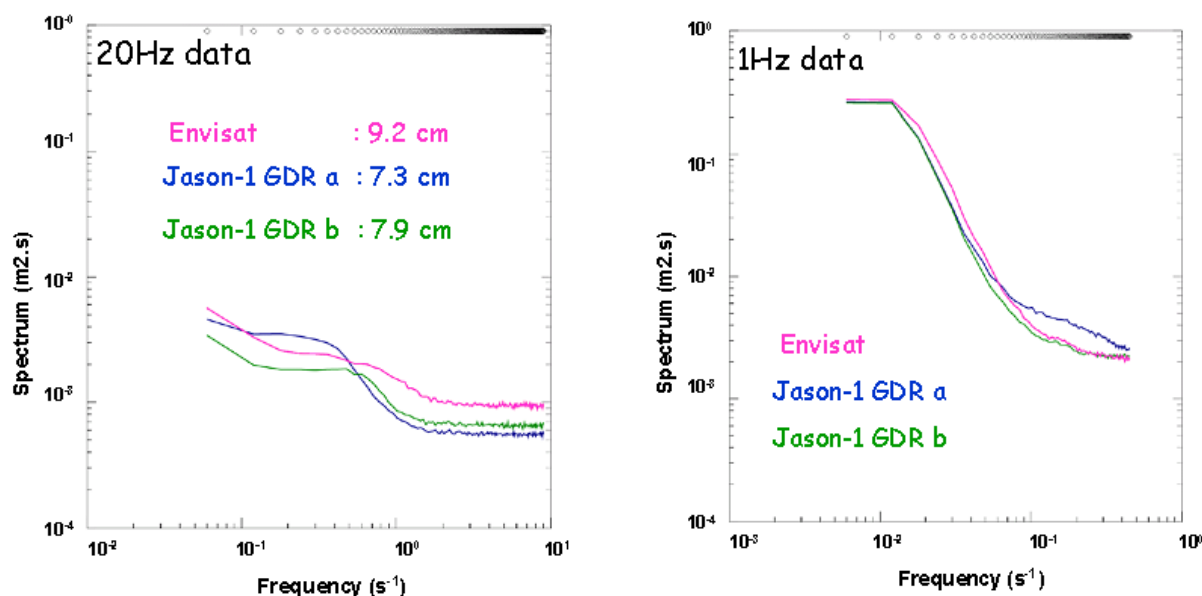


Figure 66: Spectra of Envisat and Jason-1 SLA using 20Hz measurements(left) and 1Hz measurements (right).

8.7.2 Filtering technique

Using a filtering technique described in figure 67 allows us to know the geographical distribution of the high frequency content for Envisat and Jason-1 over cycles 128-135. Figure 68 shows that the consistency between Envisat and Jason-1 is improved in wet areas.

CLS CalVal Envisat	Envisat validation and cross-calibration activities	Page : 73 Date : April 19, 2007
Ref: CLS.DOS/NT/06.300	Nom.: SALP-RP-MA-EA-21376-CLS	Issue: 0rev1

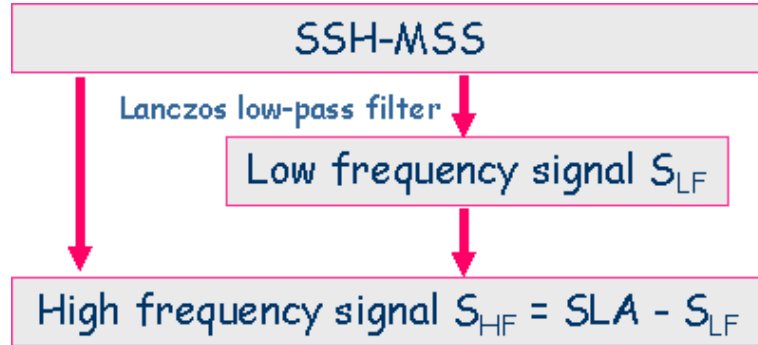


Figure 67: *Filtering technique*

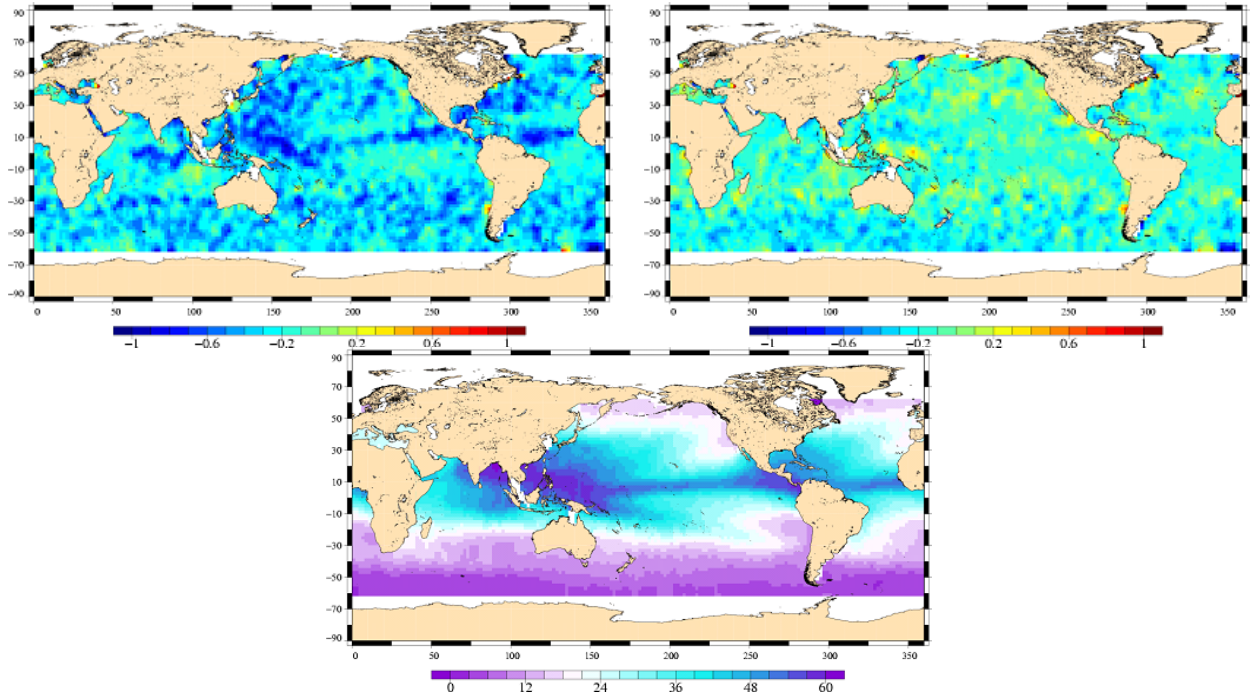


Figure 68: *Map of standard deviation of difference between $\sigma(S_{HF}(EN))$ and $\sigma(S_{HF}(J1))$ with GDR a (top left), GDR b (top right) and Envisat mean water vapour (bottom)*

CLS CalVal Envisat	Envisat validation and cross-calibration activities	Page : 74 Date : April 19, 2007
Ref: CLS.DOS/NT/06.300	Nom.: SALP-RP-MA-EA-21376-CLS	Issue: 0rev1

9 Conclusion

A statistical evaluation of Envisat altimetric measurements over ocean has been presented in this report. With four years of data now available, Envisat altimetric measurements show good general results. A very good availability on every surface and very low editing ratios over ocean are observed. One of the major improvements of the RA-2 with respect to ERS RA is the S-band allowing range corrections due to ionospheric effects. However the so-called S-Band anomaly impacts more than 4 % of the available data on average. This ratio has been improved since cycle 31 and a method is currently under development to reconstruct the impacted S-band waveforms. A new configuration (IPF5.02/CMA7), operational since September 2005, allows to strongly improve the products quality: a new orbit configuration, an improved Sea State bias modeling and new geophysical corrections such as the correction of high frequency ocean signals. The ocean-1 altimeter parameters are stable, compared to Jason-1 and ERS-2. A major anomaly impacted the USO device. A temporary correction procedure has been implemented by ESA. Using the proposed auxiliary files, Envisat Ra-2 data remain at the same high level of accuracy. The global mean [MWR-ECMWF model] wet troposphere correction difference has a strange behaviour: an increasing trend, then an decreasing trend, and finally a strong signal over 5 cycles. The crossover analysis show that, when using the USO auxiliary correction, Envisat has performances similar to Jason-1. The time invariant errors, observed on the crossover mean, are mainly due to gravity induced orbit errors and are well corrected by the use of a Grace Gravity model. The time varying errors have to be analysed further to confirm the possible error in the tide correction. Finally Envisat MSL global trend is not consistent to Jason-1 trend.

A reprocessing of the whole Envisat altimetric mission is expected in mid-2007. These new products will further improve the high quality level of the Envisat altimetric mission and will make easier the data fusion for multi-mission altimetry, as it is essential for oceanography and applications.

CLS CalVal Envisat	Envisat validation and cross-calibration activities	Page : 75 Date : April 19, 2007
Ref: CLS.DOS/NT/06.300	Nom.: SALP-RP-MA-EA-21376-CLS	Issue: 0rev1

References

- [1] Abdalla, S., "A wind retrieval algorithm for satellite radar altimeters", ECMWF Technical Memorandum, in preparation, 2006.
- [2] Ablain, M., G. Pontonnier, B. Soussi, P. Thibaut, M.H. de Launay, J. Dorandeu, and P. Vincent. 2004. Jason-1 GDR Quality Assessment Report. Cycle 079. SALP-RP-P2-EX-21072-CLS079, May.
- [3] Ablain, M., J. Dorandeu, 2006. Jason-1 Validation and Cross-calibration activities. Technical Note CLS.DOS/NT/06.302
- [4] Carrère, L., and F. Lyard, Modeling the barotropic response of the global ocean to atmospheric wind and pressure forcing - comparisons with observations. 2003. Geophys. Res. Lett., 30(6), 1275, doi:10.1029/2002GL016473.
- [5] Cazenave, A., et al.,1999: Sea Level Change from Topex/Poseidon altimetry and tide gauges, and vertical crustal motions from DORIS, G. Res. Let., 26, 2077-2080.
- [6] Celani C., B. Greco, A. Martini, M. Roca, 2002: Instruments corrections applied on RA-2 Level-1B Product. 2002: Proceeding of the Envisat Calibration Workshop.
- [7] Chambers, D., P., J. Ries, T. Urban, and S. Hayes. 2002. Results of global intercomparison between TOPEX and Jason measurements and models. Paper presented at the Jason-1 and TOPEX/Poseidon Science Working Team Meeting, Biarritz (France), 10-12 June.
- [8] Dedieu M., L. Eymard, E. Obligis, N. Tran, F. Ferreira, 2005: ENVISAT Microwave Radiometer Assessment Report Cycle 039, Technical Note CLS.DOS/NT/05.147 Available at <http://earth.esa.int/pcs/envisat/mwr/reports/>
- [9] Dorandeu, J. and P.Y. Le Traon, 1999: Effects of Global Atmospheric Pressure Variations on Mean Sea Level Changes from TOPEX/Poseidon. J. Atmos. Technol., 16, 1279-1283.
- [10] Dorandeu J., Y. Faugere, F. Mertz, F. Mercier, N. Tran, 2004a: Calibration / Validation Of Envisat GDRs Cross-calibration / ERS-2, Jason-1 Envisat and ERS Symposium, Salzburg, Austria.
- [11] Dorandeu, J., M. Ablain, Y. faugere, F. Mertz, B. Soussi, 2004b, Jason-1 global statistical evaluation and performance assessment. Calibration and cross-calibration results Mar. Geod. 27(3-4): 345-372.
- [12] Doornbos E., Scharroo R., 2005: Improved ERS and Envisat precise orbit determination, Proc. of the 2004 Envisat and ERS Symposium, Salzburg, Austria.
- [13] ECMWF, The evolution of the ECMWF analysis and forecasting system Available at: http://www.ecmwf.int/products/data/operational_system/evolution/
- [14] EOO/EOX, October 2005, Information to the Users regarding the Envisat RA2/MWR IPF version 5.02 and CMA 7.1 Available at <http://earth.esa.int/pcs/envisat/ra2/articles/>
- [15] EOP-GOQ and PCF team, 2005: Envisat Cyclic Altimetric Report, Technical Note ENVI-GSOP-EOPG-03-0011 Available at: http://earth.esa.int/pcs/envisat/ra2/reports/pcs_cyclic/
- [16] Eymard L., E. Obligis, N. Tran, February 2003, ERS2/MWR drift evaluation and correction, CLS.DOS/NT/03.688
- [17] Faugere Y., Mertz F., Dorandeu J., 2003: Envisat GDR quality assesement report (cyclic), Cycle 015. SALP-RP-P2-EX-21072-CLS015, May. Available at http://www.aviso.oceanobs.com/html/donnees/calval/validation_report/en/welcome_uk.html

CLS CalVal Envisat	Envisat validation and cross-calibration activities	Page : 76 Date : April 19, 2007
Ref: CLS.DOS/NT/06.300	Nom.: SALP-RP-MA-EA-21376-CLS	Issue: 0rev1

- [18] Faugere Y., Mertz F., Dorandeu J., 2003: Envisat validation and cross calibration activities during the verification phase. Synthesis report. Technical Note CLS.DOS/NT/03.733, ESTEC contract N°16243/02/NL/FF WP6, May 16 2003 Available at http://earth.esa.int/pcs/envisat/ra2/articles/Envisat_Verif_Phase_CLS.pdf
- [19] Faugere Y., Mertz F., Dorandeu J., 2004: Envisat RA-2/MWR ocean data validation and cross-calibration activities. Yearly report. Technical Note CLS.DOS/NT/04.289, Contract N° 03/CNES/1340/00-DSO310 Available at http://earth.esa.int/pcs/envisat/ra2/articles/Envisat_Yearly_Report_2004.pdf
- [20] Y.Faugere, J.Dorandeu, F.Lefevre, N.Picot and P.Femenias, 2005: Envisat ocean altimetry performance assessment and cross-calibration. Submitted in the special issue of SENSOR 'Satellite Altimetry: New Sensors and New Applications'
- [21] Faugere Y., Mertz F., Dorandeu J., 2005: Envisat RA-2/MWR ocean data validation and cross-calibration activities. Yearly report. Technical Note CLS.DOS/NT/04.289, Contract N° 03/CNES/1340/00-DSO310 http://www.jason.oceanobs.com/documents/calval/validation_report/en/annual_report_en_2005.pdf
- [22] Faugere, Y., Design and assessment of a method to correct the Ra2 USO anomaly, Tech. Note OSME-DPQC-SEDA-TN-06-XXX, CLS, July 2006b.
- [23] Labroue, S. and P. Gaspar, 2002: Comparison of non parametric estimates of the TOPEX A, TOPEX B and JASON 1 sea state bias. Paper presented at the Jason 1 and TOPEX/Poseidon SWT meeting, New-Orleans, 21-12 October.
- [24] Labroue S. and E. Obligis, January 2003, Neural network retrieval algorithms for the ENVISAT/MWR, Technical note CLS.DOS/NT/03.848
- [25] Labroue S., 2003: Non parametric estimation of ENVISAT sea state bias, Technical note CLS.DOS/NT/03.741, ESTEC Contract n°16243/02/NL/FF - WP3 Task 2
- [26] Labroue S., 2004: RA-2 ocean and MWR measurement long term monitoring, Final report for WP3, Task 2, SSB estimation for RA-2 altimeter, Technical Note CLS-DOS-NT-04-284
- [27] Labroue S., 2005: RA2 ocean and MWR measurement long term monitoring 2005 report for WP3, Task 2 SSB estimation for RA2 altimeter, Technical Note CLS-DOS-NT-05-200
- [28] Labroue S., 2006: Estimation du Biais d'Etat de Mer pour la mission Jason-1, Technical note CLS-DOS-NT-06-244
Labroue
- [29] Laxon and M. Roca, 2002: ENVISAT RA-2: S-BAND PERFORMANCE, S., Proceedings of the ENVISAT Calibration Workshop, Noordwijk
- [30] Le Traon, P.-Y., J. Stum, J. Dorandeu, P. Gaspar, and P. Vincent, 1994: Global statistical analysis of TOPEX and POSEIDON data. J. Geophys. Res., 99, 24619-24631.
- [31] Le Traon, P.-Y., , F. Ogor, 1998: ERS-1/2 orbit improvement using TOPEX/POSEIDON: the 2 cm challenge. J. G. Res., VOL 103, p 8045-8057, April 15, 1998.
- [32] Lefèvre, F., and E. Sénant, 2005: ENVISAT relative calibration, Technical Note CLS-DOS-NT-05.074.
- [33] Lillibridge J, R. Scharroo and G. Quartly, 2005: rain and ice flagging of Envisat altimeter and MWR data, Proc. of the 2004 Envisat and ERS Symposium, Salzburg, Austria

CLS CalVal Envisat	Envisat validation and cross-calibration activities	Page : 77 Date : April 19, 2007
Ref: CLS.DOS/NT/06.300	Nom.: SALP-RP-MA-EA-21376-CLS	Issue: 0rev1

- [34] Luthcke. S. B., N. P. Zelinsky, D. D. Rowlands, F. G. Lemoine, and T. A. Williams. 2003. The 1-Centimeter Orbit: Jason-1 Precision Orbit Determination Using GPS, SLR, DORIS, and Altimeter Data. *Mar. Geod.* 26(3-4): 399-421.
- [35] Martini A. and P. Féménias, 2000: The ERS SPTR2000 Altimetric Range Correction: Results and Validation. ERE-TN-ADQ-GSO-6001. 23 November 2000.
- [36] Martini A., 2003: Envisat RA-2 Range instrumental correction : USO clock period variation and associated auxiliary file, Technical Note ENVI-GSEG-EOPG-TN-03-0009 Available at http://earth.esa.int/pcs/envisat/ra2/articles/USO_clock_corr_aux_file.pdf
<http://earth.esa.int/pcs/envisat/ra2/auxdata/>
- [37] Martini A., P. Femenias, G. Alberti, M.P. Milagro-Perez, 2005: Ra-2 S-band anomaly detection and waveforms reconstruction, Proc. of the 2004 Envisat and ERS Symposium, Salzburg, Austria
- [38] Mertz, F., Y. Faugere and J. Dorandeu, 2003: Validation of ERS-2 OPR cycle 083-086. CLS.OC.NT/03.702 issue 083-086.
- [39] Mertz F., J. Dorandeu, N. Tran, S. Labroue, 2004, ERS-2 OPR data quality assessment. Long-term monitoring - particular investigations, Report of task 2 of IFREMER Contract n° 04/2.210.714. CLS.DOS/NT/04.277.
- [40] Mitchum, G., 1994: Comparison of TOPEX sea surface heights and tide gauge sea levels, *J. Geophys. Res.*, 99, 24541-24554.
- [41] Mitchum, G., 1998: Monitoring the stability of satellite altimeters with tide gauges, *J. Atm. Oceano. Tech.*, 15, 721-730.
- [42] Obligis E., L. Eymard, N. Tran, S. Labroue, 2005: Three years of Microwave Radiometer aboard Envisat: In-flight Calibration, Processing and validation of the geophysical products, submitted
- [43] R D Ray and R M Ponte, 2003: Barometric tides from ECMWF operational analyses, *Annales Geophysicae*, 21: 1897-1910.
- [44] Roca M., A. Martini, 2003: Level 1b Verification updates, Ra2/MWR CCVT meeting, 25-26 March 2003, ESRIN, Rome
- [45] Rudolph A., D.Kuijper, L.Ventimiglia, M.A. Garcia Matatoros, P.Bargellini, 2005: Envisat orbit control - philosophy experience and challenge, Proc. of the 2004 Envisat and ERS Symposium, Salzburg, Austria
- [46] R. Scharroo and P. N. A. M. Visser, 1998: Precise orbit determination and gravity field improvement for the ERS satellites, *J. Geophys. Res.*, 103, C4, 8113-8127
- [47] Scharroo R., A decade of ERS Satellite Orbits and Altimetry, 2002: Phd Thesis, Delft University Press science
- [48] Scharroo R., December 12, 2002, Routines for iono corrections, internet communication to the CCVT community
- [49] Scharroo R., J. L. Lillibridge, and W. H. F. Smith, Cross-Calibration and Long-term Monitoring of the Microwave Radiometers of ERS, TOPEX, GFO, Jason-1, and Envisat, *Marine Geodesy*, 27:279-297, 2004.

CLS CalVal Envisat	Envisat validation and cross-calibration activities	Page : 78 Date : April 19, 2007
Ref: CLS.DOS/NT/06.300	Nom.: SALP-RP-MA-EA-21376-CLS	Issue: 0rev1

- [50] Scharroo, R., RA-2 USO Anomaly: predictive correction model, Tech. Rep. N1-06-002, Altimetrics LLC, Cornish, New Hampshire, May 2006.
- [51] Stum J., F. Ogor, P.Y. Le Traon, J. Dorandeu, P. Gaspar and J.P. Dumont, 1998: "An intercalibration study of TOPEX/POSEIDON, ERS-1 and ERS-2 altimetric missions", Final report of IFREMER contract N_97/2 426 086/C CLS.DOS/NT/98.070.
- [52] Tran, N., D. W. Hancock III, G.S. Hayne. 2002: "Assessment of the cycle-per-cycle noise level of the GEOSAT Follow-On, TOPEX and POSEIDON." J. of Atmos. and Oceanic Technol. 19(12): 2095-2117.
- [53] Tran N. and E. Obligis, December 2003, Validation of the use of ENVISAT neural algorithm on ERS-2. CLS-DOS-NT-03.901.
- [54] Tran N., E. Obligis and L. Eymard, 2006, Envisat MWR 36.5 GHz drift evaluation and correction. CLS-DOS-NT-05.218.
- [55] Vincent, P., S. D. Desai, J. Dorandeu, M. Ablain, B. Soussi, P. S. Callahan, and B. J. Haines 2003. Jason-1 Geophysical Performance Evaluation. Mar. Geod. 26(3-4): 167-186.
- [56] Witter, D. L., D. B. Chelton, 1991: "A Geosat altimeter wind speed algorithm development", J. of Geophys. Res. (oceans), 96, 8853-8860, 1991.
- [57] Zanife, O. Z., P. Vincent, L. Amarouche, J. P. Dumont, P. Thibaut, and S. Labroue, 2003. Comparison of the Ku-band range noise level and the relative sea-state bias of the Jason-1, TOPEX and Poseidon-1 radar altimeters. Mar. Geod. 26(3-4): 201-238.

CLS CalVal Envisat	Envisat validation and cross-calibration activities	Page : 79 Date : April 19, 2007
Ref: CLS.DOS/NT/06.300	Nom.: SALP-RP-MA-EA-21376-CLS	Issue: 0rev1

10 Appendix 1: Mean Sea Level (MSL) and Sea Surface Temperature (SST) comparisons

This study has been carried out in order to monitor the MSL seen by all the operational altimeter missions. Long-term MSL change is a variable of considerable interest in the studies of global climate change. Then the objective here is on the one hand to survey the mean sea level trends and on the other hand to assess the consistency between all the MSL. Besides, the Reynolds SST is used to compare the MSL with an external data source. The mean SST is calculated in the same way as the MSL.

The following missions have been used : TOPEX/Poseidon (T/P), Jason-1 (J1), Geosat Follow-On (GFO) and Envisat. Moreover the PVA products available on the aviso web site are used to calculate an homogeneous MSL since the beginning of the T/P mission until now.

The MSL and SST time series have been plotted over global ocean. This allows us to correlate the MSL trends seen by each mission and to compare them with the SST.

In addition to these analysis, the maps of regional MSL change and SST change have been plotted for each mission over the Jason-1 period and the Envisat period. The differences of these maps have been performed; this is a way to display eventual local drifts.

10.1 SSH definition for each mission

The SSH formula is defined for all the satellites as below :

$$SSH = Orbit - Altimeter Range - \sum_{i=1}^n Correction_i$$

with :

$$\begin{aligned} \sum_{i=1}^n Correction_i = & \text{Dry troposphere correction : new S1 and S2 atmospheric tides applied} \\ & + \text{Combined atmospheric correction : MOG2D and inverse barometer} \\ & + \text{Radiometer wet troposphere correction} \\ & + \text{Filtered dual frequency ionospheric correction} \\ & + \text{Non parametric sea state bias correction} \\ & + \text{Geocentric ocean tide height, GOT 2000 : S1 atmospheric tide is applied} \\ & + \text{Solid earth tide height} \\ & + \text{Geocentric pole tide height} \end{aligned}$$

Some additional corrections have been applied :

- For Jason-1 and Envisat the wet troposphere correction has been changed by the ECMWF model in order to remove the effects of abnormal changes or trends observed on the radiometer wet troposphere correction.

CLS CalVal Envisat	Envisat validation and cross-calibration activities	Page : 80 Date : April 19, 2007
Ref: CLS.DOS/NT/06.300	Nom.: SALP-RP-MA-EA-21376-CLS	Issue: 0rev1

- For Envisat, the USO correction has been applied (drift and anomaly : see Envisat yearly report [22])
- For T/P, the radiometer wet troposphere correction has been corrected from correction (Scharroo R., 2004 [49])
- For T/P, the relative bias between TOPEX and Poseidon and between TOPEX A and TOPEX B has been taken into account
- For T/P, the drift between the TOPEX and DORIS ionosphere corrections has been corrected for on Poseidon cycles.
- For Geosat Follow-On, the GIM model has been used for the ionospheric correction.

10.2 MSL and SST time series

10.2.1 MSL over global ocean

The MSL has been monitored for each satellite altimeter over global ocean in figure 69 since the beginning of T/P mission (left figure) and since the beginning of Jason-1 mission (right figure). The observed MSL trends have a similar shape for each satellite except for Envisat. The estimation of the Envisat MSL slope seems impacted by an unexpected behaviour on the first year probably linked to a USO correction drift as explained in Faugere et al. (2005, [17]).

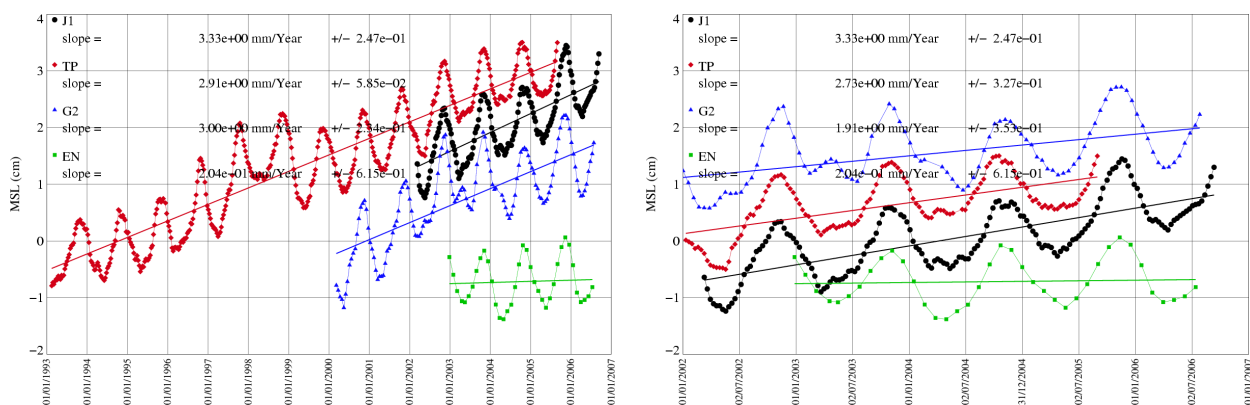


Figure 69: MSL over global ocean since the beginning of T/P mission on the left and since the beginning of Jason-1 mission on the right.

In the following figure 70, MSL have been plotted after removing annual signal, semi-annual signal, and signals lower than 60 days. The T/P, Jason-1 slopes since the beginning of Jason-1 period are still similar, with respectively 2.7 mm/year and 3.3 mm/year and an adjustment formal error around 0.1 mm/year. The GFO slope is smaller than Jason-1 one by 1.4 mm/year over the Jason-1 period. But notice that the GFO MSL slope over the global period is stronger with 3.2 mm/year.

The differences between the different global MSL slope show that the real error of the MSL slope estimation is significantly greater than the formal error adjustment which is only a mathematical error, not linked with the physical errors such as the orbit errors for instance. The formal error adjustment show here the linear evolution of the MSL and the intrinsic consistency of the data.

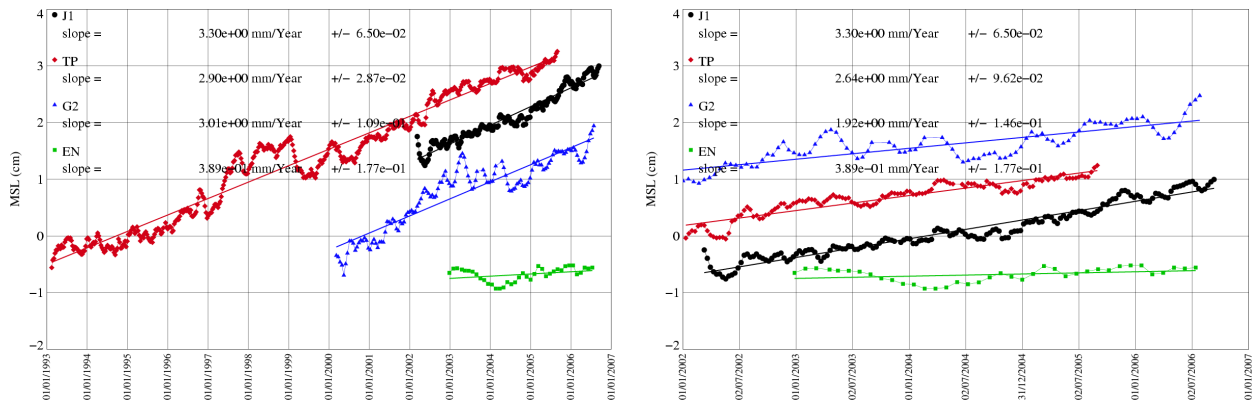


Figure 70: MSL over global ocean since the beginning of T/P mission on the left and since the beginning Jason-1 mission on the right after removing annual, semi-annual and 60-day signals.

10.2.2 SST over global ocean

In figure 71 on the left, the SST mean is compared to the MSL computed since the beginning of the T/P mission until now using the T/P and Jason-1 data. In the same figure on the right, annual signal, semi-annual signal, and signals lower than 60 days have been removed. The global MSL slope is 2.92 mm/year with a very small error adjustment (0.02 mm/year) which reveals an evolution very linear with a very good intrinsic consistency of the data. Besides, the SST increases by about 0.016 degree/year with a formal error close to 0.001 degree/year. The MSL and the SST don't have the same unit ("cm" and "degree"), thus to compare the 2 quantities, the SST scale is adjusted on the MSL scale so that the SST trend and the MSL trend are visually the same. This allows us to highlight that the SST dynamic is stronger than the MSL one. Inter-annual signal or climatic phenomena have a greater impact on the SST than on the MSL.

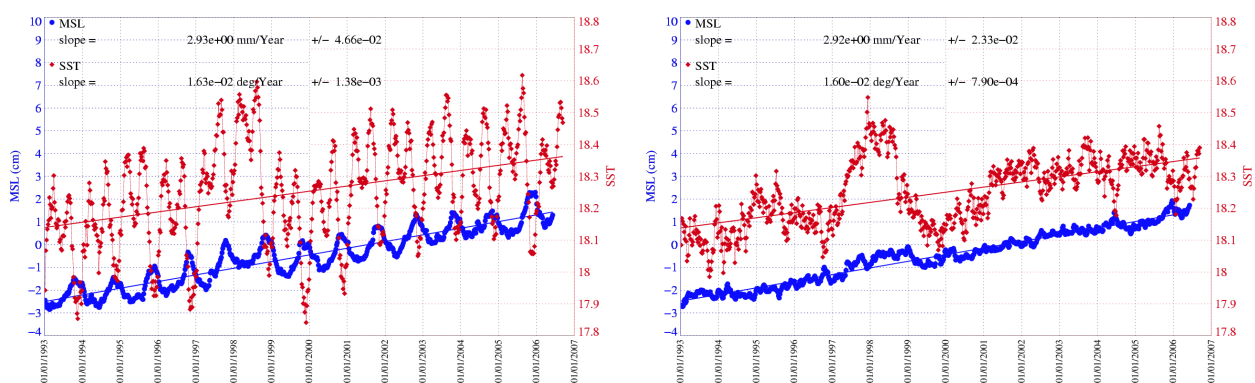


Figure 71: MSL and SST over global ocean for the T/P period on the left, and after removing annual, semi-annual and 60-day signals on the left.

CLS CalVal Envisat	Envisat validation and cross-calibration activities	Page : 82 Date : April 19, 2007
Ref: CLS.DOS/NT/06.300	Nom.: SALP-RP-MA-EA-21376-CLS	Issue: 0rev1

10.3 Spatial MSL and SST slopes

10.3.1 Methodology

In order to monitor the MSL, the spatial MSL slopes have been calculated. The SLA grids (2x2 degree bins) have been computed cycle per cycle, and the slope has been computed on each grid point. As for time analysis, 60 day, semi-annual and annual signals have been removed before estimating the slopes. Then, the MSL slopes have been mapped for each mission. These maps are used to compare the MSL slopes between each altimeter mission. This allows us to detect potential local drifts.

Besides, the SST slopes have been computed the same way in order to correlate them with the MSL slopes.

10.3.2 Spatial MSL slopes over Jason-1 period

The MSL slopes have been plotted for Jason-1 (on the right) and T/P (on the left) over Jason-1/TOPEX overlapping period in figure 72. The MSL trends seen by the two satellites are similar. However, differences greater than 10 mm/year can be observed on the T/P-Jason-1 map (bottom figure).

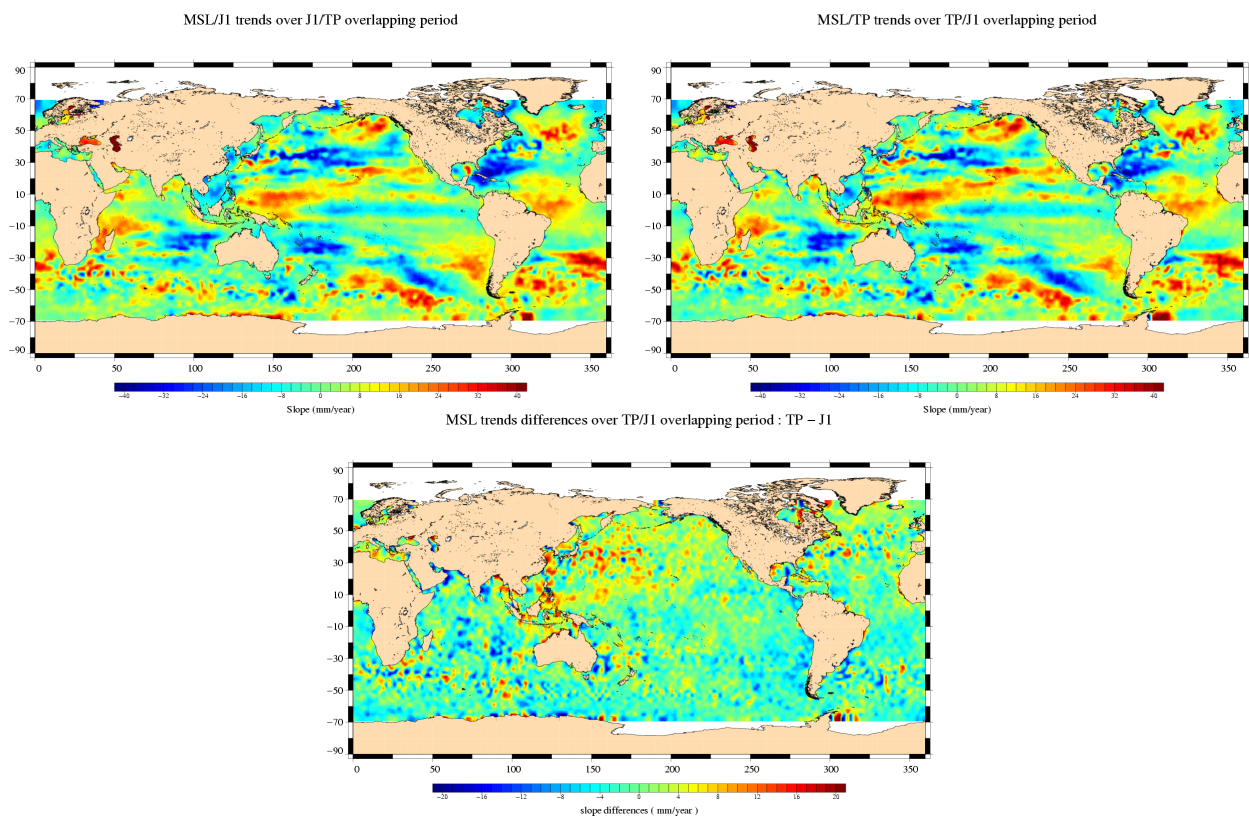


Figure 72: MSL slopes over Jason-1/TOPEX overlapping period for T/P (left) and Jason-1 (right), MSL slope differences between Jason-1 and T/P (bottom)

CLS CalVal Envisat	Envisat validation and cross-calibration activities	Page : 83 Date : April 19, 2007
Ref: CLS.DOS/NT/06.300	Nom.: SALP-RP-MA-EA-21376-CLS	Issue: 0rev1

10.3.3 Spatial MSL slopes over Envisat period

The same work has been performed over Jason-1/Envisat overlapping period using Envisat data in figure 73. The 3 maps are quite similar. They allow us to observe differences in several areas (equatorial, ...) between Jason-1 and Envisat.

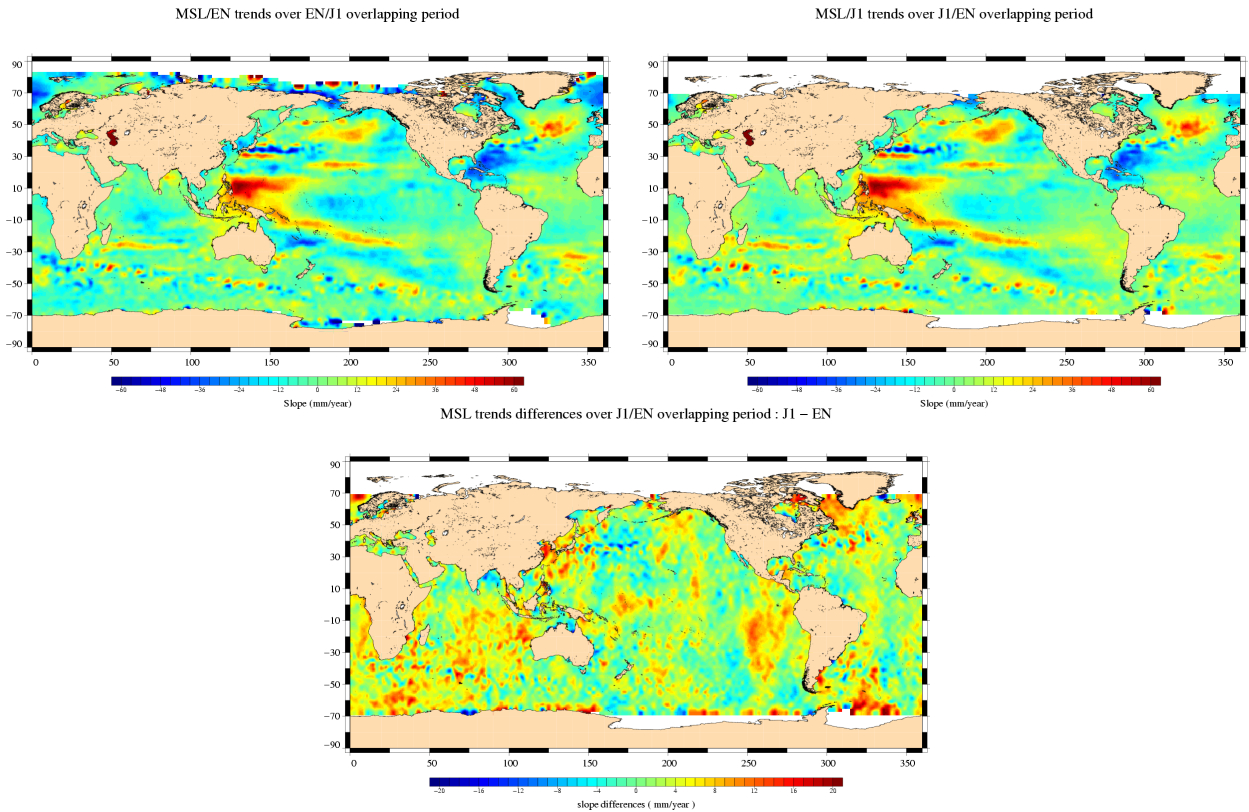


Figure 73: *MSL slopes over Envisat/Jason-1 overlapping period for Envisat (left) and Jason-1 (right), MSL slope differences between Jason-1 and Envisat (bottom)*

<p>CLS CalVal Envisat</p>	<p>Envisat validation and cross-calibration activities</p>	<p>Page : 84 Date : April 19, 2007</p>
<p>Ref: CLS.DOS/NT/06.300</p>	<p>Nom.: SALP-RP-MA-EA-21376-CLS</p>	<p>Issue: 0rev1</p>

10.3.4 Spatial SST and MSL slopes since the beginning of T/P mission

In order to compute the local MSL slopes since the beginning of the T/P mission, the PVA products (available on aviso website) are used. These products combine different altimetric data coming from T/P, Jason-1, ERS-2, Envisat, and GFO missions which allows us to increase the spatial resolution.

The MSL slopes are mapped in figure 74 on the left. In order to correlate the MSL and the SST, the SST slopes have been plotted in the same figure on the right. 14 years of altimetric data have been used to estimate the slopes which allows us to have a good estimation of the local MSL trends. The adjustment errors of the MSL and the SST slopes are mapped in figure 75.

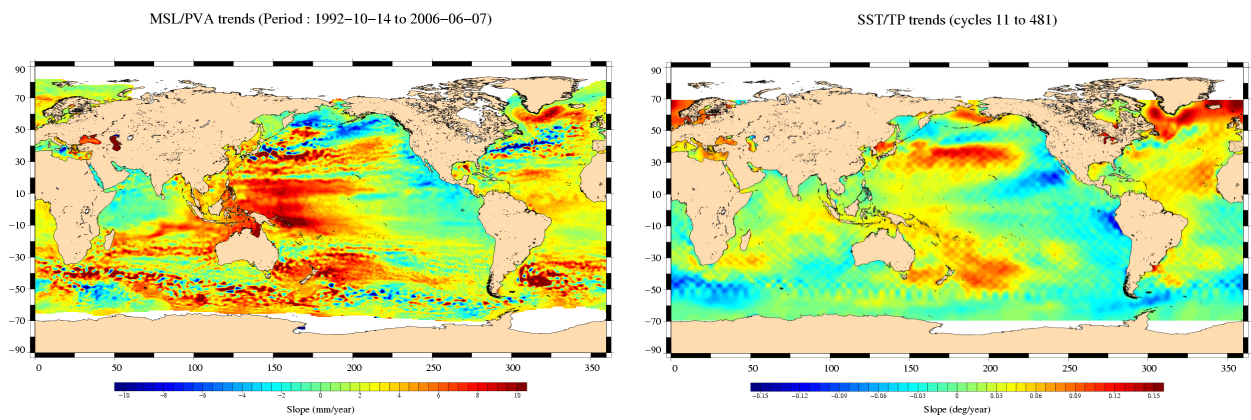


Figure 74: *T/P MSL and SST slopes over 13 years*

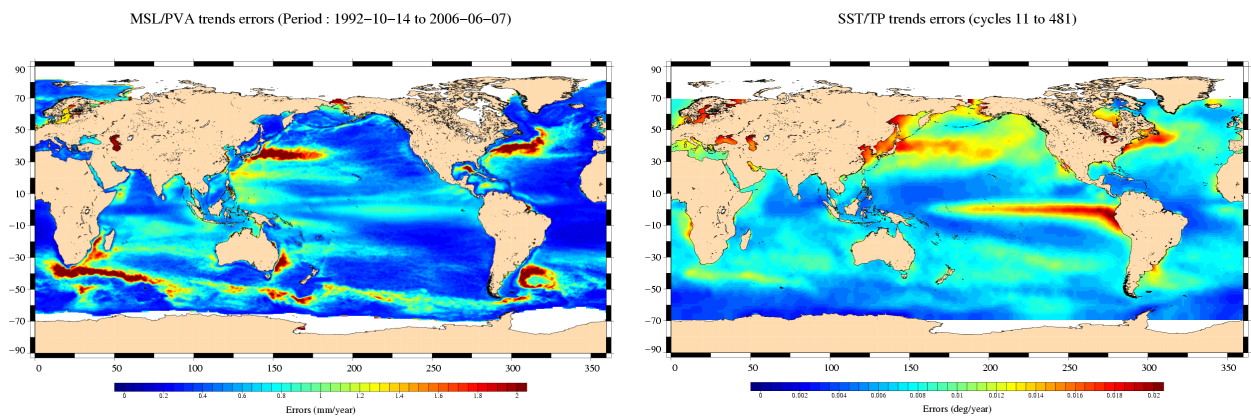


Figure 75: *Adjustment errors of T/P MSL and SST slopes over 13 years*

CLS CalVal Envisat	Envisat validation and cross-calibration activities	Page : 85 Date : April 19, 2007
Ref: CLS.DOS/NT/06.300	Nom.: SALP-RP-MA-EA-21376-CLS	Issue: 0rev1

10.3.5 "El Niño" impact on SST and MSL slope estimations

The MSL and SST regional trends are largely impacted by inter-annual signal or oceanic phenomena such as "El Niño" for instance. The 4 maps in the figure 76 show the trend for the SST and the MSL before and after "El Niño". The first period ranges from 1992 and 1996 included, whereas the second period ranges from 1999 to 2004 included.

MSL and SST trends are stronger for each period separately than for the global period. In the Pacific ocean, the absolute values are greater than 20 mm/year for the MSL and 0.3 degree/year for the SST. SST and MSL maps show a strong correlation on the two periods of time. But for both SST and MSL, the trends on the first period are very different from the trends of the second period. This is particularly true in tropical areas. Finally, these maps highlight the importance of having long time series to evaluate the regional trends with a good accuracy.

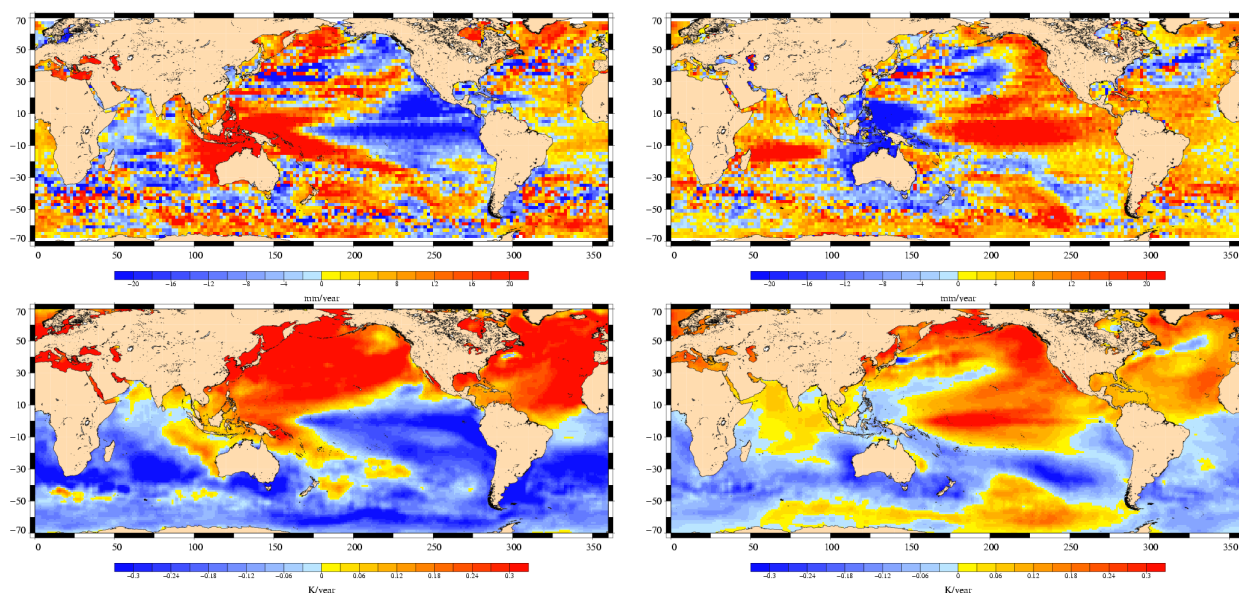


Figure 76: Adjustment errors of T/P MSL and SST slopes over 13 years before and after "El Niño"

CLS CalVal Envisat	Envisat validation and cross-calibration activities	Page : 86 Date : April 19, 2007
Ref: CLS.DOS/NT/06.300	Nom.: SALP-RP-MA-EA-21376-CLS	Issue: 0rev1

11 Appendix 2: Instrument and platform status

11.1 ACRONYMS

The main acronyms used to describe the events are explained below.

CMA: Centre Multimission Altimetrie

CTI tables: Configuration Table Interface. They contain the setting of the instruments and are uploaded on board after a switch off, a reset

HTR Refuse: Heater Refuse

ICU: Instrument Control Unit, a part of the distributed command and control function implemented on ESA spacecraft. The unit receives, decodes and executes high-level commands for its instrument, and autonomously performs health-checking and parameter monitoring. In the event of anomalies it takes autonomous recovery actions.

IPF: Instrument Processing Facilities

MCMD: Macrocommand

OBDH: On Board Data Handling

OCM: Orbit Control Mode/manoeuvre

P/L SOL: Payload Switch Off Line

SEU: Single Event Upset

SM-SOL by PMC: SM Switch Off Line by Payload Main Computer

SW: Software

TM: Telemetry

USO: Ultra Stable Oscillator

11.2 Cycle 010

- RA-2 went to STBY/Refuse (2002/10/09 09 13:34:22 to 2002/10/10 08:56:53)

11.3 Cycle 011

- Ra2 switch-down - Planned SM-SOL by PMC1 (2002/11/18 04:38:00 to 2002/11/19 19:19:21, Pass 382-429)
- DORIS Navigator switch-down - Planned SM-SOL by PMC1 (2002/11/18 04:38:02 to 2002/11/22 12:40:00, Pass 382-505)
- MWR switch-down - Planned SM-SOL by PMC1 (2002/11/18 04:37:59 to 2002/11/20 12:20:06, Pass 382-448)
- Orbit Maintenance Maneuver (2002/11/07 18:15:51 to 2002/11/07 21:06:17, Pass 83-85)
- Orbit Maintenance Maneuver (2002/11/29 03:35:30 to 2002/11/29 06:25:57, Pass 696-698)

CLS CalVal Envisat	Envisat validation and cross-calibration activities	Page : 87 Date : April 19, 2007
Ref: CLS.DOS/NT/06.300	Nom.: SALP-RP-MA-EA-21376-CLS	Issue: 0rev1

11.4 Cycle 012

- RA-2 went to HTR-0 Refuse (2002/12/21 04:31:26 to 2002/12/21 12:52:00, Pass 325-333)
- Orbit Inclination Maneuver (2002/12/18 04:28:18 to 2002/12/18 06:36:46, Pass 238-240)
- Orbit Maintenance Maneuver (2002/12/18 22:17:22 to 2002/12/19 00:17:34, Pass 259-261)

11.5 Cycle 013

- RA-2 went to HTR-0 Refuse (2003-01-16 01:52:36 to 2003-01-17 17:00:35)
- RA-2 went to suspend mode (2003-01-25 23:56:36 to 2003-01-27 19:54:02)
- Orbit Maintenance Maneuver (2003/01/14 00:55:17 to 2003/01/14 03:45:42 TAI)
- Orbit Maintenance Maneuver (2003/02/11 23:04:49 to 2003/02/12 01:04:57 TAI)

11.6 Cycle 014

- SEU's caused a Software Anomaly (2003/03/02 02:46:44 to 2003/03/03 16:46:35).
- Subsystems unavailable - Autonomous P/L switch-off (2003/03/15 04:21:08 to 2003/03/17 19:00:13)
- RA2 in HTR0/Refuse due to HPA primery bus undercurrent (2003/03/17 21:09:32 to 2003/03/18 18:50:40)
- Orbit Maintenance Maneuver (2003/02/21 03:42:57 to 2003/02/21 05:53:24)
- Orbit Maintenance Maneuver (2003/03/03 23:51:14 to 2003/03/04 01:51:22)

11.7 Cycle 015

- Wrong setting of Ra2 parameters (no CTI tables have been up-loaded on-board) from 18 Mar 2003 18:50:40 to 9 Apr 2003 17:12:24, Pass 1 to 452
- RA-2 unavailability (Format Header Error forcing ICU to RS/WT/INI) from 8 Apr 2003 15:08:57.000 to 9 Apr 2003 17:12:24.000, Pass 437 to 452
- RA-2 unavailability (Format Header Error forcing ICU to RS/WT/INI) from 8 Apr 2003 15:08:57.000 to 9 Apr 2003 17:12:24.000, Pass 613 to 624
- RA-2 unavailability: Multiple SEU caused ICU switchdown (2003/04/24 13:20:09 to 2003/04/25 09:15:36,879 to 901)
- Orbit Maintenance Maneuver (2003/04/04 00:40:48 to 2003/04/04 02:40:56 TAI)

CLS CalVal Envisat	Envisat validation and cross-calibration activities	Page : 88 Date : April 19, 2007
Ref: CLS.DOS/NT/06.300	Nom.: SALP-RP-MA-EA-21376-CLS	Issue: 0rev1

11.8 Cycle 016

- RA2 unavailability (known SEU failure) (from 5 May 2003 12:30:17.000 to 6 May 2003 10:01:10.000, Pass 191 to 215)
- RA-2 unavailability (ICU in SUSPEND due to TM FMT Error when a Reduced FMT was requested) (from 11 May 2003 11:06:33.000 to 12 May 2003 10:14:35.726, Pass 361 to 387)
- Orbit Maintenance Maneuver (from 2003/05/14 22:40:13 to 2003/05/15 00:40:19 TAI, Pass 460 to 462)
- RA-2 unavailability (Switch-down for PMC SW upgrade and OCM) from 18 May 2003 06:25:17.000 to 19 May 2003 15:59:28.000, Pass 548 to 602)
- MWR unavailability (Switch-down for PMC SW upgrade and OCM) from 18 May 2003 06:25:24.000 to 19 May 2003 14:45:40.000, Pass 548 to 602)
- DORIS unavailability (Switch-down for PMC SW upgrade and OCM) from 18 May 2003 06:25:25.000 to 19 May 2003 13:21:28.000, Pass 548 to 602)
- Orbit Inclination Maneuver (from 2003/05/20 04:11:53 to 2003/05/20 06:23:31 TAI, Pass 610 to 612)
- RA-2 unavailability (ICU went to RS/WT/INI) from 1 Jun 2003 14:36:40.000 to 2 Jun 2003 09:20:35.000, Pass 967 to 987

11.9 Cycle 017

- Orbit Maintenance Maneuver (from 2003/06/07 01:08:16 to 2003/06/07 03:08:23 TAI, Pass 119 to 122)

11.10 Cycle 018

- Orbit Maintenance Maneuver (from 2003/07/11 0:58:45 to 2003/07/11 03:49:08 TAI, Pass 90 to 94)
- RA2 unavailability (RA-2 in STBY/REF due to MCMD timeout) (from 26 Jul 2003 15:28:11 to 26 Jul 2003 17:25:35, Pass 538)
- RA2 unavailability (RA-2 picked up Mission Planning schedule) (from 31 Jul 2003 16:11:02 to 31 Jul 2003 18:06:30, Pass 682)
- Orbit Maintenance Maneuver (from 2003/07/11 0:58:45 to 2003/07/11 03:49:08 TAI, Pass 91 to 94)

CLS CalVal Envisat	Envisat validation and cross-calibration activities	Page : 89 Date : April 19, 2007
Ref: CLS.DOS/NT/06.300	Nom.: SALP-RP-MA-EA-21376-CLS	Issue: Orev1

11.11 Cycle 019

- Orbit Maintenance Maneuver (from 2003/08/15 1:31:29 to 2003/08/15 03:31:35 TAI, Pass 91 to 93)
- RA-2 went to STBY/Refuse due to Individual Echoes MCMD Timeout (from 2003-08-15 16:40:21 to 2003-08-15 18:35:35, Pass 110)
- RA-2 went to STBY/Refuse due to Individual Echoes MCMD Timeout (from 2003-08-30 15:28:00 to 2003-08-30 20:47:35, Pass 538 to 543)
- PLSOL . Instrument Switch OFF/ON (from 2003-09-04 22:52:52 to 2003-09-06 16:41:09, Pass 689 to 738)

11.12 Cycle 020

- RA-2 in STANDBY / REFUSE MODE (from 2003-09-21 15:36:40 to 2003-09-21 17:33:30, Pass 166 to 167)
- RA-2 is in RS/WT/INT mode (from 2003-09-27 00:28:08 to 2003-09-27 12:52:00, Pass 320 to 333)
- Wrong setting of Ra2 parameters (no CTI tables have been up-loaded on-board) (from 2003-09-27 12:52:00 to 2003-09-30 12:45:00, Pass 334 to 407)
- Orbit Maintenance Maneuver (2003/09/30 00:40:53 to 2003/09/30 02:41:00 TAI, Pass 405 to 407)

11.13 Cycle 021

- Orbit Inclination Maneuver (2003/10/28 04:56:18 to 2003/10/28 07:09:44 TAI, Pass 210 to 212)
- RA-2 is in RS/WT/INT mode. 29 Oct 2003 06 :47 :04 to 29 Oct 2003 12 :58 :35, Pass 242 to 247)
- Orbit Maintenance Maneuver (2003/10/31 01:13:10 to 2003/10/31 03:13:25 TAI, Pass 291 to 293)
- RA-2 is in RS/WT/INT mode. TM format header error (02 Nov 2003 15 :16 :56 to 03 Nov 2003 12 :08 :35, Pass 366 to 389)
- Orbit Maintenance Maneuver (2003/11/18 23:02:30 to 2003/11/19 01:52:55 TAI, Pass 833 to 835)

11.14 Cycle 022

- RA-2 is in RS/WT/INT mode (2003-11-26 13:31:20 to 2003-11-26 19:39:35, Pass 49 to 54)
 - RA-2 PLSOL . Instrument Switch OFF/ON (2003-12-03 07:18:43 to 2003-12-05 16:35:05, Pass 241 to 308)
 - MWR PLSOL . Instrument Switch OFF/ON (2003-12-03 07:18:43 to 2003-12-04 18:45:41)
 - RA-2 is in RS/WT/INT mode. (2003-12-06 15:55:52 to 2003-12-10 19:16:36, Pass 338 to 455)
 - Orbit Maintenance Maneuver (2003/12/15 21:02:28 to 2003/12/15 23:02:36, Pass 601 to 603)
 - Orbit Maintenance Maneuver (2003/12/26 21:03:30 to 2003/12/26 23:03:34, Pass 916 to 918)
- Proprietary information : no part of this document may be reproduced divulged or used in any form without prior permission from CNES or CLS.

CLS CalVal Envisat	Envisat validation and cross-calibration activities	Page : 90 Date : April 19, 2007
Ref: CLS.DOS/NT/06.300	Nom.: SALP-RP-MA-EA-21376-CLS	Issue: 0rev1

11.15 Cycle 023

Orbit Maintenance Maneuver (2004/01/21 23:54:27 to 2004/01/22 01:54:37))

- Orbit Maintenance Maneuver (2004/01/26 22:26:07 to 2004/01/27 00:26:11))

11.16 Cycle 024

- Orbit Inclination Maneuver (2004/02/04 04:46:39 to 2004/02/04 06:58:05)
- Orbit Maintenance Maneuver (2004/02/05 11:17:21 to 2004/02/05 13:17:23)
- Orbit Maintenance Maneuver (2004/02/24 11:48:39 to 2004/02/24 13:48:45)

11.17 Cycle 025

- Orbit Maintenance Maneuver (2004/04/07 20:05:30 to 2004/04/07 22:05:34)

11.18 Cycle 026

- RA-2 in STANDBY/REF DUE TO MCMD H202 FAILURE (2004-22-04 15:15:36 2004-22-04 17:07:05)
- RA-2 Switch down to RESET/WAIT due to too many SEU's reported. (2004-05-10 02:06:31 2004-05-10 11:27:30)
- Orbit Inclination Maneuver (2004/04/14 04:43:02 2004/04/14 06:55:00)
- Orbit Maintenance Maneuver (2004/05/07 01:08:56 2004/05/07 03:09:04)

11.19 Cycle 027

- RA2 went to suspend owing to repeated type 10 entries in report format (2004/05/31 02:45:27 to 2004/05/31 12:01:50)
- No DORIS data from 2004/06/06 13:00:00 to 2004/06/14 14:52:00. Following an onboard incident, Doris instrument has been switched to the redundant chain. Doris data are unavailable from June, 6th to June, 14th. To allow GDR production, POE with laser only data have been produced during this period.
- RA2 in SUSPEND Mode (2004/06/21 14:47:51 to 2004/06/21 19:24:30, Pass 995 to 999)

- Proprietary information : no part of this document may be reproduced divulged or used in any form without prior permission from CNES or CLS.

CLS CalVal Envisat	Envisat validation and cross-calibration activities	Page : 91 Date : April 19, 2007
Ref: CLS.DOS/NT/06.300	Nom.: SALP-RP-MA-EA-21376-CLS	Issue: 0rev1

11.20 Cycle 028

- RA2 in ICU rs/wt/ini (2004/07/18 13:47:03 to 2004/07/18 19:59:00, Pass 765 to 771)
- Orbit Maintenance Maneuver (2004/06/30 08:08:29 to 2004/06/30 10:08:35, Pass 242 to 244)

11.21 Cycle 029

RA2 in ICU RS/WT/INI. (SDU problem in RAM) (2004/08/10 15:00:39 to 2004/08/11 10:59:30, Pass 423 to 445)

- Orbit Maintenance Maneuver (2004/08/17 02:04:20 to 2004/08/17 04:04:26 , Pass 607 to 609)

11.22 Cycle 030

- RA2 in ICU RS/WT/INI. (SDU problem in RAM) (2004/09/26 13:39:50 to 2004/09/27 16:23:30, Pass 765-795)
- Abnormal behaviour of the RA-2 sensor (2004/09/27 16:23:30 to 2004-09-29 10:21:07, Pass 796-846)
- Collision avoidance Maneuver (2004/09/01 22:52:27 to 2004/09/02 00:52:37, Pass 60-62)
- Collision avoidance Maneuver (2004/09/02 23:44:27 to 2004/09/03 01:44:37, Pass 89-91)
- Orbit Inclination Maneuver (2004/09/21 04:14:37 to 2004/09/21 06:29:19, Pass 610-612)
- Orbit Maintenance Maneuver (2004/09/24 03:53:38 to 2004/09/24 05:53:46, Pass 695-697)

11.23 Cycle 031

- Collision avoidance Maneuver (2004/10/22 03:20:22 to 2004/10/22 07:00:41, Pass 495-498)
- High solar activity (Pass 974-1002)

11.24 Cycle 032

- RA2 in RS/WT/INI. 2004/11/23 13:25:58 to 2004/11/24 14:10:10, Pass 421-449
- RA2 Format header error. 2004/12/01 10:22:30 to 2004/12/01 15:34:29, Pass 647-651
- Orbit Maintenance Maneuver (2004/11/12 01:07:57 to 2004/11/12 03:08:06, Pass 91-93)

CLS CalVal Envisat	Envisat validation and cross-calibration activities	Page : 92 Date : April 19, 2007
Ref: CLS.DOS/NT/06.300	Nom.: SALP-RP-MA-EA-21376-CLS	Issue: 0rev1

11.25 Cycle 033

- RA-2 went to RS/WT/INI due RBI (2004/12/27 02:49:10 to 2004/12/27 13:49:30, 380 to 391)
- Orbit Maintenance Maneuver (2004/12/17 01:03:48 to 2004/12/17 03:03:52, 91 to 93)
- Orbit Maintenance Maneuver (2005/01/05 23:10:28 to 2005/01/06 01:10:36, 661 to 663)
- Orbit Inclination Maneuver (2005/01/07 04:25:17 to 2005/01/07 06:38:53, 696 to 698)

11.26 Cycle 034

- RA-2 went to RS/WT/INI Mode (2005/01/26 15:50:30 to 2005/01/26 21:07:30, 252 to 257)
- Orbit Maintenance Maneuver (2005/02/18 01:23:24 to 2005/02/18 03:23:28, 893 to 894)

11.27 Cycle 035

- RA-2 went to RS/WT/INI Mode (2005/03/18 04:35:34 to 2005/03/18 12:58:00, 697 to 705)
- Orbit Maintenance Maneuver (2005/03/17 04:51:26 to 2005/03/17 07:06:31, 668 to 669)

11.28 Cycle 036

- RA-2 went to RS/WT/INI mode (2005/04/18 05:01:10 to 2005/04/18 13:22:32, 583 to 591)
- RA-2 went to RS/WT/INI mode (2005/04/18 37:58:10 to 2005/04/24 11:42:30, 742 to 761)

11.29 Cycle 037

- RA-2 went to ICU in RS/WT/INI (RBI ERR 71) (2005/05/14 23:56:37 to 2005/05/15 10:53:45, 348 to 359)
- RA-2 went to ICU in RS/WT/INI (2005/05/21 00:10:45 to 2005/05/21 10:55:35, 520 to 531)

11.30 Cycle 038

- RA-2 went to ICU in RS/WT/INI (2005/07/04 04:41:10 to 2005/07/04 11:19:39, 783 to 789)

CLS CalVal Envisat	Envisat validation and cross-calibration activities	Page : 93 Date : April 19, 2007
Ref: CLS.DOS/NT/06.300	Nom.: SALP-RP-MA-EA-21376-CLS	Issue: 0rev1

11.31 Cycle 039

- RA-2 went to ICU in RS/WT/INI (2005/07/16 13:32:21 to 2005/07/16 19:58:52,135 to 141)
- RA-2 went to ICU in RS/WT/INI (2005/07/17 14:43:49 to 2005/07/17 19:20:30,165 to 169)
- RA-2 went to ICU in RS/WT/INI (2005/07/29 00:41:41 to 2005/07/29 09:58:30,492 to 501)
- Orbit Maintenance Maneuver (2005/08/09 22:45:44 to 2005/08/10 00:45:50 TAI)

11.32 Cycle 040

- RA-2 went to ICU in RS/WT/INI (2005/08/16 16:41:57 to 2005/08/16 20:22:30,24 to 27)
- RA-2 went to ICU in RS/WT/INI (2005/08/30 16:01:25 to 2005/08/30 19:43:00,424 to 427)
- RA-2 went to ICU in RS/WT/INI (2005/09/12 15:53:09 to 2005/09/12 19:47:00,796 to 799)
- Orbit Maintenance Maneuver (2005/09/07 05:19:53 to 2005/09/07 07:36:31 TAI)

11.33 Cycle 041

- RA-2 went to ICU in RS/WT/INI (2005/09/20 12:19:17 to 2005/09/20 18:56:00,19 to 25)
- RA-2 went in RS/WT/INI (2005/10/04 12:47:33 to 2005/10/04 16:35:30,420 to 423)
- Orbit Maintenance Maneuver (2005/10/06 02:19:10 to 2005/10/06 02:19:14 TAI)

11.34 Cycle 042

- RA-2 went in RS/WT/INI following Uncontrolled S/W Action (2005/10/28 05:34:13 to 2005/10/28 10:39:00,97 to 101)

11.35 Cycle 043

- RA-2 went in RS/WT/INI following Uncontrolled S/W Action (2006/01/02 12:56:35 2006/01/02 18:09:30,993 to 997)

CLS CalVal Envisat	Envisat validation and cross-calibration activities	Page : 94 Date : April 19, 2007
Ref: CLS.DOS/NT/06.300	Nom.: SALP-RP-MA-EA-21376-CLS	Issue: 0rev1

11.36 Cycle 044

- RA-2 went in RS/WT/INI following Multiple SEU Anomaly (ref AR-614) (2006/01/12 14:20:35 to 2006/01/12 19:12:30,279 to 283)
- RA-2 went in RS/WT/INI(2006/01/30 02:07:15 to 2006/01/30 11:29:00,780 to 789)
- RA-2 went in RS/WT/INI following Uncontrolled S/W Action (2006/02/01 05:17:56 to 2006/02/01 12:04:30,841 to 847)
- RA-2 went in RS/WT/INI following Uncontrolled S/W Action (2006/02/01 16:30:28 to 2006/02/01 18:36:30,854 to 855)
- Orbit Inclination Maneuver (2006/01/10 05:54:24 to 2006/01/10 06:11:24)

11.37 Cycle 045

- RA-2 went in RA2 back to operations following TM format anomaly (2006/03/13 09:36:51 to 2006/03/13 17:40:00,989 to 997))

11.38 Cycle 046

- RA-2 switch to STBY and back to measurement to get useful telemetry related to USO (2006/03/17 12:04:00 to 2006/03/17 13:26:00,104 to 107)
- Orbit Inclination Manoeuvre (2006/03/28 05:33:20 to 2006/03/28 05:52:11 TAI)
- Payload anomaly DORIS MVR switch off (no data from) (2006/04/06 02:09:00 to 2006/04/08 12:40:00 TAI)
- RA2 back to operations following TM format anomaly (2006/04/06 12:31:00 to 2006/04/08 12:31:00,664 to 735)
- Doris Doppler Instrument nominal mode with median frequency bandwidth pre-positioning (required for DORIS incident recovery) (2004/04/08 12:40:00 to 2006/04/14 09:00:00 TAI)
- Payload anomaly DORIS Reset (2006/04/14 09:00:09)

11.39 Cycle 047

- On 12th-13th May, a special operation was executed to limit RA-2 Chirp Bandwidth to 80MHz (starting from 12/05/2006 at 15:51:37, pass 710) and then 20 MHz (starting from 13/05/2006 at 03:57:57, Pass 724). The instrument was returned to 320MHz on 13/05/2006 at 15:10:17, Pass 738. Users are strongly advised not to use passes 710-738
- The instrument sub-system Radio Frequency Module (RFM) was switched to its B-side on 15 May 2006 at 14:21:50, Pass 790
- RA-2 BACK TO OPERATIONS AFTER 2 CONSECUTIVE SEU ANOMALIES (19 May 2006 09:24:32 and 19 May 2006 19:13:00)
- Proprietary information : no part of this document may be reproduced divulged or used in any form without prior permission from CNES or CLS.

CLS CalVal Envisat	Envisat validation and cross-calibration activities	Page : 95 Date : April 19, 2007
Ref: CLS.DOS/NT/06.300	Nom.: SALP-RP-MA-EA-21376-CLS	Issue: 0rev1

11.40 Cycle 048

RFM switched to its nominal configuration side (A-side) on the 2006/06/21 at 13:20:15, Pass 850

- RA-2 Back to Measurement following Uncontrolled S/W Action (2006/06/25 15:01:36 to 2006/06/25 19:46:00, passes 967-971)

11.41 Cycle 049

- none

11.42 Cycle 050

- RA-2 Back to Measurement following Multiple SEU Anomaly (2006/08/01 01:14:40 to 2006/08/01 08:54:30,6 to 13)
- Focccserver have been re-booted and is up and running. The problem was probably due to a HW failure at ESRIN (IECF) which caused all the user slots to be occupied(2006/08/17 00:00:41 to 2006/08/17 11:10:00,TAI)

11.43 Cycle 051

- -RA-2 Back to Measurement following a Service Module Anomaly (2006/09/7 16:40:30 to 2006/09/10 15:47:30,80 to 166)
- -Orbit Inclination Maneuver (2006/09/13 05:22:17 to 2006/09/13 05:40:29)
- -Interruption of the Envisat data transmission via the ESA Data Relay Satellite Artemis (anomaly with Envisat Ka-band antenna) from 2006/09/26 until 2006/10/1,630 to 641, 658 to 669, 686 to 697, 716 to 725, 744 to 755)